



AD-A283 530



Miscellaneous Paper CERC-94-14
July 1994

(1)

US Army Corps
of Engineers
Waterways Experiment
Station

Upgrade of Tropical Cyclone Surface Wind Field Model

by Vincent J. Cardone, Andrew T. Cox, J. Arthur Greenwood, Oceanweather, Inc.
Edward F. Thompson, WES



WZES

Approved For Public Release; Distribution Is Unlimited

DTIC QUALITY INSPECTED 5

94-26566



94 8 19 078

Prepared for Headquarters, U.S. Army Corps of Engineers

Upgrade of Tropical Cyclone Surface Wind Field Model

by Vincent J. Cardone, Andrew T. Cox, J. Arthur Greenwood

Oceanweather, Inc.
5 River Road, Suite 1
Cos Cob, CT 06807

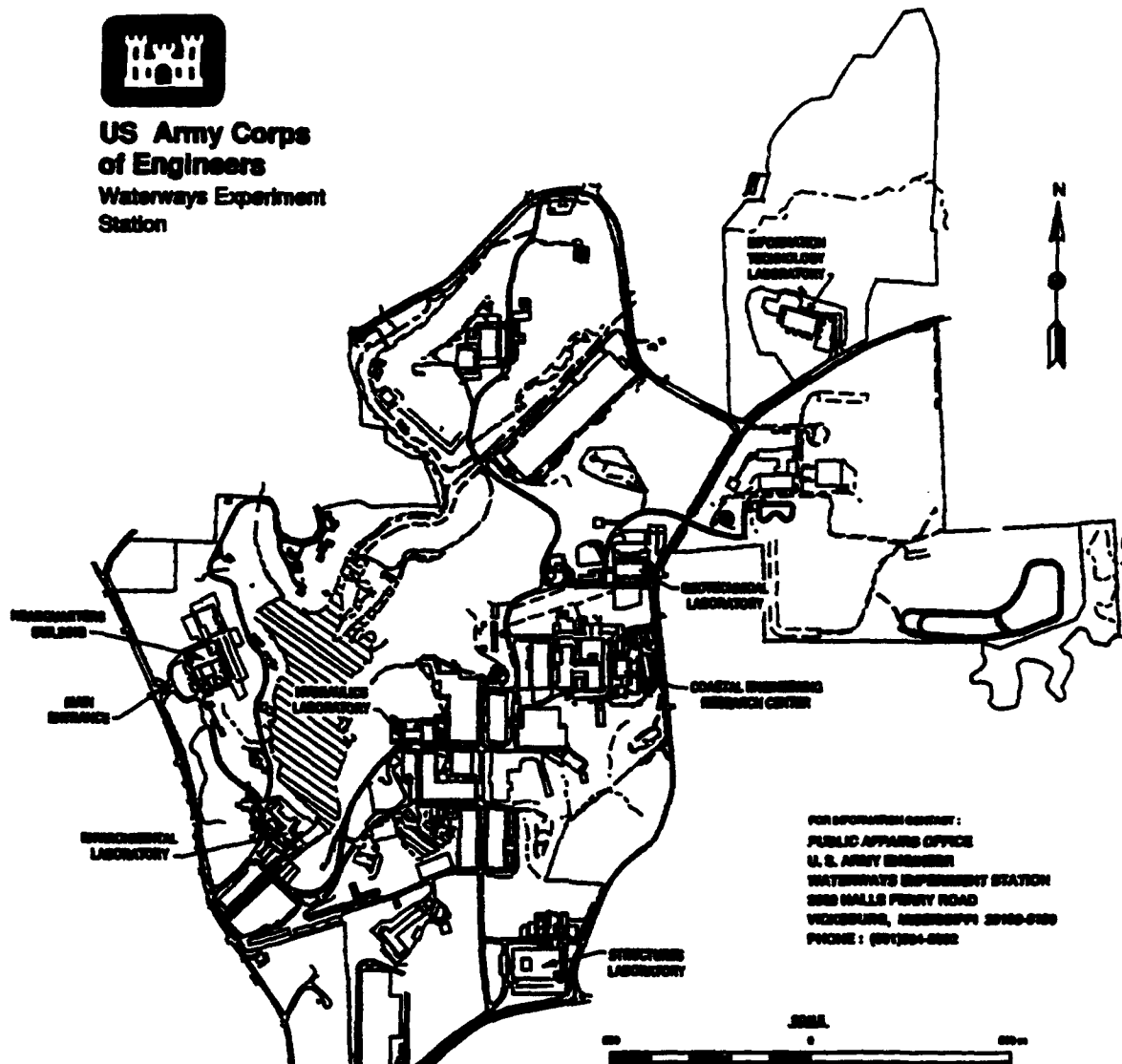
Edward F. Thompson
U.S. Army Corps of Engineers
Waterways Experiment Station
3909 Halls Ferry Road
Vicksburg, MS 39180-6199

Final report

Approved for public release; distribution is unlimited



**US Army Corps
of Engineers**
**Waterways Experiment
Station**



Waterways Experiment Station Cataloging-in-Publication Data

Upgrade of tropical cyclone surface wind field model / by Vincent J. Cardone ... [et al] ; prepared for U.S. Army Corps of Engineers.

101 p. : ill. ; 28 cm. -- (Miscellaneous paper ; CERC-94-14)

Includes bibliographic references.

1. Storm winds -- Mathematical models. 2. Hurricanes -- Mathematical models -- Data processing. 3. Windstorms -- Mathematical models -- Computer programs. 4. Cyclones -- Mathematical models. I. Cardone, Vince J. II. United States. Army. Corps of Engineers. III. U.S. Army Engineer Waterways Experiment Station. IV. Coastal Engineering Research Center (U.S.) V. Series: Miscellaneous paper (U.S. Army Engineer Waterways Experiment Station) ; CERC-94-14.

TA7 W34m no.CERC-94-14

Contents

| | |
|--|----|
| Preface | v |
| Conversion Factors, Non-SI to SI Units of Measurements | vi |
| 1—Introduction | 1 |
| Background | 1 |
| Previous Studies | 2 |
| Scope | 3 |
| 2—Existing Model Limitations | 4 |
| Physics | 4 |
| Initialization | 5 |
| Numerics | 7 |
| Summary of Limitations | 9 |
| 3—Upgraded Model | 10 |
| Increased Resolution | 10 |
| Generalized Pressure Specification | 12 |
| Pressure profile form | 12 |
| Modified outflow | 13 |
| Specification of pressure parameters | 15 |
| Sample Runs | 20 |
| 4—Summary | 25 |
| References | 26 |
| Appendix A: Comparison of Five-Nest and Seven-Nest Models for Hurricane Camille | A1 |
| Appendix B: Documentation of CE Model Upgrades | B1 |
| Appendix C: Sample Application of Upgraded CE Model to Simulation of 12 Snapshots of Hurricane Gilbert | C1 |
| Appendix D: Sample Application of Upgraded CE Model to Simulation of 36-Hr Period of Hurricane Gilbert in the Gulf of Mexico | D1 |
| SF 298 | |

List of Figures

| | | |
|-----------|---|----|
| Figure 1. | Temporal changes in the azimuthally averaged wind for NOAA reconnaissance flights into Hurricane Gilbert; changes are normalized to a 6-hr time interval (from Black and Willoughby (1992)) | 8 |
| Figure 2. | Distribution of maximum wind speed differences between 5-nest and 7-nest model runs for Hurricane Camille | 12 |
| Figure 3. | Example of Oceanweather tropical storm analysis | 17 |
| Figure 4. | Some parameters in double exponential profile | 21 |
| Figure 5. | Comparison of azimuthally averaged reconnaissance winds and fitted gradient winds in 12 cases of Hurricane Gilbert defined by Black and Willoughby (1992) | 24 |

List of Tables

| | | |
|----------|--|----|
| Table 1. | Effect of Nest Activation Parameter, INSIDE | 11 |
| Table 2. | Maximum Inflow Observed in Frictionless Stationary Vortex Solution | 14 |
| Table 3. | Empirical Correction of Inflow Angle | 15 |
| Table 4. | Parameter Definitions for Fitting Single Exponential Profile | 18 |
| Table 5. | Generalized Single Exponential Profile Fits to Selected Hurricane Gilbert Cases | 18 |
| Table 6. | Parameter Definitions for Fitting Double Exponential Profile | 20 |
| Table 7. | Observed Pressure and Azimuthally Averaged Pseudo-Gradient Wind Maxima in Hurricane Gilbert and Estimated Generalized Profile Parameters | 22 |
| Table 8. | Comparison of Measured Flight-Level Wind Maxima and Fitted Gradient Wind Maxima for Double Exponential Pressure Profile | 23 |

Preface

This report describes improvements developed for the planetary boundary layer surface wind field model traditionally used by the U.S. Army Corps of Engineers for hurricane modeling. Limitations of the model are also described. The upgraded model has increased flexibility for spatial resolution and pressure profile specification. The wind fields can be used in ocean response modeling, including wave and surge modeling activities.

This study was authorized by Headquarters, U.S. Army Corps of Engineers, under the Coastal Flooding and Storm Protection Area of the Coastal Research Program, Work Unit 32683, "Wind Estimation for Coastal Modeling." Technical Monitors were Messrs. John H. Lockhart, Jr.; John G. Housley; Barry W. Holliday; and John Saucier. Ms. Carolyn M. Holmes of the U.S. Army Engineer Waterways Experiment Station (WES), Coastal Engineering Research Center (CERC), was the Program Manager.

The study was conducted under Contract No. DACW39-93-C-0022 by Oceanweather, Inc. (OWI), Cos Cob, Connecticut. The report was prepared by Dr. Vincent J. Cardone and Messrs. Andrew T. Cox and J. Arthur Greenwood, all of OWI, and Dr. Edward F. Thompson of the Coastal Oceanography Branch (COB), Research Division (RD), CERC. Dr. Thompson was Principal Investigator of the research work unit funding this study. The work unit was under the direct supervision of Dr. Martin C. Miller, Chief, COB, and Mr. H. Lee Butler, Chief, RD, and under the general supervision of Mr. Charles C. Calhoun, Jr., Assistant Director, CERC, and Dr. James R. Houston, Director, CERC.

At the time of publication of this report, Director of WES was Dr. Robert W. Whalin. Commander was COL Bruce K. Howard, EN.

| | |
|---------------------|-------------------------------------|
| Accession For | |
| NTIS GRA&I | <input checked="" type="checkbox"/> |
| DTIC TAB | <input type="checkbox"/> |
| Unannounced | <input type="checkbox"/> |
| Justification | |
| By _____ | |
| Distribution/ _____ | |
| Availability Codes | |
| Distr | Avail and/or Special |
| A-1 | |

The contents of this report are not to be used for advertising, publication, or promotional purposes. Citation of trade names does not constitute an official endorsement or approval of the use of such commercial products.

Conversion Factors, Non-SI to SI Units of Measurement

Non-SI units of measurement used in this report can be converted to SI units as follows:

| Multiply | By | To Obtain |
|-----------------------|------------|-------------------|
| degrees (angle) | 0.01745329 | radians |
| knots (international) | 0.5144444 | meters per second |
| miles (U.S. nautical) | 1.852 | kilometers |

1 Introduction

Background

The unprecedented destruction of parts of the United States caused by hurricanes Andrew and Iniki last summer has aroused increased interest in the wind structure of tropical cyclones among the scientific and engineering communities. Unlike most past destructive storms, much of the loss in these recent storms was associated with direct wind damage. While simple parametric tropical cyclone wind models remain in use to model surface winds and to provide forcing for ocean response models, a few numerical vortex boundary layer models based upon solution of the primitive equations of motion have emerged, including most prominently the so-called U.S. Army Corps of Engineers (CE) wind model (Cardone et al. 1992). The model was developed originally at New York University in the early 1970's and later further developed at Oceanweather Inc. (OWI) under CE support in 1979. Recently the format of the CE model was modified to conform with the requirements of the CE Coastal Modeling System (Thompson 1993).

The CE numerical model was reviewed as part of a Workshop on Tropical Wind Modeling convened at the U.S. Army Engineer Waterways Experiment Station on 24-25 March, 1992. Invited participants in the review were:

- Dr. Wilson A. Schaffer, Techniques Development Laboratory, National Weather Service (NWS), National Oceanic and Atmospheric Administration (NOAA)
- Dr. Mark D. Powell, Hurricane Research Division (HRD), Atlantic Oceanographic and Meteorological Laboratory, Environmental Research Laboratories, NOAA
- Dr. Mukut B. Mathur, National Meteorological Center, NWS, NOAA
- Dr. Vincent J. Cardone, OWI

The workshop stressed the relationship between surface wind modeling and more general questions of the dynamical and thermodynamic nature of tropical cyclones. It also emphasized the need to carefully evaluate the reliability and representativeness of the scant surface marine wind data available in intense cyclones, before such data are used to further develop and validate numerical models.

The workshop addressed the potential for further development of existing numerical models, particularly the CE model. A number of specific research needs for improving wind models were identified and prioritized in terms of both importance to ocean response modeling and feasibility of success. These needs are summarized more fully in a "white paper" (Cardone and Thompson 1992).

Subsequent to the workshop, a study was initiated to address high priority upgrades to the CE model which could be accomplished with the limited funds available. The following tasks were chosen: (1) increase resolution and domain of the nested grid system; (2) generalize the surface pressure specification. The enhancements developed for the CE wind model are the subject of this report. The enhancements will be incorporated into the Coastal Modeling System in the near future.

Previous Studies

The CE wind model has been used mainly to provide wind fields in historical tropical cyclones to drive ocean response models operated in a hindcast mode (surface waves, mixed layer currents, storm surge). Those wind fields generally provide unbiased ocean predictions when used to drive CE and OWI ocean response models (e.g. Reece and Cardone 1982). They have also been used to drive ocean response models developed by other scientists independently, wherein CE model winds have also repeatedly been shown to provide unbiased hindcasts (e.g. Forristall 1980, WAMDI Group 1988, Cooper and Thompson 1989, Ly and O'Connor 1991, Grosskopf et al. 1991, Mairs et al. 1992). At OWI the model has been used in over three dozen studies to drive ocean response models to establish offshore design criteria in many parts of the world affected by tropical cyclones.

The CE model has been extensively used for both ocean wave and storm surge modeling for CE applications. Abel et al. (1989) applied the model to estimate wave statistics due to hurricanes in the Atlantic Ocean and Gulf of Mexico during 1956-75. Tracy and Hubertz (1990) estimated waves produced by 10 hurricanes impacting southern California during 1956-89. Mark and Scheffner (1993) describe a hurricane surge study for the coast of Delaware. A similar approach is presently being applied to the entire U.S. Atlantic Coast.

The generality of the CE model was also demonstrated when it was used to provide winds to test the third generation wave model (3GWAM) (WAMDI Group 1988). Winds supplied to the WAM model were exactly the same as winds for the subject storms (three intense Gulf of Mexico hurricanes) which had been used in previous studies to drive first and second generation models, and which had been used by other investigators. The WAM model was found to provide unbiased and skillful wave hindcasts in these storms, with WAM using its own calibration of source terms developed completely independently of CE winds. The same tuning on WAM has also been shown to provide

nearly perfect hindcasts in severe extratropical storms as well when driven by extremely accurate wind fields derived by direct kinematic analysis of wind measurements (Cardone et al. 1994).

Scope

In many of the studies cited above, ocean response models were used to evaluate the most extreme response (storm peak winds, waves, surge and currents) in a storm at a fixed site. In general, in storms in which the assumed storm pressure profile fits the actual radial distribution well, modeled storm peaks are unbiased in the mean and exhibit scatter index of 15 percent or less. The method is less successful in modeling the entire spatial and temporal distribution of the wind field in such storms. There are some storms in which even the storm peaks are difficult to simulate, where the storm structure departs from the simple structure implied by the presumed pressure distribution. This and other limitations of the CE model are described in more detail in Chapter 2.

In this study, two limitations of the CE tropical storm wind model are addressed and remedied. The first change is simply the addition of two additional nests to the grid system used to implement the numerical vortex model. This change provides lower truncation errors near the center of small intense storms, greater resolution near the vortex center, and an expanded solution domain. The second change is generalization of the radial surface pressure profile upon which the surface pressure initialization of the vortex model is based. The form adopted also allows the specification of profiles with two maxima in the radial pressure gradient. These changes are described in Chapter 3. A summary is given in Chapter 4.

2 Existing Model Limitations

The CE wind model developed by Cardone et al. (1992) has proved to be a powerful tool in ocean response modeling. However, the model, developed in 1979, includes a number of limitations. In light of enhanced computing power now available and the increasing field measurements and understanding of tropical storm behavior, it is timely to review the model limitations. Limitations of the CE model may be described in three basic categories: physics, initialization, and numerics.

Physics

The CE model evolved from the model of Chow (1971) who solved the momentum equations of an integrated boundary layer flow for a boundary layer of constant depth. The vertical friction force was taken parallel to the wind relative to the earth. Horizontal friction was also considered. The equations, however, were solved numerically on a nested cartesian grid system centered on the vortex and translating at constant velocity with the vortex. The steady solution in the moving coordinate system referred back to the earth yielded qualitatively realistic boundary layer wind patterns. The solution included supergradient flows inside the radius of maximum gradient wind and a decrease in the radius of maximum wind. It also included an asymmetric wind distribution with maxima in the right front quadrant for a typical superposition of a symmetric vortex and ambient gradient, and a boundary layer convergence pattern consistent with observed patterns of convection in typical storms.

Shapiro (1983) solved the same slab momentum equation as Chow (1971) but used a truncated spectral analysis in cylindrical coordinates, in order to allow a more convenient separation of the role of linear and non-linear asymmetric effects in the boundary layer flow. Chow's model and solution method provide the same patterns as that of Shapiro's model except that inside the radius of maximum wind truncation errors are larger than for the spectral solution. As a consequence, Chow's model may slightly overestimate the degree of supergradient flow inside the eye. These studies show that the essential physics governing the boundary layer flow are included in Chow's and Shapiro's models. The main physical processes missing are the feedback of

the convection (induced in part by the modelled convergence field) on the wind field, and strong non-steady effects (for example rapid deepening of the vortex in the moving frame) which may cause even the overlying vortex to be unbalanced.

The CE model is derived directly from Chow's formulation and uses Chow's numerical solution. Several improvements to Chow's solution were made to insure that it not only gives qualitatively realistic wind fields, but also provides a quantitatively correct surface stress vector distribution, from which the model diagnoses winds within the surface boundary layer as well. The main enhancements to Chow's model are in the inclusion of a similarity boundary layer formulation relating vertically integrated flow to the surface drag (magnitude and direction), adoption of more realistic boundary layer depths than considered by Chow or Shapiro, consideration of the effects of boundary layer stratification and variable surface roughness (expressed in terms of wind alone with no sea state effects considered), and incorporation of greater flexibility in the specification of the imposed pressure distribution of the vortex over the possibilities considered by Chow.

The CE model was developed with a secondary objective to provide winds over inland lake surfaces and land surfaces of arbitrary roughness. The theoretical development of this part of the model met with less success than the over-water treatment. A simplified equilibrium boundary layer approach was adopted which ignores the adjustment of the planetary boundary layer (PBL) wind field across discontinuities of roughness. Thus, while the model validation against winds measured over land indicated good agreement when the wind fetch was over a homogeneous roughness, little is known about the effect on ocean response modeling associated with failure in the CE model (probably) to resolve small scale PBL wind changes downwind of abrupt changes in roughness (e.g. the coast).

Initialization

The model is generally applied with boundary layer height in the range of 500 m - 650 m, slightly unstable stratification, a Charnock type surface roughness formulation (Charnock constant 0.035 with Karman constant 0.35), and a value of unity for the Ekman scale height parameter. This combination produces unbiased surface winds over the open sea when the model is applied to real storms and validated against measured surface wind time histories obtained by calibrated instruments (e.g. NOAA buoys, offshore rigs).

The pressure field is generally described as the superposition of the pressure gradient computed from the exponential pressure profile form for the symmetric part of the vortex:

$$p(r) = p_o + (p_\infty - p_o) e^{-\frac{r}{R_p}} \quad (1)$$

where

$p(r)$ = pressure

p_o = central pressure (at the eye)

p_∞ = axisymmetric ambient pressure (far field pressure)

R_p = scaling radius

r = radius

and an uniform ambient gradient given by

$$f \bar{k} \times \nabla_s = - \frac{1}{\rho} \nabla p_\infty \quad (2)$$

where

f = Coriolis parameter

\bar{k} = unit vector in the vertical direction

∇_s = ambient uniform geostrophic flow

ρ = mean air density

∇p_∞ = uniform ambient pressure gradient

This pressure initialization scheme (it is also a boundary condition since the model is solved to a steady state solution) often provides a very realistic simulation of the actual pressure field about a tropical cyclone. However, in some storms the actual pressure field departs from this simple picture in several possible ways. Often, particularly as a tropical cyclone enters the mid-latitudes, the ambient pressure field is inhomogeneous. The effect is especially evident if the tropical cyclone begins to interact with a frontal system or an extratropical cyclone or both. Within the tropics, some storms have been shown (Holland 1980) to follow the more general form:

$$p(r) = p_0 + (p_\infty - p_0) e^{-\left(\frac{r}{r_c}\right)^B} \quad (3)$$

where

B = constant in the general range 0.5-2.5

Finally, in some storms the radial pressure profile in the inner core is more irregular than either of the above forms, with a shape which implies two maxima in the radial pressure gradient, accompanied by two distinct maxima in the wind speed. Willoughby (1990) and Black and Willoughby (1992) have described the tendency for "concentric rings" in the radial wind distribution to be a fairly typical characteristic of intense tropical cyclones. The rings appear to be related intimately to storm intensity evolution. For example, Figure 1 shows the evolution of concentric rings in Hurricane Gilbert (1988) over a six-day period. In this storm, the CE model might be expected to provide reasonably accurate wind fields in the initial stage of vortex development and intensification between September 11-13, but it would fail to model the complicated double maxima structures later. The impact on ocean response modeling of this failure to model concentric rings is unknown.

Numerics

The CE model is computationally demanding. For example, computational considerations drove the decision to presolve the boundary layer model for spatially homogeneous (constant) boundary layer height and stability and to use a table look-up procedure for the drag coefficient during the marching of the solution toward steady state. To relax the constraint of constant boundary layer height and stability would greatly increase computer time, unless a more efficient integration scheme could be found. The minimum grid spacing on the inner nest of the solution grid (as opposed to the target grid) is 5 km, which is a bit too large to resolve details of the wind field near the center in very tight storms. (For example, as Hurricane Andrew approached the south Florida coast, the radius of maximum wind was only about 11 km.) The grid spacing is also not sufficient to resolve boundary layer adjustments near roughness discontinuities, though that physical process is not presently incorporated in the numerical model. Further, the grid spacing is too coarse to resolve detailed gradients of wind over inland bays and estuaries. Limitations in temporal resolution are less serious, within the constraint of the steady-state model, since the "time step" of the windfields is simply the temporal resolution of the storm track. That temporal resolution can be refined within reason (say to intervals of 15 minutes or so) without significant computational cost.

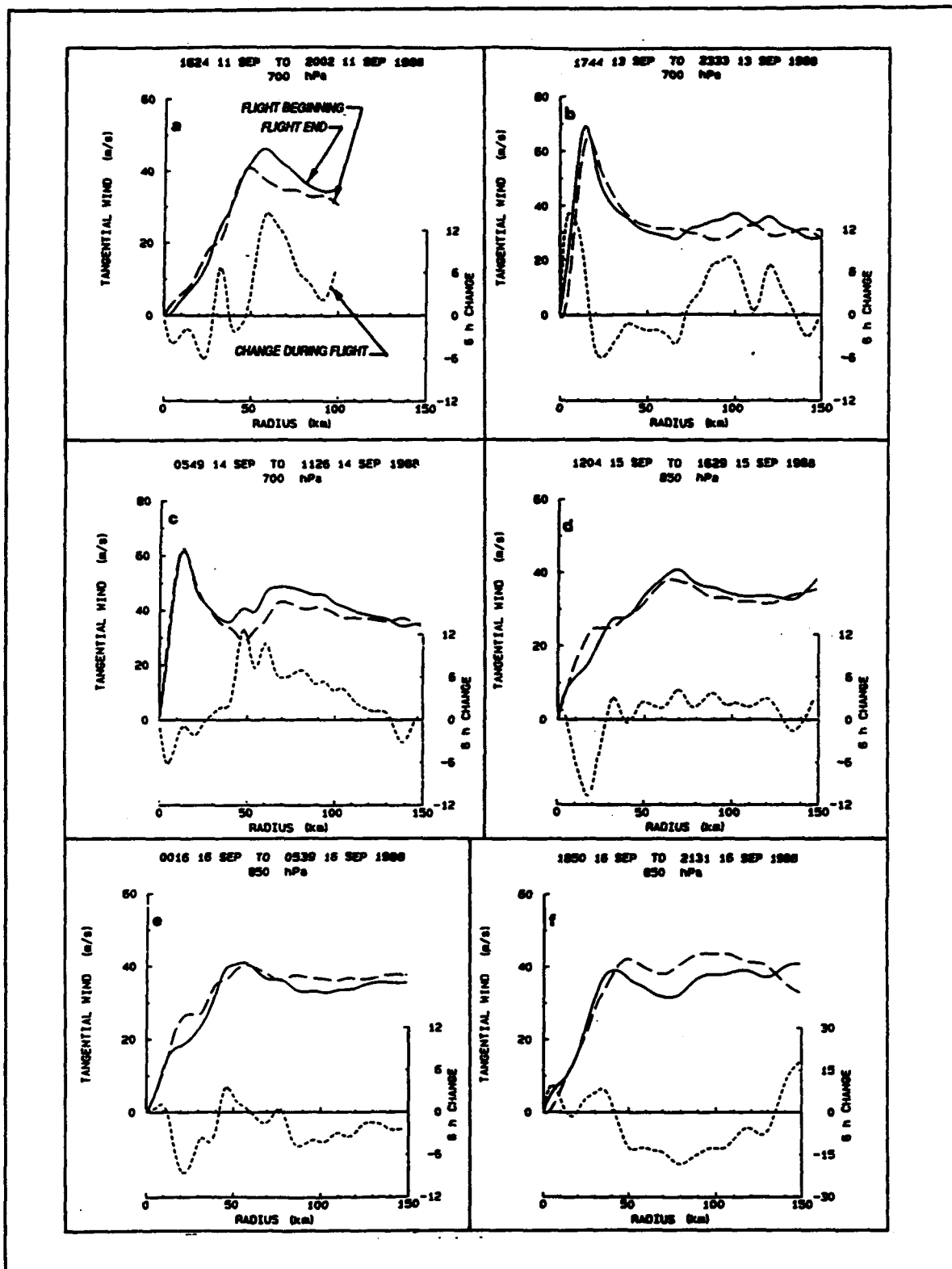


Figure 1. Temporal changes in the azimuthally averaged wind for NOAA reconnaissance flights into Hurricane Gilbert; changes are normalized to a 6-hr time interval (from Black and Willoughby (1992))

Summary of Limitations

The main model limitations described in each category above may be listed as follows:

a. Physics.

- (1) Decoupling of boundary layer from full vortex dynamics, precluding mutual adjustment of pressure and wind fields; and feedback of convective scale effects on wind field.
- (2) Simplified PBL theory (e.g. constant Ekman scale height).
- (3) Extrapolation of Charnock roughness to extreme wind speeds, with no sea state dependence.
- (4) No boundary layer adjustment across roughness discontinuity.

b. Initialization.

- (1) Constant and homogeneous boundary layer height.
- (2) Constant and homogeneous stratification.
- (3) Relatively simple pressure specification:
 - (a) Exponential pressure profile provides only one radius of maximum wind (no concentric rings).
 - (b) Pressure profile may be inadequate even for unimodal maximum gradient pressure distributions.
 - (c) Homogeneous ambient linear pressure gradient.

c. Numerics.

- (1) Practical limit of spatial resolution to 5 km may be inadequate for very tight storms.
- (2) Large number of iterations (800) required for each steady state configuration, or snapshot (using the terminology of Cardone et al. 1992).

In this study, two of the above limitations are addressed and remedied, as described in the next section.

3 Upgraded Model

Increased Resolution

The CE program consists basically of two main programs (Cardone et al. 1992). The first, SNAP, solves the numerical vortex model on a nested grid a number of times to represent the storm wind field at discrete times within an event, thereby producing a number of *snapshot* wind fields on a nested grid. SNAP also writes the snapshots to a file for use by the second main program HIST, which among other functions, interpolates the nested grid solutions to hourly intervals and then interpolates the winds to an output or *target* grid (typically that of an ocean response model).

The nested grid consists of five square 21 by 21 grid point arrays. The grid spacing increases by a factor of two from nest to nest. In the program input, the user specifies a desired spacing of the inner nest (the variable DX in name-list NAME3 of SNAP). For the default value of 5 km, the grid spacing in the coarsest nest becomes 80 km and the entire grid covers an area of (1,600 km²). While the existing CE program allows users to set DX smaller than 5 km, this is not recommended since the grid coverage shrinks commensurately. The simplified boundary condition applied on the outer boundary of the outermost nest becomes increasingly tenuous as the gridded domain shrinks.

The upgraded program allows the use of up to seven nests. However, the user may specify the number of nests (from three to seven) in a given run. The new parameter INSIDE is used to specify the number of active nests. It designates which is the finest active nest, where nests are numbered from 1 to 7 going from finest to coarsest. For example, INSIDE = 1 activates all seven nests, and INSIDE = 2 activates only nests 2 through 7. The grid spacing of nest 1, the innermost nest, is specified as before with variable DX, regardless of whether or not the nest is active. The relationships between INSIDE, active nests, and spacing of the finest active nest are summarized in Table 1. The default value of DX is 2 km. If all seven nests are exercised, the execution time per snapshot is roughly four times as long as the existing CE model. For this case the number of iterations on the inner nest is set to the default value of 3200.

Table 1
Effect of Nest Activation Parameter, INSIDE

| INSIDE | Active Nests | Spacing of Finest Active Nest |
|--------|--------------|-------------------------------|
| 1 | 1 - 7 | DX |
| 2 | 2 - 7 | 2 DX |
| 3 | 3 - 7 | 4 DX |
| 4 | 4 - 7 | 8 DX |
| 5 | 5 - 7 | 16 DX |

The program with the new nesting was tested in two ways using the Hurricane Camille snapshots as test cases. First, vortex model winds were produced by the CE model (and its OWI equivalent) for the case of $DX = 8 \text{ km}$. Then, the same SNAP inputs were used to generate winds with the new code for the case $DX = 2 \text{ km}$, $\text{INSIDE} = 3$, which provides the equivalent number of nests and inner nest grid spacing as the CE model run. Winds produced by the two alternative programs were interpolated to a target grid covering the Gulf of Mexico (nominal spacing of 0.2 deg^1), compared and found to agree to within roundoff error of the VAX computer used for these tests.

The second test compared winds for Camille produced by the new code for the case $DX = 2 \text{ km}$ and $\text{INSIDE} = 1$; that is, all seven nests are live with inner nest grid spacing of 2 km , with winds produced by the CE program with $DX = 5 \text{ km}$. These results are shown in Appendix A which gives, at 30-minute intervals, the maximum scalar wind speed, the location and the corresponding wind speeds and directions, and the same data for the maximum vector wind difference magnitude. The results (see also Figure 2) indicate that the largest differences (scalar differences of up to about 7 m/s), occur inside the eyewall, where truncation errors on the 5-km solution are expected to be large for an intense tight vortex such as Camille. Maximum scalar wind speed differences in the area of the eyewall are generally less than 1 m/sec . However, maximum vector difference magnitudes of up to 9 m/sec were observed occasionally in the vicinity of the eyewall reflecting a tendency for the wind direction on the 2-km solution to be turned systematically in the direction of less inflow, by up to 10 deg from the 5-km solution. The 2-km solutions are no doubt the more accurate solutions.

¹ A table of factors for converting non-SI units of measurement to SI units is presented on page vi.

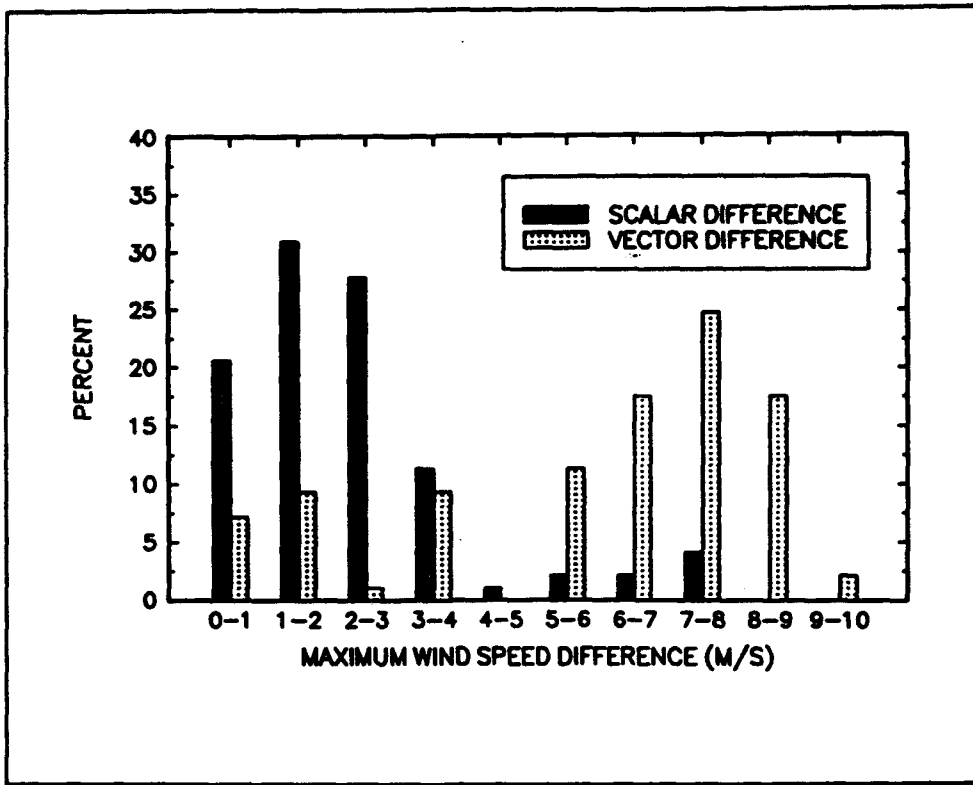


Figure 2. Distribution of maximum wind speed differences between 5-nest and 7-nest model runs for Hurricane Camille

Generalized Pressure Specification

Pressure profile form

The upgrade to the pressure specification uses a generalized form of Holland's (1980) exponential pressure profile

$$p(r) = p_o + \sum_{i=1}^n dp_i e^{-\left(\frac{R_p}{r}\right)^{n_i}} \quad (4)$$

where

n = number of components

dp_i = pressure anomaly for the i 'th component ($dp_1+dp_2+\dots+dp_n=p_o-p_e$)

R_{pi} = scaling radius for the i 'th component

B_i = Holland's B coefficient for the i 'th component

The corresponding tangential and radial pressure gradients are:

$$\frac{\partial p}{\partial \theta} = 0 \quad (\text{tangential}) \quad (5)$$

$$\frac{\partial p}{\partial r} = \sum_{i=1}^n B_i \frac{dp_i}{dr} \left(\frac{R_{pi}}{r} \right)^n \left(\frac{1}{r} \right) e^{-\left(\frac{R_{pi}}{r}\right)^n} \quad (\text{radial})$$

The CE model was modified to provide options for a single or double exponential component ($n = 1$ or $n = 2$). This form allows the specification of pressure profiles with two separate maxima in the radial pressure gradient, though the mere form does not guarantee two maxima. For example, the sum of two exponentials also allows the modeling of pressure profiles which have only one maximum but with shapes very different from those predicted by the single exponential even with the variable B included.

Incorporation of this model into the seven-nest version of the program led to extensive changes to program SNAP, in particular to Subroutines GRAD and PXYM and further changes to namelist NAME3, as documented in Appendix B. One immediate consequence of this model is that the quadrantal specification of profile parameters allowed in the single exponential form with $B = 1$ is lost. To retain this option in the CE model portfolio, two versions of the upgraded program were developed as follows:

SNAP_ADC.7NE and HIST_ADC.7NE - This version only upgrades the current CE program (which includes quadrantal variation of parameters for a single exponential with $B = 1$) to incorporate the additional nests.

SNAP_HOL.7NE - This version upgrades the current CE model to allow both 7 nests and the generalized pressure specification scheme, but without quadrantal variation. Note, however, that asymmetry in the pressure field is still modeled through superposition of the vortex pressure field and the background steering gradient. The background pressure gradient is required to be homogeneous (that is, the parameter ST12 is eliminated).

Modified outflow

In early tests of the upgraded CE program with hypothetical snapshot inputs estimated roughly to apply to several stages of Hurricane Gilbert (inputs for

Gilbert snapshots were derived more rigorously as described below), it was demonstrated that the program could produce the pattern of annular concentric wind maxima. However, it was noticed that the inflow characteristics of the model appeared to have changed somewhat from the unimodal mode!. In the standard CE model, Subroutine OUTFLOW serves to remove 8 degrees of inflow from the snapshot solution throughout the domain to compensate approximately for inflow believed to be spuriously introduced through the numerical solution. This spurious inflow is revealed by solving the model for a motionless vortex with all friction terms deactivated and comparing the modeled wind direction to the purely circular flow expected of a vortex in gradient balance.

The frictionless, motionless vortex test was repeated with the upgraded model for the series of nine snapshots indicated in Table 2. For the unimodal case (Case 1) and the bimodal cases with $B = 1$ for both exponentials (cases 2 and 6), the maximum inflow (which tends to occur just outside the wind maxima) averages 7.5 deg. As the value of B increases, however, there is a proportional increase in the inflow. In the bimodal profile with B varying between the two exponentials, the inflow varies with radius. Subroutine OUTFLOW was modified to compensate for dependence of spurious inflow on B (Table 3).

Table 2
Maximum Inflow Observed in Frictionless Stationary Vortex Solution¹

| Case | p_0 mb | R_{in} mm | R_{ex} mm | Δp_1 mb | Δp_2 mb | B_1 | B_2 | (Max inflow) ₁ deg | (Max inflow) ₂ deg |
|------|-------------|----------------|----------------|--------------------|--------------------|-------|-------|-------------------------------------|-------------------------------------|
| 1 | 970 | 27 | 0 | 40 | 0 | 1.00 | 0.00 | 7.2 | — |
| 2 | 915 | 8 | 58 | 68 | 27 | 1.00 | 1.00 | 7.3 | 7.3 |
| 3 | 915 | 8 | 58 | 68 | 27 | 1.00 | 2.00 | 6.6 | 13.1 |
| 4 | 915 | 8 | 58 | 68 | 27 | 2.52 | 1.00 | 18.7 | 6.6 |
| 5 | 915 | 8 | 58 | 68 | 27 | 2.52 | 2.00 | 28.8 | 16.5 |
| 6 | 890 | 6 | 42 | 53 | 67 | 1.00 | 1.00 | 8.0 | 7.7 |
| 7 | 890 | 6 | 42 | 53 | 67 | 1.00 | 1.26 | 8.1 | 9.1 |
| 8 | 890 | 6 | 42 | 53 | 67 | 2.52 | 1.00 | 12.7 | 7.5 |
| 9 | 890 | 6 | 42 | 53 | 67 | 2.52 | 1.26 | 15.1 | 9.0 |

¹ All runs were done with the upgraded CE model with 7 nests and generalized pressure specification; $p_0 = 1010$ mb for all runs

Table 3
Empirical Correction of Inflow Angle

| Exponential | Reduction Applied To Inflow Angle deg |
|---------------------|--|
| Unimodal $B = 1$ | 8 |
| Unimodal $B \neq 1$ | 8.8 |
| Bimodal | $8 \left(\frac{B_1 + B_2}{2} \right)$ |

Specification of pressure parameters

Single Exponential Profile: $B = 1$. In the standard CE model, the pressure profile may be specified in basically two ways. The most fundamental way is to fit the profile to sea level pressure measurements available at different radii at a given time, or transformed from time to space using single station data acquired at a station in the path of the storm. There are several examples of this approach as applied to historical U.S. Gulf of Mexico and East Coast hurricanes in Graham and Hudson (1960). The eye pressure may be prescribed, if it is known, for a more accurate fit, or the eye pressure may be extrapolated from a fit determined exclusively from data outside the center. A simplification to this procedure is often followed for oceanic storms, for which eye pressure may be known from aircraft dropsonde data, far field pressure is estimated from weather maps, and a few estimates of pressure at various radii about the storm are known from ship or island station synoptic reports. Then, the unknown parameter scale radius may be estimated from Equation 1 as follows for each such report and an average or weighted average of the estimates taken to represent the storm profile at map time:

$$R_p = -r \ln \left(\frac{p(r) - p_o}{p_m - p_o} \right) \quad (6)$$

If there are insufficient pressure data but eye pressure is known and an estimate of the radius of maximum wind, R_m , is known (e.g. from aircraft vortex message reports filed upon penetration of the eye and assuming that R_m at flight level is the same as R_m at the surface, or more crudely from radar or satellite eye diameter estimates), R_p may be estimated directly from R_m using the average relationship found between these two variables by the vortex model.

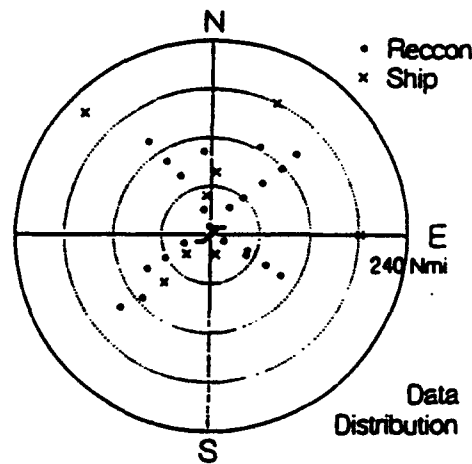
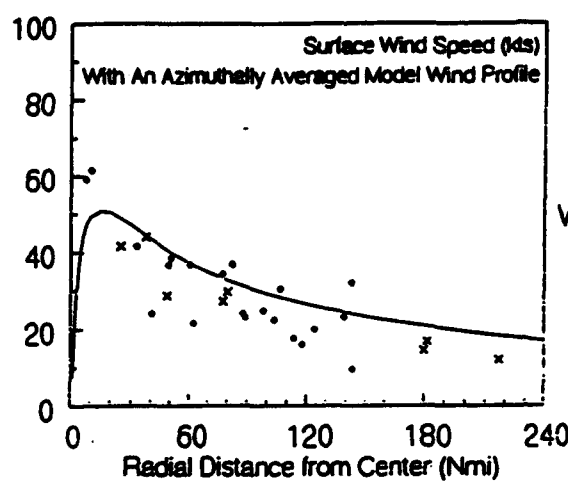
Single Exponential Profile: Variable B . Variants of these same two approaches may be followed to estimate the parameters of the generalized unimodal model, for which the additional parameter B must also be specified. Again, if there are sufficient pressure data, the profile may be fitted directly. For example, Figure 3 shows the screen display of a PC-based interactive system developed at OWI using a commercially available plotting/statistical analysis software package. The pressure data are composited (see window in upper right hand corner of screen) as a function of radius in a South China Sea typhoon from reduced (from flight level) aircraft pressures and pressures reported by ships within a 3-hr time window of analysis time. The aircraft also provided estimates of eye pressure (note the two conflicting estimates at the origin in the lower window of Figure 3). Far field pressure was estimated from weather maps. The best fit shown is for $p_e = 968$ mb, $B = 0.8$, and $R_s = (14 \text{ nm})^{0.8}$. The window at the upper left of the screen compares the azimuthally averaged solution for the model surface wind (downloaded from a run made on a VAX) and reduced aircraft and ship reports of wind.

The second approach is more indirect and emphasizes the use of aircraft wind data. In recent years such data have become quite accurate after the introduction of inertial navigation systems, onboard processing and the availability of coded messages (so-called supplementary or peripheral flight level winds) containing measured winds at flight level outside the eye. Figure 1 shows the complete analysis carried out by Black and Willoughby (1992) of flight data acquired over the main lifetime of Hurricane Gilbert in the Caribbean Sea and Gulf of Mexico. These curves show 12 separate radial profiles of the azimuthally averaged flight level (700 mb or 850 mb) tangential wind speed composited from flight legs near the indicated times. Most of the wind profiles exhibit two distinct wind maxima. On the assumption that the azimuthally averaged flow is approximately in gradient balance with the axisymmetric pressure field, the pressure profile associated with double concentric wind maxima should also exhibit two local maxima in the pressure gradient. Therefore they might be fitted by a double exponential profile. Even those profiles which do not exhibit two distinct peaks, such as those in panels *b*, *d*, and *e*, exhibit atypical shapes for tropical cyclones, with a single maximum and broad regions with little or no change of wind speed with radius. Nevertheless, we have selected five of these cases to illustrate the fitting of the single exponential profile using aircraft wind data and eye pressure. Parameters are defined in Table 4 and results from the fitting process are given in Table 5.

The fitting method is basically a systematic search of many possible solutions of the single exponential for that solution whose radial distribution of implied gradient wind provides a close match to the location and magnitude of the azimuthal average flight level wind. This searching program (implemented in a preprocessing program called 1EYEWALL.nJL) requires the input information listed in Table 5. Additional documentation is given in Appendix B. The searching program fixes the profile anomaly parameter ($p_e - p_o$), loops through possible values of the scale radius R_s (from R_m to $2R_m$) and B (from 0.5 to 2.52) and finds the pressure profile whose gradient wind simultaneously

Oceanweather Tropical System Analysis
 Surface Winds and Pressures Estimated from
 Recon, Vortex and Periperal Data Messages

Typhoon WAYNE86
 86090212 +/- 3hrs



Created on Aug 16, 1993 3:52:20 pm

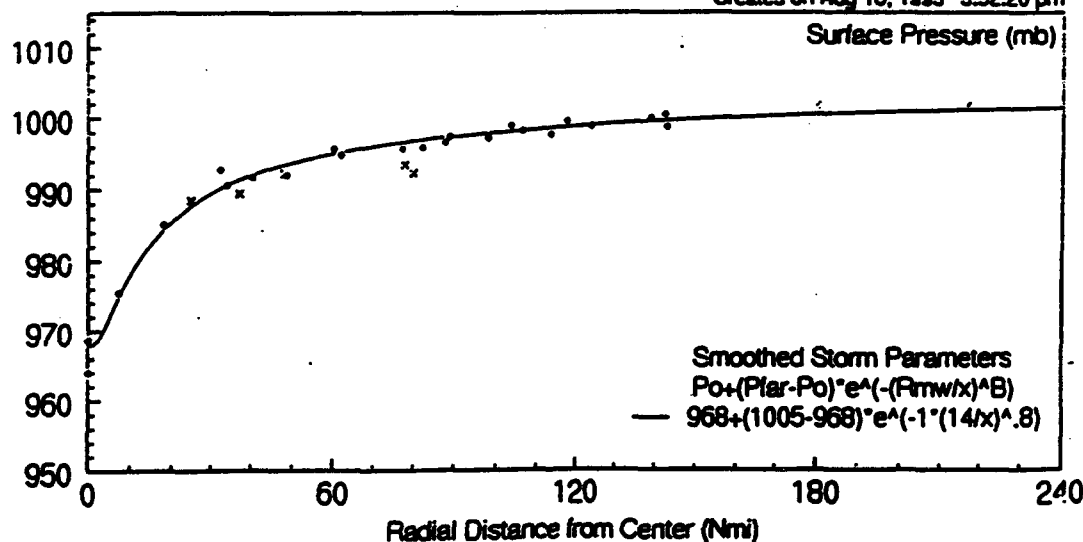


Figure 3. Example of Oceanweather tropical storm analysis

Table 4
Parameter Definitions for Fitting Single Exponential Profile

| Parameter | Definition |
|------------|---|
| R_m | Observed radius of maximum wind |
| V_m | Azimuthally averaged tangential flight level wind at R_m |
| V_{m150} | Azimuthally averaged tangential flight level wind at 150 km from center |
| r_p | Scale radius of single exponential profile |
| dp | Storm pressure anomaly parameter of single exponential profile |
| B | Holland's B |
| R_{pm} | Radius of maximum gradient of fitted pressure profile |
| V_{pm} | Maximum gradient wind of fitted pressure profile |
| V_{p150} | Gradient wind of fitted profile 150 km from center |

Table 5
Generalized Single Exponential Profile Fits to Selected Hurricane Gilbert Cases

| Case | Input | | | | | | Output | | | | | |
|------|-------------|--------------------|-------------|--------------|-------------------|-------------|------------|------|-----------------|----------------|-------------------|--|
| | P_o mb | P_{∞} mb | R_m km | V_m m/s | V_{m150} m/s | r_p km | dp mb | B | V_{pm} m/s | R_{pm} km | V_{p150} m/s | |
| 3 | 905 | 1012 | 16 | 65 | 30 | 20 | 107 | 1.50 | 67.2 | 20 | 21 | |
| 4 | 888 | 1012 | 13 | 69 | 30 | 16 | 124 | 1.41 | 70.3 | 16 | 20 | |
| 7 | 951 | 1012 | 65 | 38 | 36 | 97 | 61 | 1.00 | 39.3 | 87 | 36 | |
| 8 | 950 | 1012 | 69 | 41 | 38 | 92 | 62 | 1.12 | 42.2 | 85 | 38 | |
| 9 | 949 | 1010 | 57 | 40 | 37 | 85 | 61 | 1.12 | 41.9 | 79 | 37 | |

best matches the observed wind speeds at R_m and at 150 km in terms of absolute difference. For example, in Case 3 of Table 5 the selected profile gradient wind (not shown) is within 1 m/s of the V_m of 65 m/s at R_m . However the searching program places the absolute profile maximum of 67.2 m/s at a radius of 20 km, and fails to maintain the observed broad region of little change in wind speed between 50 and 150 km, resulting in a profile wind speed of only 21 m/s at 150 km, about 10 m/s lower than measured. Cases 7, 8 and 9 are somewhat more successful. The parameter B varies between 1.0 and 1.5 for these fits, or in the same general range reported by Holland for a single exponential.

Double Exponential Profile. While it is conceivable that there may be sufficiently voluminous and accurate pressure data in some tropical cyclones to

attempt to directly fit a double exponential profile to measurements of surface pressure as a function of radius, we have not attempted to construct such a data set and perform such a fit. We did try, without success, to develop useful fits to the profile from just the total storm anomaly, estimates of the two radii of maximum wind and a single pressure along the profile in the region between the two maxima. However, a generalization of the searching algorithm described above for a single exponential has met with some success.

The searching algorithm (called 2EYEWALL.HOL) as applied to a double exponential is documented in Appendix B. Parameters involved are defined in Table 6 and Figure 4. The searching program fixes the total storm anomaly, assumes the scale radius for the inner exponential is equal to the observed radius of maximum wind of the inner maximum, or ring, and loops through ranges of the outer scale radius, R_{p2} (from R_{m2} to $2R_{m2}$), inner and outer B (from 0.5 to 2.52) and the ratio of dp_1/dp_2 (from 1/8 to 8). The algorithm seeks the combination whose pressure profile provides a gradient wind profile that has maxima at R_{m1} and R_{m2} within ± 1 m/s of observed and which maximizes the following:

$$V_{g1} + V_{g2} - 2 V_{gm} \quad (7)$$

where

$$V_{gm} = \text{gradient wind at } (R_{m1} + R_{m2})/2$$

If it succeeds in finding such a profile it checks that the wind at 150 km is lower than the outer maximum, V_{m2} , and if it is, prints the solution. If these conditions are not met, another cycle is attempted. The matching criterion is relaxed to ± 2 m/s, this time requiring that the wind at $(R_{m1} + R_{m2})/2$ is less than the winds prescribed at R_{m1} and R_{m2} , and minimizing the wind at 150 km. The program also prints the profile parameters for the selected profile. If, after the second cycle the program still does not find a successful fit, it prints the closest fit found in each cycle.

Table 7 shows the results of the application of this searching algorithm to all 12 of the azimuthal average tangential flight level wind profiles in Hurricane Gilbert derived by Black and Willoughby (1992). The double exponential appears to require large values of B to resolve two distinct peaks in the radial profile of gradient wind, at least for most of these cases. Table 8 compares the location and magnitude of the double wind maxima derived from the fitted profile to those observed. Figure 5 compares the fitted and observed radial profiles of pseudo-gradient wind. The inner ring is usually fitted very closely. In 11 out of 12 of the cases a distinct outer wind maximum is resolved, and it is usually placed within ± 20 km of the observed maximum. In 9 out of those 11 cases, the maximum is within about ± 2 m/s of that observed. Case 8 is the poorest fit, but in practice Case 7 and Case 8 are so close in time

Table 6
Parameter Definitions for Fitting Double Exponential Profile

| Parameter | Definition |
|-----------|---|
| R_{m1} | Radius of maximum wind, inner ring |
| R_{m2} | Radius of maximum wind, outer ring |
| V_{m1} | Azimuthally averaged tangential flight level wind, inner ring |
| V_{m2} | Azimuthally averaged tangential flight level wind, outer ring |
| R_{p1} | Scale radius, inner exponential |
| R_{p2} | Scale radius, outer exponential |
| dp_1 | Pressure anomaly, inner exponential |
| dp_2 | Pressure anomaly, outer exponential |
| B_1 | Holland's B , inner exponential |
| B_2 | Holland's B , outer exponential |
| R_g1 | Radius of maximum gradient wind of fitted profile, inner ring |
| R_g2 | Radius of maximum gradient wind of fitted profile, outer ring |
| V_{g1} | Maximum gradient wind of fitted profile, inner ring |
| V_{g2} | Maximum gradient wind of fitted profile, outer ring |

(in fact they are derived from the same flight) that Case 7 may be used to represent this phase of the storm history.

Sample Runs

The upgraded program, including seven nests and the generalized pressure specification, has been applied to provide sample wind fields on target grids using as test input the snapshots developed for Hurricane Gilbert. Two runs were made. The first generates a snapshot wind field for each of the 12 Gilbert cases (including realistic forward motion and steering flow parameters) and interpolates each snapshot to a polar grid using a test history table. Interpolations are also made from pairs of adjacent snapshots (equal time weight). Winds for the 23 wind fields so produced on the polar grid are then azimuthally averaged. These results are given in Appendix C.

A second test run was made which modeled Gilbert during its passage across the Gulf of Mexico between 1200 UT 15 September through 0000 UT 17 September, 1988. Snapshots for this run consisted of Cases 7, 9, 11, and 12. The target grid for this run was a grid of nominal 12 nm spacing covering the Gulf of Mexico. The wind fields were output at 12-hourly intervals. Additional details and surface wind field plots are given in Appendix D.

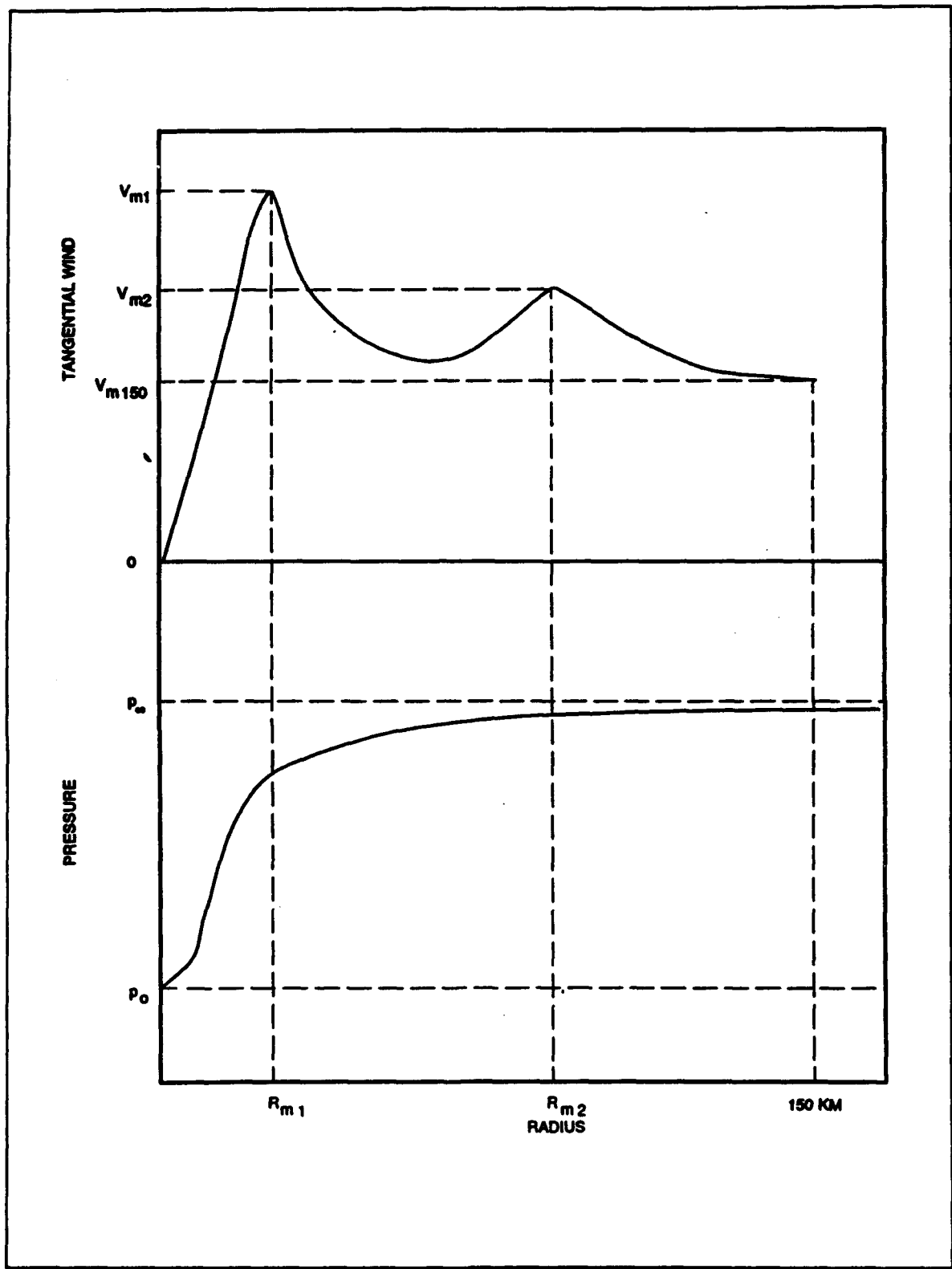


Figure 4. Some parameters in double exponential profile

Table 7
**Observed Pressure and Azimuthally Averaged Pseudo-Gradient Wind Maxima
In Hurricane Gilbert¹ and Estimated Generalized Profile Parameters**

| Case | Date/ Time (UTC) | Input | | | | | | | Output | | | | | |
|------|------------------------|-------------|-------------|----------------|----------------|-----------------|-----------------|----------------|----------------|--------------|--------------|-------|-------|--|
| | | p_o mb | p_e mb | R_{m1} km | R_{m2} km | V_{m1} m/s | V_{m2} m/s | R_{p1} km | R_{pe} km | dp_1 mb | dp_2 mb | B_1 | B_2 | |
| 1 | 11/1624 | 972 | 1011 | 47 | 90 | 40 | 35 | 47 | 127 | 23 | 16 | 2.52 | 2.52 | |
| 2 | 11/2002 | 968 | 1011 | 58 | 108 | 47 | 36 | 58 | 162 | 32 | 11 | 2.52 | 2.52 | |
| 3 | 13/1744 | 905 | 1012 | 16 | 111 | 65 | 32 | 16 | 125 | 94 | 13 | 1.68 | 2.39 | |
| 4 | 13/2333 | 888 | 1012 | 13 | 100 | 69 | 38 | 13 | 100 | 110 | 14 | 1.59 | 2.52 | |
| 5 | 14/0549 | 893 | 1012 | 13 | 70 | 62 | 44 | 13 | 70 | 101 | 18 | 1.41 | 2.52 | |
| 6 | 14/1126 | 890 | 1012 | 13 | 69 | 62 | 48 | 13 | 69 | 102 | 20 | 1.41 | 2.52 | |
| 7 | 15/1204 | 951 | 1012 | 22 | 65 | 25 | 38 | 22 | 87 | 45 | 16 | 0.56 | 2.52 | |
| 8 | 15/1629 | 950 | 1012 | 32 | 69 | 28 | 41 | 32 | 103 | 35 | 27 | 0.94 | 2.51 | |
| 9 | 16/0016 | 949 | 1010 | 22 | 57 | 27 | 40 | 22 | 81 | 41 | 20 | 0.75 | 2.52 | |
| 10 | 16/0539 | 950 | 1011 | 55 | 120 | 41 | 37 | 55 | 170 | 52 | 9 | 1.12 | 2.24 | |
| 11 | 16/1850 | 953 | 1010 | 50 | 100 | 42 | 43 | 50 | 119 | 47 | 10 | 1.33 | 2.52 | |
| 12 | 16/2131 | 954 | 1009 | 40 | 100 | 39 | 40 | 40 | 112 | 45 | 10 | 1.19 | 2.52 | |

¹ Cases correspond to Black and Willoughby's (1992) analysis of aircraft data in Hurricane Gilbert

Table 8
**Comparison of Measured Flight-Level Wind Maxima and Fitted
 Gradient Wind Maxima for Double Exponential Pressure Profile¹**

| Case | Inner Ring | | | | Outer Ring | | | | |
|------|----------------|-----------------|----------------|-----------------|----------------|-----------------|------------------|-------------------|--------------------------|
| | Measured | | Fitted | | Measured | | Fitted | | |
| | R_{m1} km | V_{m1} m/s | R_{g1} km | V_{g1} m/s | R_{m2} km | V_{m2} m/s | R_{g2} km | V_{g2} m/s | V_g at R_{m2} m/s |
| 1 | 47 | 40 | 47 | 39.6 | 90 | 35 | 110 | 37.1 | 35.7 |
| 2 | 58 | 47 | 58 | 46.6 | 108 | 36 | 108 ² | 35.7 ² | — |
| 3 | 16 | 65 | 16 | 66.7 | 111 | 32 | 105 | 33.7 | 33.6 |
| 4 | 13 | 69 | 13 | 70.3 | 100 | 38 | 85 | 37.2 | 36.3 |
| 5 | 13 | 62 | 13 | 63.5 | 70 | 44 | 59 | 46.2 | 45.4 |
| 6 | 13 | 62 | 13 | 63.7 | 69 | 48 | 59 | 48.4 | 47.3 |
| 7 | 22 | 25 | 22 | 26.3 | 65 | 38 | 82 | 39.2 | 36.1 |
| 8 | 32 | 28 | 30 | 29.7 | 69 | 41 | 98 | 48.1 | 39.2 |
| 9 | 22 | 27 | 21 | 28.9 | 57 | 40 | 78 | 43.4 | 38.1 |
| 10 | 55 | 41 | 55 | 39.2 | 120 | 37 | 120 | 37.1 | — |
| 11 | 50 | 42 | 50 | 40.7 | 100 | 43 | 93 | 41.5 | 41.3 |
| 12 | 40 | 39 | 40 | 32.9 | 100 | 40 | 92 | 38.4 | 38.2 |

¹ Cases correspond to Black and Willoughby's (1992) analysis of Hurricane Gilbert

² Second ring maximum not resolved, profile gradually decays from inner maximum

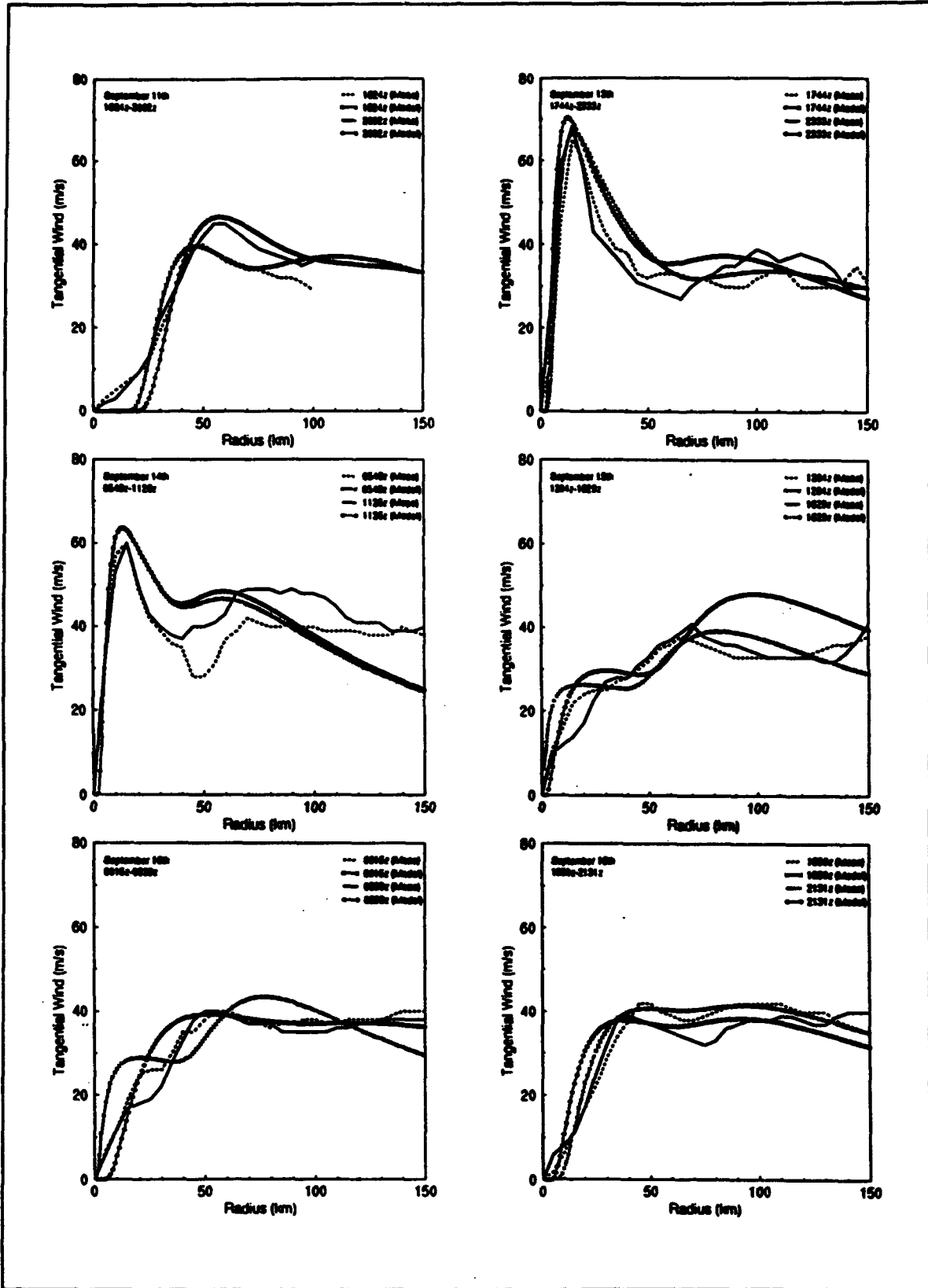


Figure 5. Comparison of azimuthally averaged reconnaissance winds and fitted gradient winds in 12 cases of Hurricane Gilbert defined by Black and Willoughby (1992)

4 Summary

The CE tropical cyclone surface wind field model has been a very useful tool in ocean response modeling for more than a decade. The model continues to be used regularly. The CE recently held a workshop to reassess model assumptions, particularly in light of modern advances in computing technology and field measurement of hurricane structure. Model limitations were identified and evaluated in terms of their perceived importance to ocean response modeling and the level of effort required to develop improved solutions. The limitations are summarized in this report.

Two aspects of the CE model were targeted for improvement. This report describes the improvements developed for the upgraded model. First, the standard CE model represents a compromise between spatial resolution in the central region of very high gradients, coverage of the full ocean area affected by the tropical cyclone, and computer requirements. Computing resources are much more available now than at the time the model was developed in the late 1970's. The model was upgraded to include more computationally intensive options which give improved resolution and areal coverage. Up to seven nested grids are now available, compared to only five nests in the standard model. In a typical application, this upgrade can be used to achieve 2-km resolution around the eye (as compared to 5-km resolution often used in the standard model) and an expanded total coverage area.

The second upgrade to the standard CE model allows a more general specification of the axisymmetric pressure profile. This upgrade can be used to create wind fields with maxima at two different radii or with a broad maximum extending over a range of radii. It also provides more flexibility in fitting the shape of single peaked wind profiles.

The upgraded model is demonstrated with historical hurricanes. The five-nest and seven-nest models are applied to Hurricane Camille. The fully upgraded model, with seven nests and general pressure specification, is applied to Hurricane Gilbert. This hurricane was chosen because it is well-documented by Black and Willoughby (1992) and it evolved into some non-traditional storm structures. The upgraded model was more effective than the standard CE model in simulating the storm.

References

- Abel, C. E., Tracy, B. A., Vincent, C. L., and Jensen, R. E. (1989). "Hurricane hindcast methodology and wave statistics for Atlantic and Gulf hurricanes from 1956-1975," WIS Report 19, U.S. Army Engineer Waterways Experiment Station, Vicksburg, MS.
- Black, M. L., and Willoughby, H. E. (1992). "The concentric eyewall cycle of Hurricane Gilbert," *Mon. Weather Rev.*, American Meteorological Society, 120, 947-957.
- Cardone, V. J., and Thompson, E. F. (1992). "Numerical modeling of tropical cyclone boundary layer winds: status, limitations and priorities," unpublished report prepared for U.S. Army Engineer Waterways Experiment Station, Vicksburg, MS.
- Cardone, V. J., Graber, H. C., Jensen, R. E., Hasselmann, S., and Caruso, M. J. (1994). "In search of the true surface wind field in SWADE IOP-1: ocean wave modelling perspective," to be submitted to *Atmosphere-Ocean System Journal*.
- Cardone, V. J., Greenwood, C. V., and Greenwood, J. A. (1992). "Unified program for the specification of hurricane boundary layer winds over surfaces of specified roughness," Contract Report CERC-92-1, U.S. Army Engineer Waterways Experiment Station, Vicksburg, MS.
- Chow, S. H. (1971). "A study of the wind field in the planetary boundary layer of a moving tropical cyclone," M. S. thesis in Meteorology, School of Engineering and Science, New York University, New York, N.Y.
- Cooper, C., and Thompson, J. D. (1989). "Hurricane-generated currents on the outer continental shelf, 1, model formulation and verification," *J. Geophys. Res.* 94(C9), 12513-12540.
- Forristall, G. Z. (1980). "A two-layer model for hurricane driven currents on an irregular grid," *J. Phys. Oceanogr.* 10(9), 1417-1438.

- Graham, H. E., and Hudson, G. N. (1960). "Surface winds near the center of hurricanes and other cyclones," National Hurricane Research Project Report No. 39, Wash., DC.
- Grosskopf, W. D., Griffon, D. L., Berek, E. P., and Sharma, J. N. (1991). "Gulf of Mexico wind, wave, and current database," *Proc., Offshore Tech. Conf.* OTC 6539, Houston, TX, 1, 357-364.
- Holland, G. J. (1980). "An analytic model of the wind and pressure profiles in hurricanes," *Mon. Weather Rev.* 108, 1212-1218.
- Ly, L. N., and O'Connor, W. P. (1991). "Gulf coast hurricane surge simulations using a numerical ocean circulation model," *Proc., MTS '91 Conf.*, Marine Technology Society, New Orleans, LA.
- Mairs, H. L., Koch, S. P., Gordon, R. B., and Cuellar, R., Jr. (1992). "The storm current response of Gulf of Mexico hurricanes," *Proc., Offshore Tech. Conf.* OTC 6833, Houston, TX, 235-242.
- Mark, D. J., and Scheffner, N. W. (1993). "Validation of a continental-scale storm surge model for the coast of Delaware," *Proc. Estuarine and Coastal Modeling Conference*, ASCE, Chicago, IL, 249-263.
- Reece, A. M., and Cardone, V. J. (1982). "Test of wave hindcast model results against measurements during four different meteorological systems," *Proc., Offshore Tech. Conf.* OTC 4323, Houston, TX, 269-293.
- Shapiro, L. J. (1983). "The asymmetric boundary layer flow under a translating hurricane," *J. Atmospheric Sci.* 39(Feb.).
- Thompson, E. F. (1993). "HURWIN: Tropical Storm Planetary Boundary Layer Wind Model," *Coastal Modeling System (CMS) User's Manual*, Instruction Report CERC-91-1, Supplement 2, M. A. Cialone, ed., U.S. Army Engineer Waterways Experiment Station, Vicksburg, MS.
- Tracy, B. A., and Hubertz, J. M. (1990). "Hindcast hurricane swell for the coast of southern California," WIS Report 21, U.S. Army Engineer Waterways Experiment Station, Vicksburg, MS.
- WAMDI Group. (1988). "The WAM model - a third generation ocean wave prediction model," *J. Phys. Oceanog.* 18, 1275-1810.
- Willoughby, H. E. (1990). "Temporal changes of the primary circulation in tropical cyclones," *J. Atmospheric Sci.* (47), 242-264.

Appendix A

Comparison of Five-Nest and Seven-Nest Models for Hurricane Camille

Comparison of modeled winds at 20-m height and at 30-min intervals in alternative hindcasts of Hurricane Camille in the Gulf of Mexico during August 1969. The run labelled "5-Nests" used the standard CE model with 5-km spacing on the inner nest. The run labelled "7-Nests" used the upgraded CE model with seven-nests and grid spacing of 2 km on the inner nest. The first (second) line at each time step gives: maximum scalar (vector magnitude) wind speed difference found on the grid between the two runs, latitude and longitude of the grid point, and wind speed and direction of the alternative solutions at that grid point.

Table A1

Comparison of Wind Estimates from 5-Nest and 7-Nest Models,
Hurricane Camille

| Day/ Hour | Max. Speed Diff. m/s | Grid Point Coord. | | 5-Nest Model | | 7-Nest Model | |
|--------------|----------------------------|-------------------|--------------|--------------|----------------|--------------|----------------|
| | | Lat. deg | Long. deg | Speed m/s | Dir. deg az | Speed m/s | Dir. deg az |
| 161200 | 7.1 | 24.1 | -85.7 | 27.9 | 151.7 | 20.8 | 162.6 |
| | 8.4 | 24.1 | -85.7 | 27.9 | 151.7 | 20.8 | 162.6 |
| 161230 | 3.0 | 24.1 | -86.0 | 39.7 | 338.6 | 36.7 | 342.5 |
| | 6.0 | 24.1 | -85.7 | 42.0 | 172.2 | 43.1 | 180.1 |
| 161300 | 1.2 | 24.1 | -85.7 | 41.6 | 181.0 | 42.8 | 183.7 |
| | 7.0 | 24.3 | -86.0 | 52.6 | 47.1 | 52.9 | 54.6 |
| 161330 | 2.2 | 24.3 | -86.0 | 43.6 | 78.8 | 41.4 | 88.0 |
| | 7.2 | 24.3 | -86.0 | 43.6 | 78.8 | 41.4 | 88.0 |
| 161400 | 1.5 | 24.3 | -86.0 | 38.1 | 131.1 | 36.7 | 140.6 |
| | 6.7 | 24.3 | -86.2 | 51.0 | 2.0 | 50.1 | 9.5 |
| 161430 | 3.4 | 24.3 | -86.2 | 40.7 | 359.4 | 37.3 | 5.4 |
| | 7.3 | 24.3 | -86.0 | 43.5 | 150.1 | 45.2 | 159.3 |
| 161500 | 2.1 | 24.3 | -86.2 | 21.2 | 312.9 | 23.2 | 306.1 |
| | 5.3 | 24.5 | -86.2 | 53.0 | 52.8 | 54.0 | 58.3 |
| 161530 | 2.4 | 24.3 | -86.2 | 31.2 | 240.3 | 33.6 | 242.5 |
| | 8.2 | 24.5 | -86.2 | 49.6 | 80.5 | 49.2 | 90.0 |
| 161600 | 1.0 | 24.3 | -86.4 | 46.5 | 312.6 | 45.5 | 316.1 |
| | 8.9 | 24.5 | -86.2 | 47.6 | 106.6 | 46.9 | 117.4 |
| 161630 | 3.8 | 24.5 | -86.4 | 39.5 | 16.6 | 35.7 | 22.6 |
| | 6.2 | 24.5 | -86.2 | 46.3 | 138.6 | 47.9 | 145.9 |
| 161700 | 1.5 | 24.5 | -86.4 | 9.8 | 339.9 | 8.4 | 342.7 |
| | 3.6 | 24.8 | -86.4 | 53.0 | 57.2 | 54.1 | 60.8 |
| 161730 | 1.9 | 24.5 | -86.4 | 23.2 | 226.5 | 25.1 | 232.6 |
| | 5.4 | 24.8 | -86.4 | 52.2 | 74.4 | 52.9 | 80.2 |
| 161800 | 2.0 | 24.5 | -86.4 | 36.8 | 209.7 | 38.8 | 212.5 |
| | 6.9 | 24.8 | -86.4 | 49.9 | 103.1 | 51.0 | 110.8 |
| 161830 | 3.4 | 24.8 | -86.7 | 43.7 | 27.9 | 40.3 | 36.3 |
| | 7.0 | 24.8 | -86.7 | 43.7 | 27.9 | 40.3 | 36.3 |
| 161900 | 2.1 | 24.8 | -86.7 | 14.7 | 2.9 | 12.7 | 359.3 |
| | 3.0 | 25.0 | -86.7 | 53.2 | 53.0 | 54.2 | 55.9 |
| 161930 | 2.8 | 24.8 | -86.7 | 25.2 | 226.3 | 28.0 | 231.6 |
| | 6.0 | 25.0 | -86.7 | 52.0 | 76.3 | 52.6 | 82.9 |
| 162000 | 1.9 | 24.8 | -86.7 | 36.1 | 217.8 | 38.0 | 219.8 |
| | 7.0 | 25.0 | -86.7 | 48.9 | 102.0 | 49.9 | 111.1 |
| 162030 | 3.1 | 25.0 | -86.9 | 44.4 | 20.2 | 41.3 | 28.9 |
| | 7.2 | 25.0 | -86.9 | 44.4 | 20.2 | 41.3 | 28.9 |

(Sheet 1 of 6)

Table A1 (Continued)

| Day/ Hour | Max. Speed Diff. m/s | Grid Point Coord. | | 5-Nest Model | | 7-Nest Model | |
|--------------|----------------------------|-------------------|----------------|--------------|----------------|--------------|----------------|
| | | Lat. deg | Long. deg | Speed m/s | Dir. deg az | Speed m/s | Dir. deg az |
| 162100 | 1.2 3.2 | 25.0 25.0 | -86.7 -86.7 | 44.1 44.1 | 159.6 159.6 | 45.3 45.3 | 163.4 163.4 |
| 162130 | 2.4 6.8 | 25.0 25.3 | -86.9 -86.9 | 24.7 51.9 | 255.5 68.2 | 27.0 52.2 | 257.8 75.7 |
| 162200 | 1.7 9.3 | 25.2 25.2 | -86.9 -86.9 | 47.8 47.8 | 95.4 95.4 | 46.2 46.2 | 106.5 106.5 |
| 162230 | 2.8 7.6 | 25.2 25.2 | -87.1 -86.9 | 45.4 46.9 | 13.3 132.4 | 42.6 46.9 | 22.2 141.6 |
| 162300 | 1.6 3.7 | 25.2 25.2 | -86.9 -86.9 | 43.4 43.4 | 163.1 163.1 | 44.9 44.9 | 167.5 167.5 |
| 162330 | 2.1 7.7 | 25.2 25.4 | -87.1 -87.1 | 26.5 51.0 | 267.8 64.2 | 28.6 51.3 | 268.0 72.8 |
| 170000 | 1.8 8.2 | 25.4 25.4 | -87.1 -87.1 | 44.0 44.0 | 94.1 94.1 | 42.2 42.2 | 104.8 104.8 |
| 170030 | 1.2 6.1 | 25.4 25.4 | -87.4 -87.4 | 48.6 48.6 | 345.6 345.6 | 47.3 47.3 | 352.7 352.7 |
| 170100 | 2.2 7.2 | 25.4 25.6 | -87.4 -87.4 | 41.8 51.9 | 313.1 29.6 | 39.6 51.8 | 318.0 37.5 |
| 170130 | 2.4 5.0 | 25.6 25.6 | -87.4 -87.1 | 31.0 45.7 | 7.0 149.9 | 28.6 46.8 | 6.2 155.9 |
| 170200 | 0.9 7.8 | 22.6 25.8 | -88.5 -87.4 | 8.4 51.4 | 265.9 54.0 | 7.4 51.4 | 271.6 62.7 |
| 170230 | 7.3 9.0 | 25.8 25.8 | -87.4 -87.4 | 19.8 19.8 | 104.9 104.9 | 12.6 12.6 | 124.3 124.3 |
| 170300 | 3.5 6.7 | 25.8 26.0 | -87.4 -87.4 | 28.9 51.2 | 221.5 81.4 | 32.3 52.0 | 226.8 88.8 |
| 170330 | 1.0 7.5 | 26.0 26.0 | -87.6 -87.4 | 51.3 42.1 | 7.4 121.2 | 50.4 41.2 | 14.3 131.4 |
| 170400 | 2.8 5.5 | 26.0 26.0 | -87.6 -87.4 | 38.2 41.5 | 333.4 175.3 | 35.4 42.9 | 336.4 182.5 |
| 170430 | 2.9 7.6 | 26.2 26.2 | -87.6 -87.6 | 45.2 45.2 | 39.4 39.4 | 42.3 42.3 | 48.6 48.6 |
| 170500 | 1.3 3.7 | 26.2 26.4 | -87.4 -87.6 | 44.2 53.4 | 161.7 53.5 | 45.5 54.4 | 164.7 57.3 |
| 170530 | 1.7 8.1 | 26.2 26.4 | -87.6 -87.6 | 32.2 46.2 | 250.2 78.9 | 34.1 45.2 | 251.5 89.0 |

(Sheet 2 of 6)

Table A1 (Continued)

| Day/ Hour | Max. Speed Diff. m/s | Grid Point Coord. | | 5-Nest Model | | 7-Nest Model | |
|--------------|----------------------------|-------------------|--------------|--------------|----------------|--------------|----------------|
| | | Lat. deg | Long. deg | Speed m/s | Dir. deg az | Speed m/s | Dir. deg az |
| 170600 | 6.9 | 26.4 | -87.6 | 22.5 | 163.9 | 15.7 | 177.4 |
| | 8.1 | 26.4 | -87.6 | 22.5 | 163.9 | 15.7 | 177.4 |
| 170630 | 2.5 | 26.4 | -87.6 | 37.7 | 192.9 | 40.2 | 190.6 |
| | 5.2 | 26.4 | -87.6 | 37.7 | 192.9 | 40.2 | 190.6 |
| 170700 | 4.0 | 26.6 | -87.8 | 42.8 | 29.2 | 38.8 | 36.7 |
| | 6.7 | 26.6 | -87.8 | 42.8 | 29.2 | 38.8 | 36.7 |
| 170730 | 2.4 | 26.6 | -87.8 | 6.5 | 353.2 | 4.1 | 20.6 |
| | 3.4 | 26.6 | -87.8 | 6.5 | 353.2 | 4.1 | 20.6 |
| 170800 | 3.2 | 26.6 | -87.8 | 30.1 | 229.2 | 33.2 | 234.5 |
| | 7.9 | 26.8 | -87.8 | 51.4 | 81.1 | 51.1 | 89.9 |
| 170830 | 1.5 | 26.8 | -88.0 | 49.3 | 7.7 | 47.8 | 16.1 |
| | 7.3 | 26.8 | -87.8 | 41.8 | 129.6 | 40.9 | 139.7 |
| 170900 | 2.9 | 26.8 | -88.0 | 35.2 | 344.8 | 32.3 | 345.8 |
| | 6.3 | 26.8 | -87.8 | 43.9 | 163.9 | 45.6 | 171.6 |
| 170930 | 0.9 | 24.5 | -80.1 | 8.8 | 290.2 | 8.0 | 206.4 |
| | 8.6 | 27.0 | -88.0 | 49.4 | 53.7 | 48.5 | 63.7 |
| 171000 | 5.9 | 27.0 | -88.0 | 19.5 | 102.7 | 13.6 | 113.0 |
| | 6.6 | 27.0 | -88.0 | 19.5 | 102.7 | 13.6 | 113.0 |
| 171030 | 1.4 | 27.0 | -88.3 | 45.3 | 342.6 | 43.9 | 349.2 |
| | 6.4 | 27.0 | -88.0 | 32.6 | 186.0 | 33.3 | 187.1 |
| 171100 | 2.0 | 27.0 | -88.3 | 39.4 | 312.5 | 37.3 | 315.8 |
| | 7.1 | 27.2 | -88.3 | 51.2 | 31.4 | 50.1 | 39.4 |
| 171130 | 2.3 | 27.2 | -88.3 | 26.3 | 24.5 | 24.0 | 20.5 |
| | 5.3 | 27.2 | -88.0 | 48.7 | 145.2 | 49.6 | 151.4 |
| 171200 | 1.0 | 27.2 | -88.0 | 45.1 | 168.0 | 46.1 | 170.2 |
| | 6.3 | 27.4 | -88.3 | 52.9 | 64.7 | 53.4 | 70.4 |
| 171230 | 3.7 | 27.4 | -88.3 | 39.6 | 96.0 | 35.9 | 102.8 |
| | 5.8 | 27.4 | -88.3 | 39.6 | 96.0 | 35.9 | 102.8 |
| 171300 | 1.8 | 27.4 | -88.5 | 44.1 | 346.3 | 42.4 | 352.7 |
| | 7.1 | 27.4 | -88.3 | 35.3 | 180.2 | 33.6 | 191.7 |
| 171330 | 1.7 | 27.4 | -88.5 | 40.1 | 313.1 | 38.4 | 316.2 |
| | 7.5 | 27.6 | -88.3 | 50.7 | 111.3 | 51.0 | 119.7 |
| 171400 | 1.4 | 27.6 | -88.5 | 28.0 | 12.5 | 26.6 | 8.4 |
| | 5.9 | 27.6 | -88.3 | 48.2 | 149.0 | 49.5 | 155.8 |
| 171430 | 2.3 | 27.6 | -88.5 | 30.2 | 280.3 | 32.6 | 279.7 |
| | 8.4 | 27.8 | -88.5 | 48.7 | 58.4 | 47.3 | 68.2 |

(Sheet 3 of 6)

Table A1 (Continued)

| Day/ Hour | Max Speed Diff. m/s | Grid Point Coord. | | 5-Nest Model | | 7-Nest Model | |
|--------------|---------------------------|-------------------|----------------|--------------|----------------|--------------|----------------|
| | | Lat. deg | Long. deg | Speed m/s | Dir. deg az | Speed m/s | Dir. deg az |
| 171500 | 6.0 6.8 | 27.8 27.8 | -88.5 -88.5 | 19.3 19.3 | 114.2 114.2 | 13.3 13.3 | 125.6 125.6 |
| 171530 | 1.7 6.5 | 27.8 28.0 | -88.7 -88.5 | 45.9 52.5 | 338.5 81.4 | 44.2 53.2 | 342.8 88.4 |
| 171600 | 1.6 7.6 | 28.0 28.0 | -88.5 -88.5 | 41.8 41.8 | 126.4 126.4 | 40.1 40.1 | 136.8 136.8 |
| 171630 | 1.7 7.5 | 28.0 28.0 | -88.7 -88.5 | 34.0 45.2 | 338.7 169.1 | 32.3 46.3 | 338.4 178.4 |
| 171700 | 3.1 7.5 | 28.3 28.3 | -88.7 -88.7 | 44.9 44.9 | 45.2 45.2 | 41.8 41.8 | 54.2 54.2 |
| 171730 | 2.0 3.2 | 28.3 28.5 | -88.7 -88.7 | 6.9 53.8 | 324.1 59.8 | 4.9 53.9 | 340.6 63.2 |
| 171800 | 2.6 8.5 | 28.3 28.5 | -88.7 -88.7 | 33.7 47.2 | 240.9 81.6 | 36.4 45.0 | 246.3 91.9 |
| 171830 | 7.8 8.3 | 28.5 28.5 | -88.7 -88.7 | 24.5 24.5 | 167.5 167.5 | 16.7 16.7 | 175.6 175.6 |
| 171900 | 2.5 8.9 | 28.5 28.7 | -88.7 -88.7 | 38.2 50.1 | 214.3 97.5 | 40.7 49.6 | 221.1 107.7 |
| 171930 | 2.9 7.7 | 28.7 28.7 | -89.0 -88.7 | 41.2 41.2 | 1.6 154.8 | 38.3 40.8 | 6.5 165.5 |
| 172000 | 1.8 7.2 | 28.7 28.9 | -88.7 -89.0 | 43.2 50.0 | 192.8 38.1 | 45.0 49.0 | 197.7 46.4 |
| 172030 | 1.5 7.1 | 28.9 28.9 | -88.7 -88.7 | 47.9 47.9 | 150.2 150.2 | 49.4 49.4 | 158.3 158.3 |
| 172100 | 2.0 8.2 | 28.9 29.1 | -89.0 -89.0 | 31.1 47.6 | 283.6 55.6 | 33.2 46.1 | 283.5 65.4 |
| 172130 | 3.1 3.5 | 29.1 29.1 | -89.0 -89.0 | 15.6 15.6 | 79.7 79.7 | 12.5 12.5 | 86.5 86.5 |
| 172200 | 3.6 8.5 | 29.1 29.3 | -89.0 -89.0 | 27.7 50.1 | 250.0 72.7 | 31.3 49.6 | 255.4 82.6 |
| 172230 | 7.2 8.2 | 29.3 29.3 | -89.0 -89.0 | 23.8 23.8 | 135.6 135.6 | 16.6 16.6 | 147.2 147.2 |
| 172300 | 1.6 7.1 | 29.3 29.5 | -89.0 -89.0 | 37.8 51.5 | 205.3 93.0 | 39.4 52.0 | 214.6 100.9 |
| 172330 | 2.2 6.2 | 29.5 29.5 | -89.2 -89.0 | 44.9 39.1 | 7.8 143.3 | 42.7 37.6 | 15.1 152.3 |

(Sheet 4 of 6)

Table A1 (Continued)

| Day/ Hour | Max. Speed Diff. m/s | Grid Point Coord. | | 5-Nest Model | | 7-Nest Model | |
|--------------|----------------------------|-------------------|--------------|--------------|----------------|--------------|----------------|
| | | Lat. deg | Long. deg | Speed m/s | Dir. deg az | Speed m/s | Dir. deg az |
| 180000 | 1.7 | 29.5 | -89.0 | 43.4 | 188.7 | 45.1 | 195.4 |
| | 5.5 | 29.5 | -89.0 | 43.4 | 188.7 | 45.1 | 195.4 |
| 180030 | 1.8 | 29.7 | -89.2 | 27.4 | 30.7 | 25.6 | 26.6 |
| | 6.0 | 29.7 | -89.0 | 49.7 | 142.6 | 50.7 | 149.4 |
| 180100 | 3.2 | 29.7 | -89.2 | 27.0 | 274.3 | 30.2 | 276.4 |
| | 8.4 | 29.9 | -89.2 | 50.6 | 62.6 | 49.5 | 72.1 |
| 180130 | 6.9 | 29.9 | -89.2 | 20.1 | 126.8 | 13.2 | 141.7 |
| | 8.0 | 29.9 | -89.2 | 20.1 | 126.8 | 13.2 | 141.7 |
| 180200 | 1.4 | 29.9 | -89.2 | 36.5 | 197.3 | 37.9 | 208.1 |
| | 7.1 | 29.9 | -89.2 | 36.5 | 197.3 | 37.9 | 208.1 |
| 180230 | 2.9 | 30.1 | -89.4 | 43.9 | 16.8 | 41.0 | 24.2 |
| | 9.2 | 30.1 | -89.2 | 46.9 | 132.5 | 45.5 | 143.9 |
| 180300 | 1.4 | 30.1 | -89.2 | 45.9 | 176.3 | 47.3 | 181.7 |
| | 6.0 | 30.3 | -89.4 | 52.0 | 47.1 | 52.1 | 53.6 |
| 180330 | 2.5 | 30.3 | -89.4 | 23.1 | 71.2 | 20.6 | 66.5 |
| | 3.3 | 30.3 | -89.2 | 49.9 | 139.7 | 50.5 | 143.4 |
| 180400 | 1.9 | 30.3 | -89.4 | 24.1 | 245.7 | 26.0 | 252.7 |
| | 3.6 | 30.3 | -89.4 | 24.1 | 245.7 | 26.0 | 252.7 |
| 180430 | 0.9 | 28.3 | -92.2 | 8.4 | 293.9 | 7.5 | 299.6 |
| | 1.4 | 30.3 | -89.4 | 38.9 | 234.0 | 39.7 | 235.6 |
| 180500 | 0.9 | 28.3 | -92.2 | 8.3 | 291.2 | 7.5 | 296.5 |
| | 1.4 | 29.5 | -94.0 | 4.4 | 353.8 | 4.3 | 11.9 |
| 180530 | 0.9 | 28.5 | -92.2 | 8.8 | 292.6 | 7.9 | 298.1 |
| | 1.5 | 30.3 | -89.4 | 39.5 | 236.7 | 38.8 | 234.8 |
| 180600 | 0.9 | 28.5 | -92.4 | 7.8 | 293.4 | 7.0 | 299.2 |
| | 1.4 | 29.5 | -93.3 | 6.5 | 334.2 | 6.0 | 345.8 |
| 180630 | 0.9 | 28.7 | -92.4 | 7.5 | 293.6 | 6.6 | 299.3 |
| | 1.3 | 29.7 | -92.9 | 8.0 | 328.1 | 7.2 | 336.0 |
| 180700 | 0.9 | 29.5 | -92.6 | 7.6 | 315.2 | 6.7 | 322.1 |
| | 1.3 | 29.5 | -92.6 | 7.6 | 315.2 | 6.7 | 322.1 |
| 180730 | 0.9 | 29.5 | -92.6 | 6.7 | 310.7 | 5.8 | 317.2 |
| | 1.1 | 29.5 | -92.6 | 6.7 | 310.7 | 5.8 | 317.2 |
| 180800 | 0.9 | 29.5 | -92.4 | 6.8 | 301.6 | 5.9 | 306.7 |
| | 1.1 | 29.5 | -92.4 | 6.8 | 301.6 | 5.9 | 306.7 |
| 180830 | 0.9 | 29.7 | -92.2 | 7.2 | 298.6 | 6.3 | 302.9 |
| | 1.0 | 29.7 | -92.0 | 8.2 | 294.2 | 7.3 | 298.0 |

(Sheet 5 of 6)

Table A1 (Concluded)

| Day/ Hour | Max. Speed Diff. m/s | Grid Point Coord. | | 5-Nest Model | | 7-Nest Model | |
|--------------|----------------------------|-------------------|--------------|--------------|----------------|--------------|----------------|
| | | Lat. deg | Long. deg | Speed m/s | Dir. deg az | Speed m/s | Dir. deg az |
| 180900 | 0.9 | 29.7 | -92.0 | 7.2 | 289.3 | 6.3 | 292.2 |
| | 0.9 | 29.7 | -92.0 | 7.2 | 289.3 | 6.3 | 292.2 |
| 180930 | 0.9 | 29.7 | -92.0 | 6.3 | 282.5 | 5.5 | 284.1 |
| | 0.9 | 30.3 | -89.4 | 17.4 | 218.1 | 17.3 | 215.2 |
| 181000 | 0.8 | 29.7 | -92.0 | 5.5 | 275.1 | 4.7 | 274.8 |
| | 0.8 | 30.3 | -89.4 | 15.8 | 216.9 | 15.8 | 213.8 |
| 181030 | 0.7 | 29.7 | -92.0 | 4.8 | 265.3 | 4.1 | 262.5 |
| | 0.8 | 30.3 | -86.4 | 11.9 | 161.5 | 12.1 | 165.0 |
| 181100 | 0.5 | 29.7 | -91.7 | 4.9 | 253.5 | 4.3 | 249.7 |
| | 0.8 | 30.3 | -86.4 | 11.4 | 162.2 | 11.5 | 165.9 |
| 181130 | 0.4 | 28.3 | -83.4 | 8.2 | 156.8 | 8.5 | 160.7 |
| | 0.8 | 30.1 | -85.7 | 10.0 | 160.4 | 10.2 | 164.6 |
| 181200 | 0.4 | 29.7 | -93.8 | 3.1 | 170.9 | 3.5 | 170.8 |
| | 0.8 | 30.3 | -86.4 | 10.3 | 163.0 | 10.4 | 167.3 |

(Sheet 6 of 6)

Appendix B

Documentation of CE Model Upgrades

This appendix provides brief documentation of new and modified programs in the upgraded CE tropical cyclone surface wind field model. The material is a supplement to the primary documentation of Cardone et al. (1992). Five FORTRAN programs are discussed. The programs HIST_ADC.7NE, SNAP_ADC.7NE, and SNAP_HOL.7NE are modified versions of the previous HIST and SNAP programs. Programs 1EYEWALL.HOL and 2EYEWALL.HOL are new. They are helpful in implementing the new generalized surface pressure specification.

Program HIST_ADC.7NE

HIST_ADC.7NE is a slight modification of HIST_ADC.F. All input files except LSNAP, and all output files, are unchanged from HIST_ADC.F to HIST_ADC.7NE. The changes to file LSNAP are as follows:

- pressure arrays, formerly dimensioned (21,21,5), are now dimensioned (21,21,7);
- wind arrays, formerly dimensioned (21,21,10), are now dimensioned (21,21,14);
- in the variables at the end of records in LSNAP, variable DX is followed by the new variable INSIDE. INSIDE is an integer indexing the innermost live nest of the 7 nests supported, so that the effective grid spacing is $DX*2^{**}(INSIDE-1)$.

Program SNAP_ADC.7NE

SNAP_ADC.7NE is derived from SNAP_ADC.F. The modifications allow the user to run up to 7 grid nests rather than the previous mandatory 5 nests.

Arrays of pressure, pressure gradient, wind, formerly dimensioned (21,21,5), are now dimensioned (21,21,7). Two changes are made to namelist /NAME3/ as follows:

- a variable name NOMEN (CHARACTER*4) for storm identification has been included;
- integer variable INSIDE has been added. INSIDE indexes the finest live nest of the 7 nests provided. Thus the number of live nests is (8-INSIDE), and the grid spacing of the finest live nest is $DX*2^{**}(INSIDE-1)$. Default values are DX = 2, and INSIDE = 1, yielding a 2 km grid spacing and an execution time roughly 4 times as long as the existing 5-nest model. The combination DX = 6.25, INSIDE = 3, (lines 304, 305) reproduces the 25 km spacing often used by the CE for global studies. In the great majority of applications, the useful values of INSIDE are 1, 2, and 3. INSIDE = 4 may be tried for running a quick preliminary study on a coarse grid.

Program SNAP_HOL.7NE

SNAP_HOL.7NE is an extensive modification of SNAP_ADC.7NE to include the generalized pressure profile as well as the capability for modeling up to 7 nests. The variable ST12 and the quadrantal variation of PFAR and RADIUS have been excised. In OWI's experience with the hurricane model, they have been used only once: for hurricane Eloise, September 13, 1975. Variable ITRACK has been excised: its use pertained to a 1969 study in which direction was specified in points. Namelist /NAME3/ is changed materially. Each variable and array in /NAME3/ is documented below. The method of computation of pressure and pressure gradient is discussed in a later part on Mathematical Method.

Revisions at beginning of program

```
REAL RADIUS(2),DPRESS(2),HOLL(2)
CHARACTER*4 NOMEN
EQUIVALENCE (RAD1,RADIUS), (RAD2,RADIUS(2)), (B1,HOLL),
$ (B2,HOLL(2)), (DP1,DPRESS), (DP2,DPRESS(2))
NAMELIST /NAME3/ SGW, AN1, NOMEN,
$ EYELAT, EYLONG, DIREC, SPEED, EYPRES, RADIUS, RAD1,
$ RAD2, PFAR, NM, DX, INSIDE, HOLL, B1, B2, DPRESS, DP1,
$ DP2
```

Definition of variables in namelist NAME3

| | |
|-----------|--|
| SGW | Magnitude of surface geostrophic wind, m/sec |
| AN1 | Angle between SGW and east, counterclockwise from east |
| NOMEN | Designator for tropical storm, e.g. two digits and one letter |
| EYELAT | Latitude of eye of storm at snap time, north positive |
| EYLONG | Longitude of eye of storm at snap time, east positive (EYLONG is included for archival purposes but not presently used in computation) |
| DIREC | Direction of forward motion of storm, clockwise from north |
| SPEED | Speed of forward motion, in kt (but redefinable according to the switch variable UNITS) |
| EYPRES | Pressure at eye of storm, in mb |
| RADIUS | Scale radius of the two components of exponential pressure profile |
| RAD1,RAD2 | Alternate names for specifying RADIUS; convenient when only one exponential is modeled |
| PFAR | Ambient pressure exterior to storm, in mb |
| NM | Number of computational cycles in nest 1; NM should be a multiple of 64 (default: NM = 3200) |
| DX | Grid spacing in nest 1, in km (default: DX = 2.) |
| INSIDE | Index of finest nest actually used for computations; the finest active grid spacing is DX*2** (INSIDE-1) (default: INSIDE = 1) |
| HOLL | Power to which radius is raised in the modified Holland's (1980) pressure profile model. When HOLL(2) = 0., only one exponential is used; RADIUS(2) and DPRESS(2) are then ignored. |
| B1,B2 | Alternate names for specifying HOLL; convenient when only one exponential is modeled. Default values are B1 = 1., B2 = 0. These defaults are reinstated for every snapshot. Use of the defaults reverts to a standard exponential pressure profile, as used in SNAP_ADC.7NE. |
| DPRESS | DPRESS(I) is the pressure difference associated with RADIUS(I) and HOLL(I) in OWI's double-eyewall extension of Holland's (1980) modified exponential profile. |
| DP1,DP2 | Alternate names for specifying DPRESS. As explained in the part on Mathematical Method, it is never advantageous to include DP2 in an input list; it is in the NAMELIST in order to force its appearance in the output file. |

SPECIAL WARNING: Do not input both members of an equivalence. Input either RADIUS or RAD and RAD2; either HOLL or B1 and B2; either DPRESS or DP1 and DP2. The program imposes consistency checks on RADIUS, HOLL, and DPRESS; it does not check EYPRES and PFAR, so that it remains the user's duty to verify that PFAR > EYPRES.

Mathematical method

The program performs the following consistency checks:

1. If $B1 < 0$ or $B2 < 0$, stop.
2. If $B2 = 0$, run Holland's modified exponential model (ignore RAD2 and DP2).
 - 2.1 If $RAD1 \leq 0$, stop.
 - 2.2 If DP1 not specified, compute it as PFAR-EYPRES.
 - 2.3 If DP1 specified, but inconsistent with PFAR-EYPRES, stop.
 - 2.4 Set N = 1.
3. If $B2 > 0$, run OWI's extension of Holland's pressure profile.
 - 3.1 If $RAD1 \leq 0$ or $RAD2 \leq 0$, stop.
 - 3.2 If DP2 not specified, compute it as PFAR-EYPRES-DP1.
 - 3.3 If DP2 specified, but inconsistent with PFAR-EYPRES-DP1, stop.
 - 3.4 Set N = 2.

Program 1EYEWALL.HOL

Program 1EYEWALL.HOL attempts to fit snapshot parameters to a guessed wind profile. It considers only the case of one exponential ($B2 = 0.0$). 1EYEWALL.HOL requires the following input arguments (in namelist /INN/):

| | |
|--------|--|
| BLAT | Absolute value of latitude of eye, degrees & decimals; used in computation of the Coriolis parameter. Also, the value BLAT=99 is used as a flag to stop computation. |
| EYPRES | Pressure at eye, in mb |
| PFAR | Pressure at large (theoretically infinite) distance from eye, in mb |
| RW1 | Radius at which a wind speed is guessed, in km |
| SP1 | Wind speed corresponding to RW1, in m/sec |
| V150 | Wind speed at radius of 150 km, in m/sec |

The following outputs are printed:

1. In namelist /INN/:

SP11, SP12 = SP1 minus & plus 1 m/sec
SP31, SP32 = V150 minus & plus 1 m/sec
DP2 = pressure difference (far field minus eye), in pascal

2. In namelist /VORTEX/:

COR = Coriolis parameter, $2*\omega*\sin(\text{BLAT})$

FR22 = the quantity $0.5 * \text{COR} * \text{RW1}$ (used in the computation of gradient wind)

FR23 = $0.5 * \text{COR} * r$, where r is 150000 m or 150 km

PEYE = pressure at eye, in pascal

3. Below namelist /VORTEX/, six parameters are printed, defined from left to right as:

3.1 DP2 (see above)

3.2 Fitted value of scale radius, in m

3.3 Fitted value of Holland's exponent

3.4 Fitted value of gradient wind at radius RW1, in m/sec
(in a good fit, this will be nearly equal to SP1)

3.5 Fitted value of gradient wind at radius 150 km, in m/sec
(in a good fit, this will be nearly equal to V150)

3.6 Goodness of fit measure: absolute value of gradient wind minus in put wind at radius RW1, plus the same at radius 150 km. A value less than 3.0 implies a tolerably well-fitting solution.

4. Table with 6 columns and 150 lines:

4.1 Radius, in km

4.2 Pressure, in mb

4.3 First component of pressure gradient, in pascal/m

4.4 Second component (this is zero, since only one exponential was fitted)

4.5 Pressure gradient (here equal to output #4.3)

4.6 Gradient wind, m/sec

5. Below the table are numbers that, if the fit is satisfactory, the user can insert into namelist /NAME3/ of SNAP_HOL.7NE:

EYELAT = echo of the input BLAT

EYPRES = echo of input

PFAR = echo of input

RAD1 = scale radius, in nm

HOLL = two values of Holland's exponent; the second value is zero, because only one exponential was fitted

Program 2EYEWALL.HOL

Program 2EYEWALL.HOL attempts to fit snapshot parameters to a guessed wind profile. It considers the case of two exponentials ($B2 > 0.0$).
2EYEWALL.HOL requires the following inputs in namelist /INN/:

BLAT Same usage as in 1EYEWALL.HOL

EYPRES Same usage as in 1EYEWALL.HOL

PFAR Same usage as in 1EYEWALL.HOL

| | |
|-------|--|
| RS1 | Scale radius of inner ring, in km (numerical experiments with this scheme have shown that the inner scale radius can safely be taken equal to the inner radius to local maximum wind) |
| RW2 | Radius to maximum wind of outer ring, in km |
| DRING | An integer switch variable indexing the shape of the wind profile |

DRING = 1: the maximum wind is greater in the inner ring
 DRING = 2: the maximum wind is greater in the outer ring

| | |
|-----|--|
| SP1 | Desired wind speed at radius RS1, in m/sec |
| SP2 | Desired wind speed at radius RW2, in m/sec |

The following outputs are printed:

1. In namelist /INN/:

SP11, SP12 = SP1 minus and plus 1 m/sec
 SP21, SP22 = SP2 minus and plus 1 m/sec

2. In namelist /VORTEX/:

BLAT = echo of input
 COR = same usage as in 1EYEWALL.HOL
 RAD1 = RS1, in m
 RAD2 = RW2, in m
 RAD3 = $0.5*(RAD1+RAD2)$; a local minimum of wind speed, if found, will be near RAD3
 RAD4 = 150000 m (= 150 km)
 FR21 = the quantity $0.5*COR*RAD1$; used in the computation of gradient wind
 FR22 = the quantity $0.5*COR*RAD2$
 FR23 = the quantity $0.5*COR*RAD3$
 PEYE = same usage as in 1EYEWALL.HOL
 DP = pressure difference (far field minus eye), in pascal

3. Below namelist /VORTEX/, nine parameters are printed, defined from left to right as:

- 3.1 Fitted value of DP1 (partial pressure difference for first exponential), in pascal
- 3.2 Fitted value of DP2 (partial pressure difference for second exponential), in pascal
- 3.3 Scale radius of second exponential, in m (the scale radius of first exponential has been fixed at RAD1)
- 3.4 Exponent for first exponential (Holland 1980)
- 3.5 Exponent for second exponential (OWI extension of Holland (1980))
- 3.6 Fitted wind speed at radius RAD1, m/sec
- 3.7 Fitted wind speed at radius RAD2, m/sec

3.8 Fitted wind speed at radius RAD3, m/sec
3.9 (printed below 3.1): fitted wind speed at radius 150 km

4. Second printing of namelist /INN/, if given:

The fit in the above two-line summary was unsatisfactory in that the wind at 150 km was greater than the wind at RAD2; a second fit will be attempted, this time minimizing the wind speed at 150 km.

SP11, SP12 = SP1 minus and plus 2 m/sec
SP21, SP22 = SP2 minus and plus 2 m/sec

5. Below second printing of /INN/: the same nine parameters as in #3 above, for the second attempted fit.

6. Table with 6 columns and 150 lines:

6.1 Radius, in km
6.2 Pressure, in mb
6.3 First component of pressure gradient, in pascal/m
6.4 Second component of pressure gradient, in pascal/m
6.5 Pressure gradient (sum of the two components), in pascal/m
6.6 Gradient wind, in m/sec

7. Below the table are numbers that, if the fit is satisfactory, the user can insert into namelist /NAME3/ of SNAP_HOL.7NE:

EYELAT = echo of the input BLAT
EYPRES = echo of input
PFAR = echo of input
RADIUS = two values of scale radius, in nm
HOLL = two values of Holland's exponent
DP1 = pressure difference for first component, in mb
(program SNAP_HOL.7NE computes DP2 by subtraction)

Appendix C

Sample Application of Upgraded CE Model to Simu- lation of 12 Snapshots of Hurricane Gilbert

This appendix provides input file information used by OWI in test runs with the upgraded CE model, including seven nests and the generalized pressure specification. Snapshots were generated at 6-hr intervals for Hurricane Gilbert, which occurred during September 1988. The first snapshot represents 1200 UTC (Universal Time Coordinate, formerly known as Greenwich Mean Time) 15 September 1988. In all, 12 snapshots were generated. Inputs for the programs SNAP_HOL.7NE and HIST_ADC.7NE are included as implemented on the OWI VAX computer. The listed values of parameter AN1 follow a meteorological convention (deg azimuth coming from) rather than the convention used by the Cardone et al. (1992).

Listings of the full field of surface (19-m elevation) wind speed and direction were generated on a polar output grid. They are included here at 6-hr intervals (snapshot times). Wind speed is in m/sec. Wind direction is in deg azimuth coming from. Printed output of the azimuthally averaged, surface wind speed and inflow angle is also given in this appendix. In addition to the 12 snapshot wind fields, this output includes a wind field interpolated halfway between each pair of snapshots.

```

S ASSIGN GRID.312    FDR012
S ASSIGN 05GILBERT21 FDR005
S ASSIGN GILB.WIN021 FDR052
S RUN MOLL3
SNAME1
KZM      =      8309,
KDM      =     151200,
KMIN     =      180,
DX       =   2.000030      ,
KSTRES   =          0,
NSTRES   =     17227,
KWIND    =      19,
NWIND    =     312,
MM       =  500.0030      ,
INSIDE   =          1,
KTIME    =          1
SEND
SNAME2
EYELAT  =  16.00030      ,
DIREC   =  290.0030      ,
SPEED   =  11.03030      ,
EYPRES   =  972.0030      ,
PFAR    =  1011.030      ,
RAD1    =  25.38030      ,
RAD2    =  68.73030      ,
RADIUS   =  25.38030      ,  68.73000      ,
DP1     =  22.85030      ,
DP2     =  16.15030      ,
DPRES   =  22.85030      ,  16.15000      ,
B1      =  2.520030      ,
B2      =  2.520030      ,
HOLL    =  2*2.520030
SGW     =  7.000030      ,
AN1     =  110.0030      ,
ST12    =  0.0000030E+00
SEND
SNAME2
EYELAT  =  16.00030      ,
DIREC   =  290.0030      ,
SPEED   =  11.00030      ,
EYPRES   =  968.0030      ,
PFAR    =  1011.030      ,
RAD1    =  31.32030      ,
RAD2    =  87.37030      ,
RADIUS   =  31.32030      ,  87.37000      ,
DP1     =  31.77030      ,
DP2     =  11.23030      ,
DPRES   =  31.77030      ,  11.23000      ,
B1      =  2.520030      ,
B2      =  2.520030      ,
HOLL    =  2*2.520030
SGW     =  7.000030      ,
AN1     =  110.0030      ,
ST12    =  0.0000030E+00
SEND

```

Snapshot 1

Snapshot 2

Figure C1. Program inputs, Hurricane Gilbert (Sheet 1 of 6)

| | | |
|--------|----------------|---|
| SNAME2 | | |
| EYELAT | = 19.00000 | , |
| DIREC | = 290.00000 | , |
| SPEED | = 11.00000 | , |
| EYPRES | = 905.00000 | , |
| PFAR | = 1012.000 | , |
| RAD1 | = 8.640000 | , |
| RAD2 | = 67.28000 | , |
| RADIUS | = 8.640000 | , |
| DP1 | = 93.83000 | , |
| DP2 | = 13.17000 | , |
| DPRES | = 93.83000 | , |
| B1 | = 1.680000 | , |
| B2 | = 2.380000 | , |
| HOLL | = 1.680000 | , |
| SGW | = 7.000000 | , |
| AN1 | = 110.0000 | , |
| ST12 | = 0.000000E+00 | |
| SEND | | |
| SNAME2 | | |
| EYELAT | = 20.00000 | , |
| DIREC | = 290.00000 | , |
| SPEED | = 11.00000 | , |
| EYPRES | = 888.00000 | , |
| PFAR | = 1012.000 | , |
| RAD1 | = 7.020000 | , |
| RAD2 | = 54.00000 | , |
| RADIUS | = 7.020000 | , |
| DP1 | = 110.2200 | , |
| DP2 | = 13.78000 | , |
| DPRES | = 110.2200 | , |
| B1 | = 1.590000 | , |
| B2 | = 2.520000 | , |
| HOLL | = 1.590000 | , |
| SGW | = 7.000000 | , |
| AN1 | = 110.0000 | , |
| ST12 | = 0.000000E+00 | |
| SEND | | |
| SNAME2 | | |
| EYELAT | = 20.00000 | , |
| DIREC | = 290.00000 | , |
| SPEED | = 11.00000 | , |
| EYPRES | = 893.00000 | , |
| PFAR | = 1012.000 | , |
| RAD1 | = 7.020000 | , |
| RAD2 | = 37.80000 | , |
| RADIUS | = 7.020000 | , |
| DP1 | = 101.1200 | , |
| DP2 | = 17.88000 | , |
| DPRES | = 101.1200 | , |
| B1 | = 1.410000 | , |
| B2 | = 2.520000 | , |
| HOLL | = 1.410000 | , |
| SGW | = 7.000000 | , |
| AN1 | = 110.0000 | , |
| ST12 | = 0.000000E+00 | |
| SEND | | |

Snapshot 3

Snapshot 4

Snapshot 5

Figure C1. (Sheet 2 of 6)

| | | | | |
|--------|---|---------------|---|-----------|
| SNAME2 | | | | |
| EYELAT | = | 21.00000 | , | |
| DIREC | = | 290.00000 | , | |
| SPEED | = | 11.00000 | , | |
| EYPRES | = | 890.00000 | , | |
| PFAR | = | 1012.000 | , | |
| RAD1 | = | 7.020000 | , | |
| RAD2 | = | 37.26000 | , | |
| RADIUS | = | 7.020000 | , | 37.26000 |
| DP1 | = | 101.80000 | , | |
| DP2 | = | 20.20000 | , | |
| DPRES | = | 101.80000 | , | 20.20000 |
| B1 | = | 1.410000 | , | |
| B2 | = | 2.520000 | , | |
| HOLL | = | 1.410000 | , | 2.520000 |
| SGW | = | 7.000000 | , | |
| AN1 | = | 110.0000 | , | |
| ST12 | = | 0.000000E+00 | | |
| SEND | | | | |
| SNAME2 | | | | |
| EYELAT | = | 22.00000 | , | |
| DIREC | = | 290.00000 | , | |
| SPEED | = | 11.00000 | , | |
| EYPRES | = | 951.00000 | , | |
| PFAR | = | 1012.000 | , | |
| RAD1 | = | 11.88000 | , | |
| RAD2 | = | 46.85000 | , | |
| RADIUS | = | 11.88000 | , | 46.85000 |
| DP1 | = | 45.07000 | , | |
| DP2 | = | 15.93000 | , | |
| DPRES | = | 45.07000 | , | 15.93000 |
| B1 | = | 0.5600000 | , | |
| B2 | = | 2.5200000 | , | |
| HOLL | = | 0.5600000 | , | 2.5200000 |
| SGW | = | 7.000000 | , | |
| AN1 | = | 110.0000 | , | |
| ST12 | = | 0.0000000E+00 | | |
| SEND | | | | |
| SNAME2 | | | | |
| EYELAT | = | 22.00000 | , | |
| DIREC | = | 290.00000 | , | |
| SPEED | = | 11.00000 | , | |
| EYPRES | = | 950.00000 | , | |
| PFAR | = | 1012.000 | , | |
| RAD1 | = | 17.28000 | , | |
| RAD2 | = | 55.82000 | , | |
| RADIUS | = | 17.28000 | , | 55.82000 |
| DP1 | = | 34.57000 | , | |
| DP2 | = | 27.43000 | , | |
| DPRES | = | 34.57000 | , | 27.43000 |
| B1 | = | 0.9400000 | , | |
| B2 | = | 2.5200000 | , | |
| HOLL | = | 0.9400000 | , | 2.5200000 |
| SGW | = | 7.000000 | , | |
| AN1 | = | 110.0000 | , | |
| ST12 | = | 0.0000000E+00 | | |
| SEND | | | | |

Snapshot 6

Snapshot 7

Snapshot 8

Figure C1. (Sheet 3 of 6)

```

SNAME2
EYELAT = 23.00000 , Snapshot 9
DIREC = 290.00000 ,
SPEED = 11.00000 ,
EYPRES = 949.00000 ,
PFAR = 1010.000 ,
RAD1 = 11.89000 ,
RAD2 = 43.53000 ,
RADIUS = 11.88000 , 43.53000 ,
DP1 = 40.67000 ,
DP2 = 20.33000 ,
DPRES = 40.67000 , 20.33000 ,
B1 = 0.7500000 ,
B2 = 2.5200000 ,
HDLL = 0.7500000 , 2.5200000 ,
SGW = 7.0000000 ,
AN1 = 110.00000 ,
ST12 = 0.0000000E+00
SEND

SNAME2
EYELAT = 23.00000 , Snapshot 10
DIREC = 290.00000 ,
SPEED = 11.00000 ,
EYPRES = 950.00000 ,
PFAR = 1011.000 ,
RAD1 = 29.70000 ,
RAD2 = 91.63000 ,
RADIUS = 29.70000 , 91.63000 ,
DP1 = 51.84000 ,
DP2 = 9.1600000 ,
DPRES = 51.84000 , 9.1600000 ,
B1 = 1.1200000 ,
B2 = 2.2400000 ,
HDLL = 1.1200000 , 2.2400000 ,
SGW = 7.0000000 ,
AN1 = 110.00000 ,
ST12 = 0.0000000E+00
SEND

SNAME2
EYELAT = 24.00000 , Snapshot 11
DIREC = 290.00000 ,
SPEED = 11.00000 ,
EYPRES = 953.00000 ,
PFAR = 1010.000 ,
RAD1 = 27.00000 ,
RAD2 = 64.21000 ,
RADIUS = 27.00000 , 64.21000 ,
DP1 = 46.62000 ,
DP2 = 10.38000 ,
DPRES = 46.62000 , 10.38000 ,
B1 = 1.3300000 ,
B2 = 2.5200000 ,
HDLL = 1.3300000 , 2.5200000 ,
SGW = 7.0000000 ,
AN1 = 110.00000 ,
ST12 = 0.0000000E+00
SEND

```

Figure C1. (Sheet 4 of 6)

```

SNAME2
EYELAT = 24.00000 , 
DIREC = 290.00000 , 
SPEED = 11.00000 , 
EYPRES = 954.00000 , 
PFAIR = 1009.000 , 
RAD1 = 21.60000 , 
RAD2 = 60.61000 , 
RADIUS = 21.60000 , 60.61000 , 
DP1 = 44.98000 , 
DP2 = 10.02000 , 
DPRES = 44.98000 , 10.02000 , 
B1 = 1.190000 , 
B2 = 2.520000 , 
HOLL = 1.190000 , 2.520000 , 
SGW = 7.000000 , 
AN1 = 110.00000 , 
ST12 = 0.000000E+00
SEND
SNAME2
EYELAT = 999.00000 , 
DIREC = 290.00000 , 
SPEED = 11.00000 , 
EYPRES = 954.00000 , 
PFAIR = 1009.000 , 
RAD1 = 0.000000E+00, 
RAD2 = 0.000000E+00, 
RADIUS = 2#0.000000E+00, 
DP1 = 0.000000E+00, 
DP2 = 0.000000E+00, 
DPRES = 2#0.000000E+00, 
B1 = 1.000000 , 
B2 = 0.000000E+00, 
HOLL = 1.000000 , 0.0000000E+00, 
SGW = 7.000000 , 
AN1 = 110.00000 , 
ST12 = 0.000000E+00
SEND

```

| 0 | 20 | 0 | 0 | 0 | 1 | 0 |
|-----|----|---|---|---|----|---|
| 2 | 20 | 0 | 0 | 0 | 2 | 0 |
| 4 | 20 | 0 | 0 | 0 | 3 | 0 |
| 6 | 20 | 0 | 0 | 0 | 4 | 0 |
| 8 | 20 | 0 | 0 | 0 | 5 | 0 |
| 10 | 20 | 0 | 0 | 0 | 6 | 0 |
| 12 | 20 | 0 | 0 | 0 | 7 | 0 |
| 14 | 20 | 0 | 0 | 0 | 8 | 0 |
| 16 | 20 | 0 | 0 | 0 | 9 | 0 |
| 18 | 20 | 0 | 0 | 0 | 10 | 0 |
| 20 | 20 | 0 | 0 | 0 | 11 | 0 |
| 22 | 20 | 0 | 0 | 0 | 12 | 0 |
| 999 | 0 | 0 | 0 | 0 | 0 | 0 |

Figure C1. (Sheet 5 of 6)

| HOUR | LAT | LONG | STORM HISTORY SNAPS | ZERO HOUR IS INTERP ROT | 8809 151200 |
|------|-----|------|---------------------|-------------------------|-------------|
| 0 | 20 | 0 | 0 0 1 0 | 0.0000 | 0 |
| 1 | 20 | 0 | 0 0 1 2 | 0.5000 | 0 |
| 2 | 20 | 0 | 0 0 2 0 | 0.0000 | 0 |
| 3 | 20 | 0 | 0 0 2 3 | 0.5000 | 0 |
| 4 | 20 | 0 | 0 0 3 0 | 0.0000 | 0 |
| 5 | 20 | 0 | 0 0 3 4 | 0.5000 | 0 |
| 6 | 20 | 0 | 0 0 4 0 | 0.0000 | 0 |
| 7 | 20 | 0 | 0 0 4 5 | 0.5000 | 0 |
| 8 | 20 | 0 | 0 0 5 0 | 0.0000 | 0 |
| 9 | 20 | 0 | 0 0 5 6 | 0.5000 | 0 |
| 10 | 20 | 0 | 0 0 6 0 | 0.0000 | 0 |
| 11 | 20 | 0 | 0 0 6 7 | 0.5000 | 0 |
| 12 | 20 | 0 | 0 0 7 0 | 0.0000 | 0 |
| 13 | 20 | 0 | 0 0 7 8 | 0.5000 | 0 |
| 14 | 20 | 0 | 0 0 8 0 | 0.0000 | 0 |
| 15 | 20 | 0 | 0 0 8 9 | 0.5000 | 0 |
| 16 | 20 | 0 | 0 0 9 0 | 0.0000 | 0 |
| 17 | 20 | 0 | 0 0 9 10 | 0.5000 | 0 |
| 18 | 20 | 0 | 0 0 10 0 | 0.0000 | 0 |
| 19 | 20 | 0 | 0 0 10 11 | 0.5000 | 0 |
| 20 | 20 | 0 | 0 0 11 0 | 0.0000 | 0 |
| 21 | 20 | 0 | 0 0 11 12 | 0.5000 | 0 |
| 22 | 20 | 0 | 0 0 12 0 | 0.0000 | 0 |

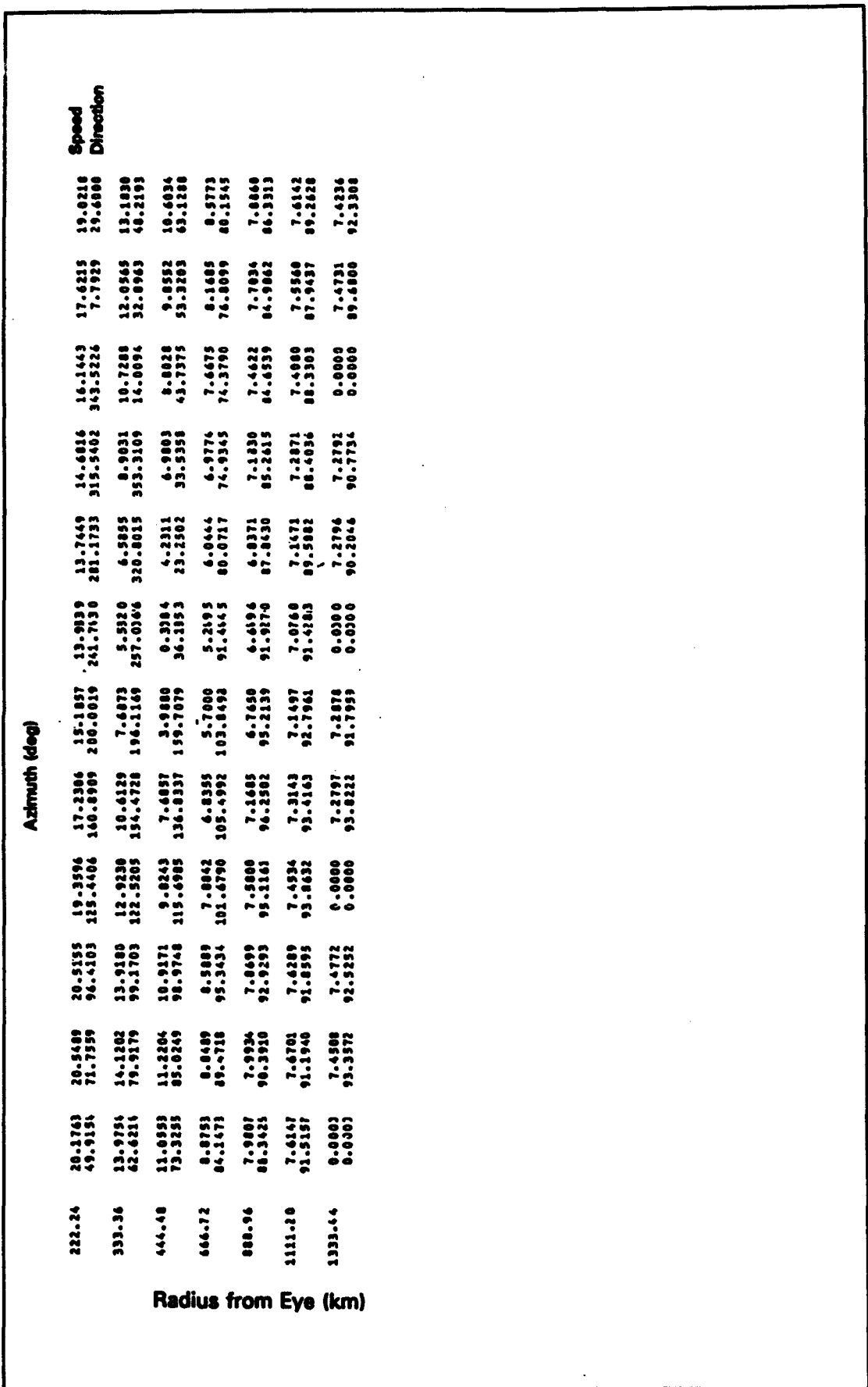
\$WHAT
 KSTEP2 = 22
 \$END
 WORKK: 0 8809 151200
 WORKK: 1 8809 151500
 WORKK: 2 8809 151800
 WORKK: 3 8809 152100
 WORKK: 4 8809 160000
 WORKK: 5 8809 160300
 WORKK: 6 8809 160600
 WORKK: 7 8809 160900
 WORKK: 8 8809 161200
 WORKK: 9 8809 161500
 WORKK: 10 8809 161800
 WORKK: 11 8809 162100
 WORKK: 12 8809 170000
 WORKK: 13 8809 170300
 WORKK: 14 8809 170600
 WORKK: 15 8809 170900
 WORKK: 16 8809 171200
 WORKK: 17 8809 171500
 WORKK: 18 8809 171800
 WORKK: 19 8809 172100
 WORKK: 20 8809 180000
 WORKK: 21 8809 180300
 WORKK: 22 8809 180600
 END OF STRESS RUN

Figure C1. (Sheet 6 of 6)

| Hour | Radius from Eye (km) | Azimuth (deg) | | | | | | | | | | | | Speed Direction |
|--------|----------------------|---------------|---------|---------|---------|---------|---------|---------|---------|---------|---------|---------|---------|--------------------|
| | | 0. | 30. | 60. | 90. | 120. | 150. | 180. | 210. | 240. | 270. | 300. | 330. | |
| 1.85 | 5.2191 | 5.2045 | 5.0998 | 5.0868 | 5.0242 | 5.0450 | 5.0535 | 5.0752 | 5.0781 | 5.0587 | 5.0396 | 5.0228 | 5.0474 | 98.6693 |
| 3.70 | 5.0953 | 5.0707 | 5.0574 | 5.0731 | 5.0165 | 5.0367 | 5.0306 | 5.0111 | 6.0155 | 6.0031 | 5.9781 | 5.9342 | 5.9342 | 98.5902 |
| 5.56 | 5.0887 | 5.0381 | 5.0130 | 5.0349 | 5.0075 | 5.0668 | 6.0199 | 6.0671 | 6.0521 | 6.0429 | 6.0169 | 5.9667 | 5.9667 | 99.4205 |
| 7.43 | 5.0663 | 5.0081 | 5.0649 | 5.0764 | 5.0964 | 5.0836 | 5.0507 | 6.0029 | 6.0006 | 6.0066 | 6.0031 | 6.0009 | 6.0009 | 100.3353 |
| 9.26 | 5.0583 | 5.0813 | 5.1133 | 5.1486 | 5.0467 | 5.0662 | 6.0331 | 6.1189 | 6.1304 | 6.1428 | 6.1333 | 6.0610 | 6.0610 | 102.4407 |
| 11.11 | 5.0602 | 5.0649 | 5.0661 | 5.0882 | 5.0429 | 6.0117 | 6.1163 | 6.1807 | 6.2273 | 6.2359 | 6.1741 | 6.1741 | 6.1741 | 101.3340 |
| 12.96 | 5.0181 | 5.0660 | 5.0923 | 5.0334 | 5.0082 | 5.0233 | 6.0255 | 6.1500 | 6.1925 | 6.2732 | 6.4462 | 6.4462 | 6.4462 | 103.7215 |
| 14.82 | 5.0015 | 5.0091 | 5.0234 | 5.0666 | 5.0212 | 6.0349 | 6.1339 | 6.2316 | 6.4952 | 6.9506 | 7.1461 | 7.1547 | 7.1547 | 103.7215 |
| 16.67 | 5.0062 | 5.0973 | 5.4917 | 5.2330 | 5.0279 | 5.0943 | 6.1598 | 6.2660 | 6.2947 | 6.3797 | 6.7210 | 6.9364 | 6.9364 | 105.0828 |
| 18.52 | 5.0065 | 6.0193 | 5.0063 | 5.2179 | 5.0923 | 5.0600 | 5.0750 | 5.0650 | 5.0650 | 5.0591 | 5.0591 | 5.0591 | 5.0591 | 102.0374 |
| 27.78 | 32.0373 | 24.3052 | 21.3874 | 18.7590 | 15.5180 | 11.9773 | 11.5172 | 21.4211 | 36.7541 | 41.4234 | 44.2547 | 42.3971 | 42.3971 | 44.0079 |
| 37.04 | 46.2677 | 46.0264 | 33.2342 | 29.2763 | 27.3211 | 26.8793 | 32.0644 | 40.2791 | 43.2172 | 44.8667 | 46.8933 | 47.3146 | 47.3146 | 44.0079 |
| 46.30 | 45.5667 | 43.5132 | 37.4322 | 35.4423 | 32.9499 | 34.1627 | 37.0834 | 39.7371 | 41.2559 | 42.8003 | 44.4066 | 45.2970 | 45.2970 | 44.0079 |
| 55.56 | 43.2333 | 43.2629 | 39.0072 | 35.5084 | 36.4821 | 35.3937 | 36.7984 | 37.8656 | 38.9099 | 40.4397 | 41.9891 | 42.8609 | 42.8609 | 41.9891 |
| 74.08 | 40.2472 | 40.5314 | 39.2017 | 36.5206 | 35.2295 | 33.9128 | 33.0255 | 34.7682 | 35.2842 | 36.6579 | 38.1599 | 39.2419 | 39.2419 | 38.1599 |
| 92.40 | 37.4363 | 37.9756 | 37.6074 | 35.7166 | 33.8160 | 32.3110 | 31.7723 | 31.9663 | 32.5325 | 33.9074 | 35.2797 | 36.5343 | 36.5343 | 35.2797 |
| 130.90 | 30.2692 | 30.7611 | 30.7445 | 29.4682 | 27.5210 | 25.7919 | 24.7662 | 24.9025 | 26.9451 | 26.2332 | 27.6136 | 29.0277 | 29.0277 | 27.6136 |
| 166.68 | 26.2361 | 26.4758 | 26.7038 | 25.5612 | 23.4929 | 21.1182 | 20.3507 | 20.1863 | 20.7486 | 22.1619 | 23.5127 | 24.9486 | 24.9486 | 23.5127 |
| 174.00 | 23.2022 | 27.7149 | 26.7039 | 25.9559 | 16.2286 | 19.8186 | 23.4804 | 27.0124 | 27.0124 | 27.0124 | 27.0124 | 26.5199 | 26.5199 | 26.5199 |

Figure C2. Wind speed and direction fields, Snapshot 1, Hurricane Gilbert (Continued)

Figure C2. (Concluded)



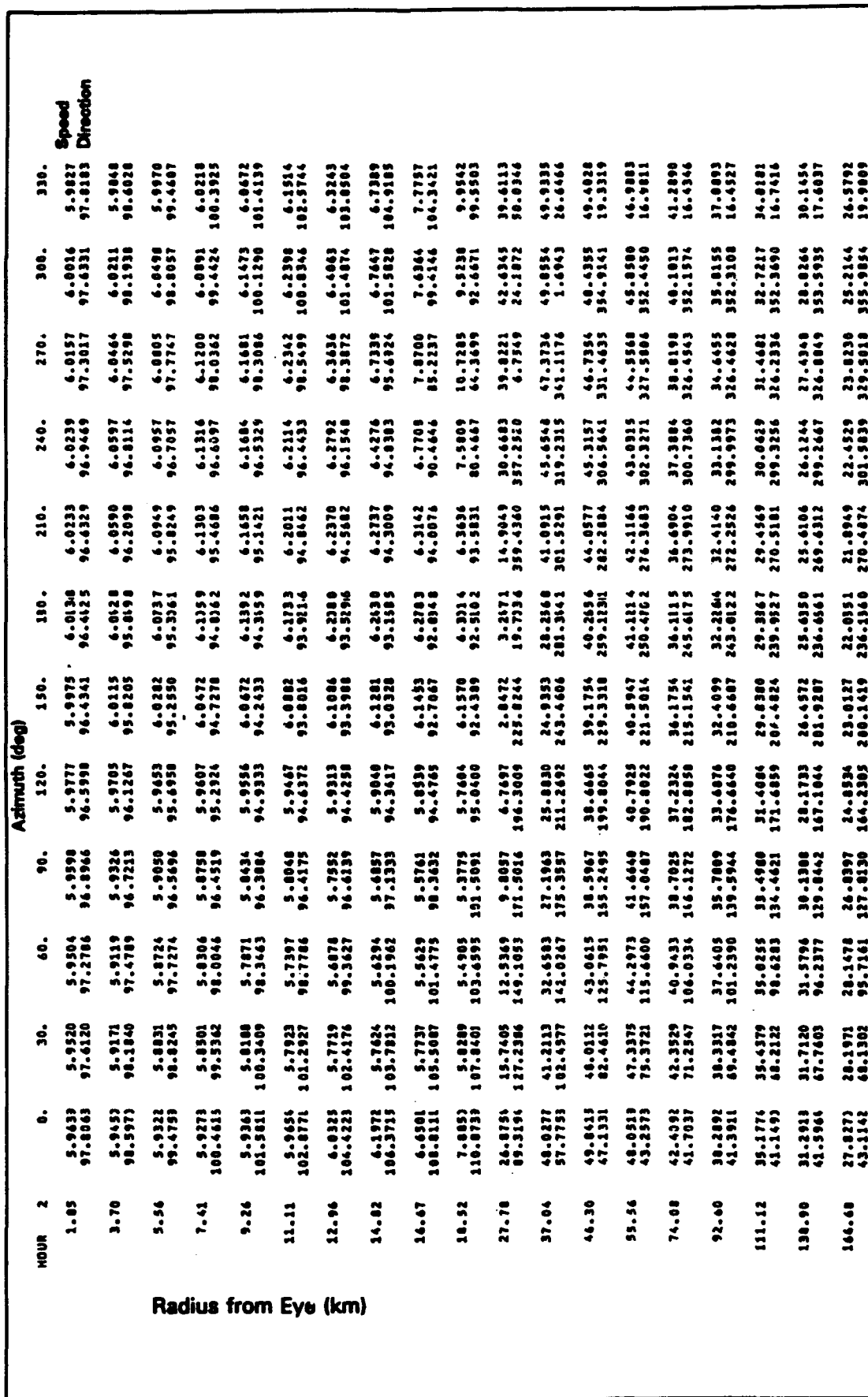


Figure C3. Wind speed and direction fields, Snapshot 2, Hurricane Gilbert (Continued)

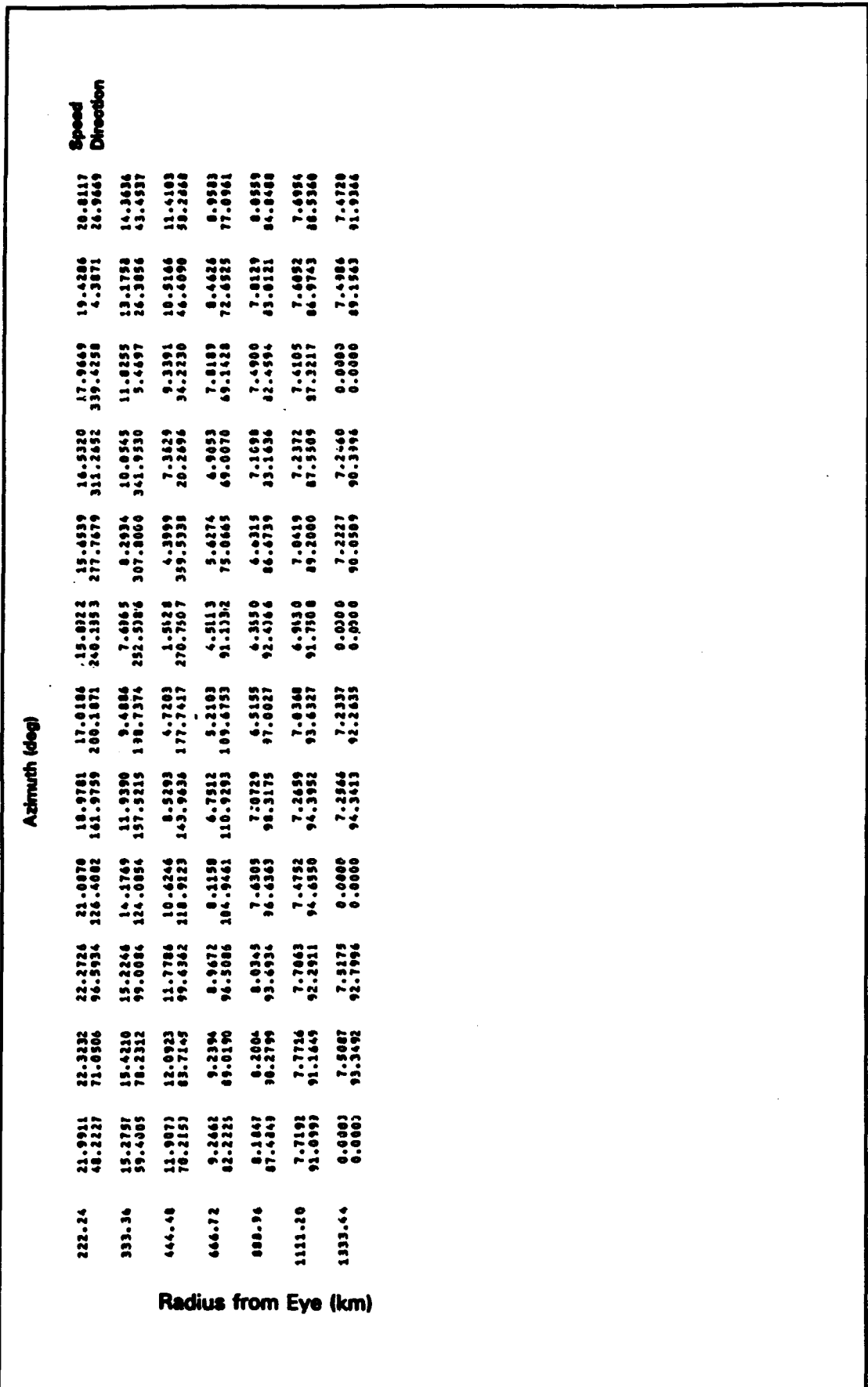


Figure C3. (Concluded)

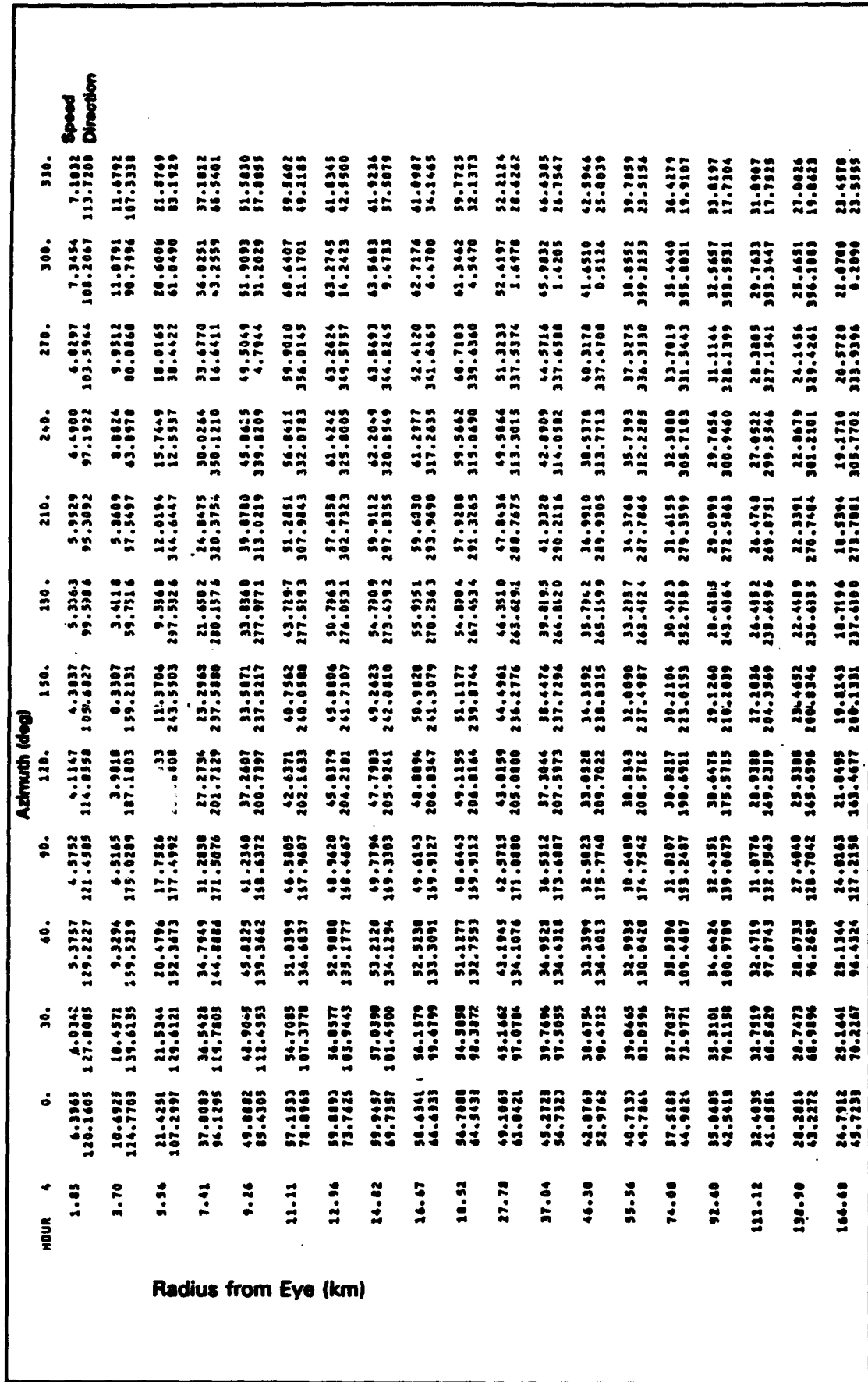


Figure C4. Wind speed and direction fields, Snapshot 3, Hurricane Gilbert (Continued)

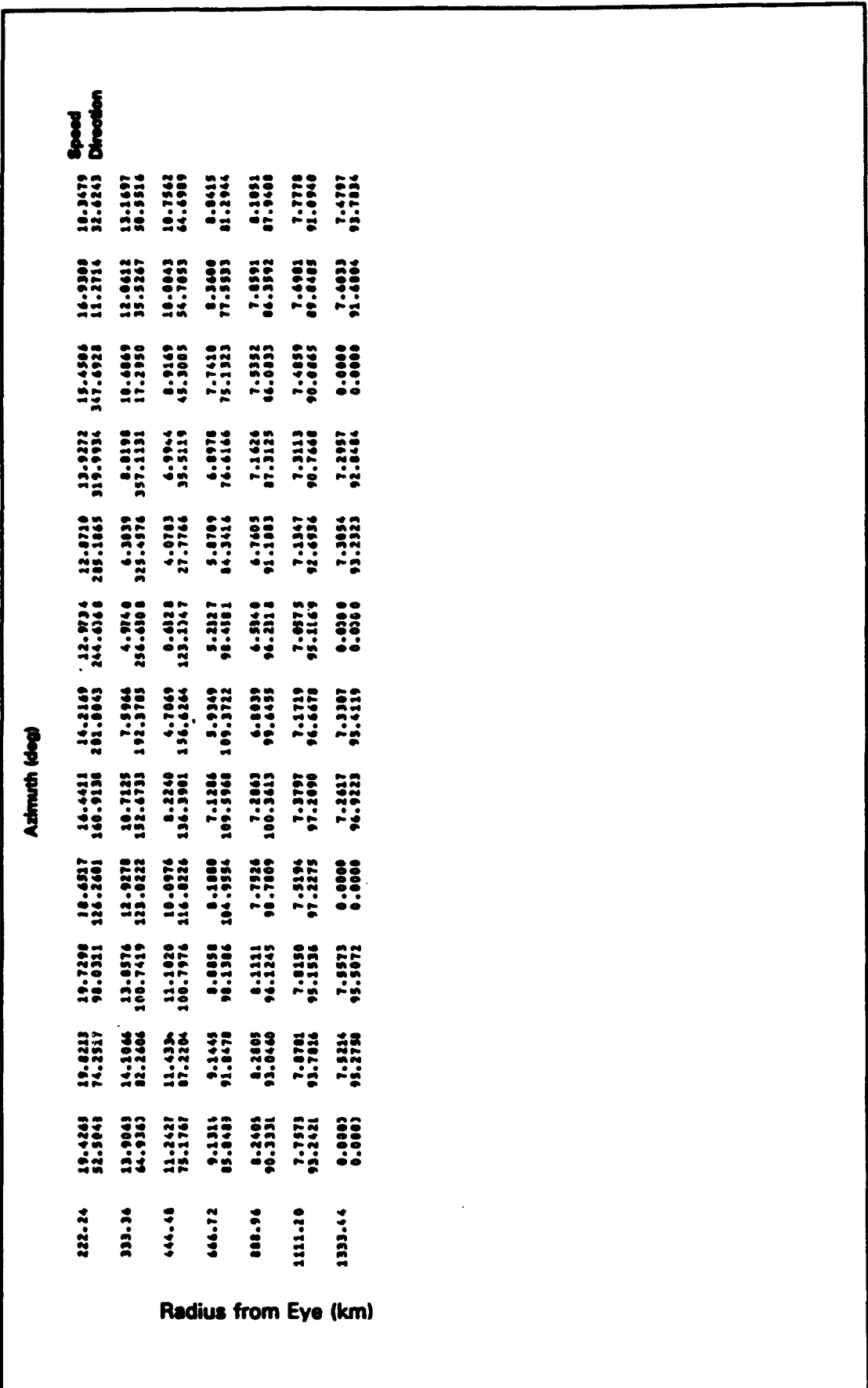


Figure C4. (Concluded)

| Hour | 6. | Azimuth (deg) | | | | | | | | | | Speed Direction |
|----------|----------|---------------|----------|----------|----------|----------|----------|----------|----------|----------|----------|--------------------|
| | | 30. | 60. | 90. | 120. | 150. | 180. | 210. | 240. | 270. | 300. | |
| 1.45 | 8.7587 | 8.8469 | 7.3751 | 6.2912 | 2.9668 | 2.7953 | 6.3706 | 6.2876 | 6.6405 | 6.6346 | 9.4994 | 9.8593 |
| 136.1323 | 144.1176 | 153.1153 | 155.2415 | 156.7932 | 158.7933 | 92.6150 | 75.2947 | 81.8592 | 95.7165 | 103.4593 | 114.1064 | |
| 3.70 | 18.8375 | 19.1938 | 18.1798 | 16.5379 | 12.9362 | 8.7114 | 6.3546 | 9.5660 | 13.7629 | 15.3382 | 17.4939 | 19.7043 |
| 116.3443 | 130.2980 | 150.3503 | 154.0237 | 209.0165 | 215.5932 | 321.2597 | 319.1177 | 26.7669 | 52.7107 | 70.0027 | 92.7229 | |
| 5.16 | 27.5673 | 36.8985 | 35.8393 | 31.5210 | 26.9226 | 23.0200 | 21.5235 | 24.4005 | 26.9389 | 32.3592 | 35.3477 | 37.1543 |
| 95.0591 | 119.5443 | 144.4468 | 171.3501 | 202.3593 | 218.3506 | 200.2772 | 321.0060 | 351.1961 | 18.9060 | 44.2365 | 69.2312 | |
| 7.41 | 52.3123 | 51.7840 | 48.8768 | 63.8776 | 39.4607 | 35.9773 | 36.1742 | 41.3764 | 46.8507 | 50.9407 | 54.2249 | |
| 83.7693 | 110.5392 | 137.4012 | 156.9833 | 199.4220 | 236.5291 | 276.5392 | 311.6202 | 339.1288 | 5.1511 | 31.0071 | 56.8460 | |
| 9.26 | 69.2722 | 58.3196 | 54.4180 | 49.4179 | 45.6254 | 43.7122 | 46.7360 | 50.4535 | 56.4512 | 61.0504 | 63.1035 | 62.2220 |
| 74.3502 | 104.9284 | 136.3890 | 166.1550 | 200.7326 | 239.1822 | 276.5372 | 307.2585 | 312.3792 | 356.6454 | 21.5529 | 48.5523 | |
| 11.11 | 61.7753 | 59.2260 | 55.3876 | 51.2279 | 48.1242 | 48.5398 | 53.3904 | 60.4504 | 65.7414 | 65.5473 | 65.2947 | 63.7561 |
| 72.4413 | 102.2594 | 133.6112 | 157.2567 | 203.7365 | 261.7421 | 276.0103 | 303.1263 | 326.7779 | 310.5916 | 15.0671 | 42.6163 | |
| 12.96 | 61.2395 | 58.3482 | 54.4777 | 51.2481 | 51.7784 | 57.3164 | 61.9924 | 64.4035 | 64.4035 | 65.6483 | 65.3220 | 63.4411 |
| 69.4763 | 100.8050 | 133.7936 | 169.1574 | 204.5296 | 243.0662 | 274.3847 | 299.2185 | 322.2239 | 346.0483 | 10.7110 | 38.2669 | |
| 14.82 | 59.8243 | 56.6528 | 53.1556 | 50.5644 | 50.0220 | 53.9123 | 58.3169 | 61.5660 | 63.3714 | 64.5352 | 64.3750 | 62.3946 |
| 67.5272 | 99.9166 | 134.2455 | 171.3573 | 208.4510 | 243.2396 | 271.3716 | 295.6800 | 318.7166 | 342.8263 | 7.7321 | 35.6183 | |
| 16.67 | 57.4673 | 54.6111 | 51.3413 | 49.4066 | 50.9395 | 52.7386 | 57.5953 | 60.2171 | 61.6226 | 62.7707 | 63.8473 | 63.4411 |
| 66.6825 | 99.6381 | 130.4933 | 172.7232 | 209.8978 | 242.6661 | 269.3732 | 293.6667 | 316.7347 | 340.5663 | 5.6432 | 33.5158 | |
| 18.52 | 55.4693 | 52.3469 | 49.3679 | 47.8010 | 49.4753 | 52.1007 | 55.4111 | 58.9281 | 60.4404 | 60.8260 | 61.3083 | 59.7045 |
| 64.5177 | 99.5459 | 135.2461 | 173.6429 | 210.2333 | 241.4376 | 247.4376 | 271.4279 | 291.1797 | 314.7228 | 330.9867 | 3.9918 | 31.9120 |
| 27.79 | 58.1195 | 45.7728 | 41.1246 | 43.2747 | 42.7690 | 44.4606 | 46.3540 | 47.9773 | 49.4243 | 51.3451 | 52.4901 | 51.1543 |
| 60.0335 | 100.9063 | 140.0168 | 177.4193 | 210.2338 | 239.2319 | 264.8191 | 288.0164 | 312.7312 | 336.5460 | 6.2422 | 26.8616 | |
| 37.84 | 47.3952 | 42.0494 | 37.3719 | 36.9136 | 38.1612 | 39.5896 | 40.8154 | 42.1046 | 43.4624 | 45.0299 | 46.5221 | 47.3943 |
| 52.1713 | 93.4259 | 140.2711 | 178.4746 | 210.9635 | 237.0774 | 262.9564 | 287.4566 | 311.6602 | 335.6173 | 356.7277 | 23.3724 | |
| 46.30 | 44.6671 | 43.0687 | 37.9987 | 35.4313 | 35.5413 | 36.4519 | 37.5746 | 39.3551 | 41.5723 | 42.5760 | 43.5639 | 42.9014 |
| 47.7362 | 81.1588 | 126.2334 | 170.9221 | 204.7558 | 232.5748 | 258.3649 | 283.3655 | 307.9482 | 332.8180 | 356.6253 | 26.9060 | |
| 55.56 | 42.3251 | 42.2377 | 39.3022 | 36.2876 | 35.1939 | 34.9469 | 35.0557 | 36.1846 | 37.9296 | 38.4960 | 40.0002 | 41.0002 |
| 44.5223 | 74.1461 | 110.6455 | 157.2176 | 182.7632 | 223.4742 | 251.9712 | 278.0220 | 304.2259 | 329.9261 | 356.4931 | 38.3977 | |
| 74.88 | 38.4597 | 29.0402 | 38.2046 | 36.3213 | 34.8021 | 33.9439 | 32.3117 | 32.9778 | 33.2506 | 34.4683 | 36.0990 | 37.3913 |
| 41.4574 | 68.7123 | 160.5228 | 137.4882 | 174.4264 | 207.9711 | 248.3510 | 269.4181 | 298.0038 | 325.1468 | 351.1395 | 15.8077 | |
| 92.44 | 34.7072 | 35.1943 | 35.9497 | 33.5277 | 31.5231 | 29.8140 | 28.9198 | 28.0042 | 29.2471 | 30.5728 | 31.9501 | 33.3974 |
| 130.98 | 24.9083 | 26.3179 | 26.3597 | 25.4229 | 23.2679 | 21.2990 | 20.3232 | 19.3443 | 20.3927 | 21.7892 | 23.2420 | 24.4644 |
| 144.68 | 22.7019 | 22.7141 | 22.7297 | 21.7449 | 19.4088 | 17.2160 | 16.0168 | 15.0073 | 16.5463 | 16.9889 | 19.5601 | 21.0074 |
| 48.7092 | 72.2471 | 97.3235 | 126.3743 | 137.4489 | 158.0082 | 219.1773 | 277.9183 | 310.9147 | 339.0566 | 359.8434 | 22.2374 | |

Radius from Eye (km)

Figure C5. Wind speed and direction fields, Snapshot 4, Hurricane Gilbert (Continued)

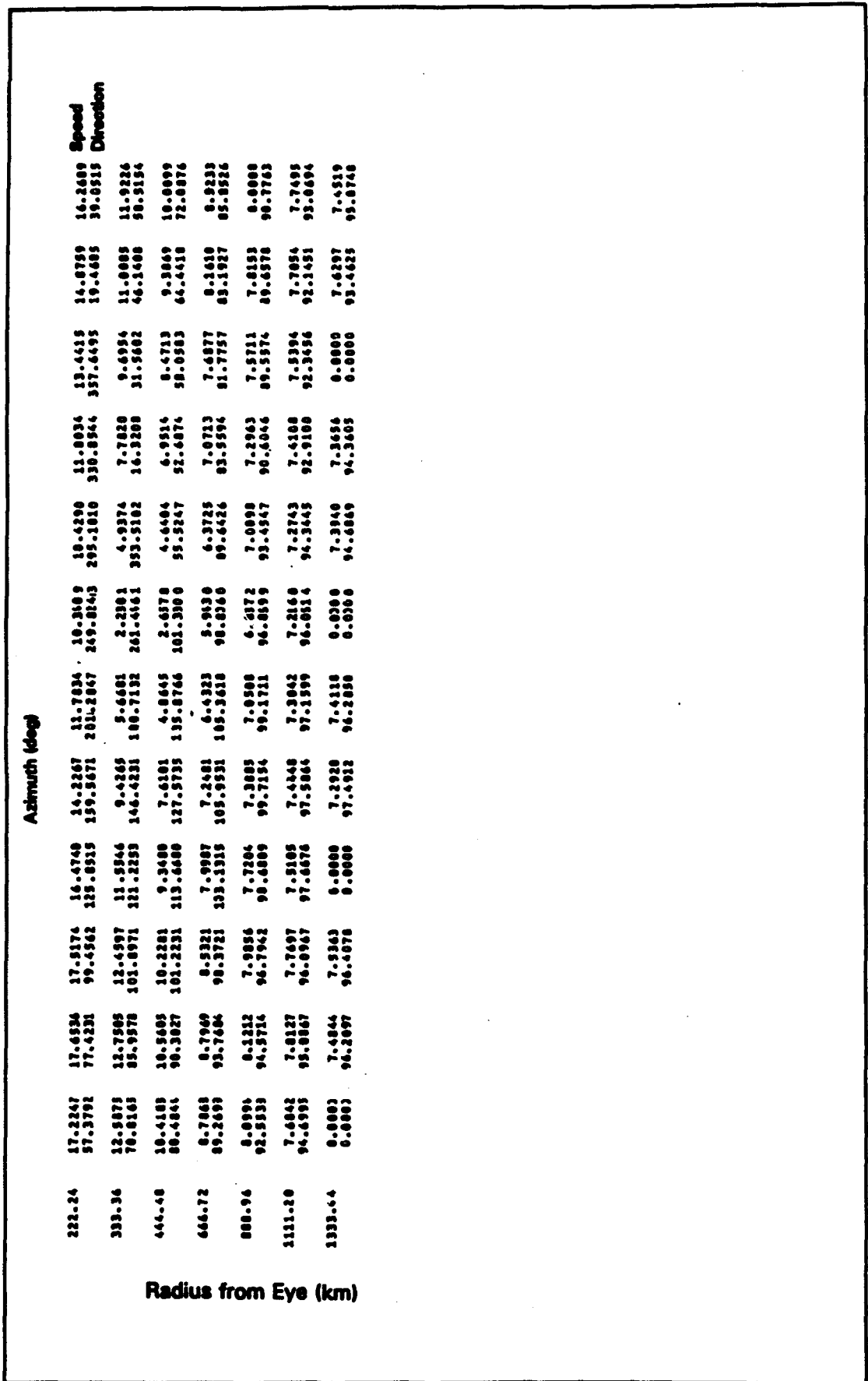


Figure C5. (Concluded)

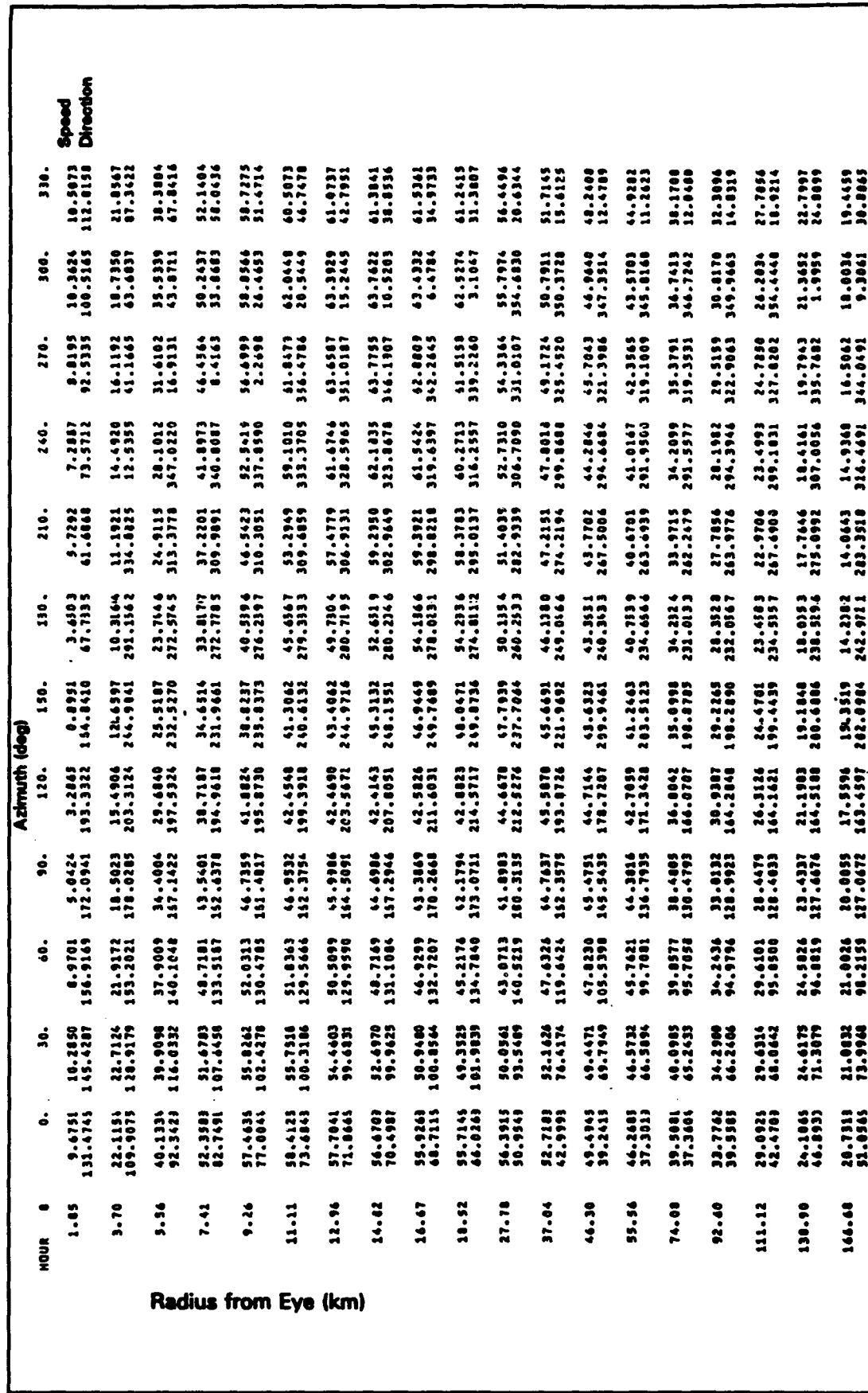


Figure C6. Wind speed and direction fields, Snapshot 5, Hurricane Gilbert (Continued)

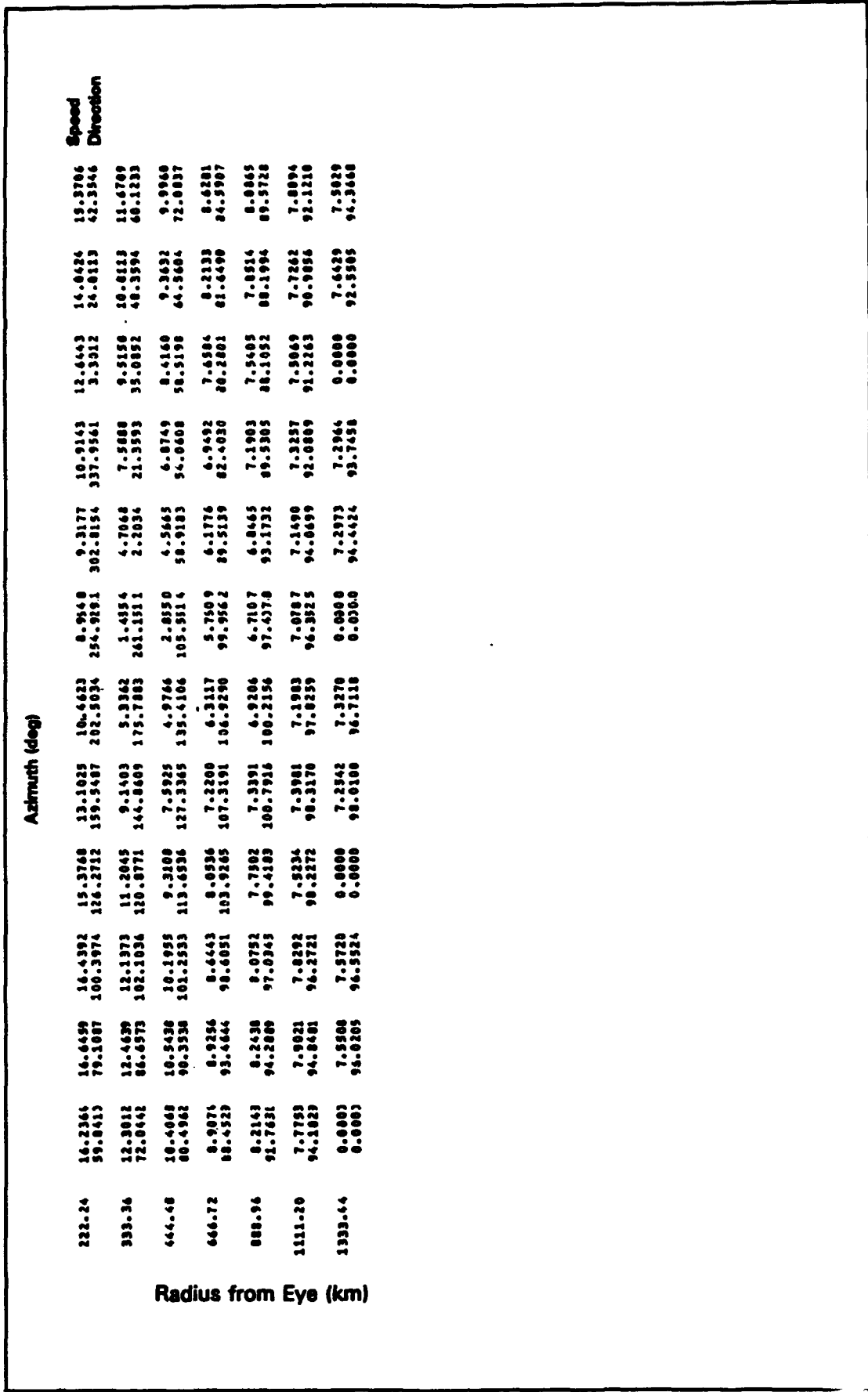
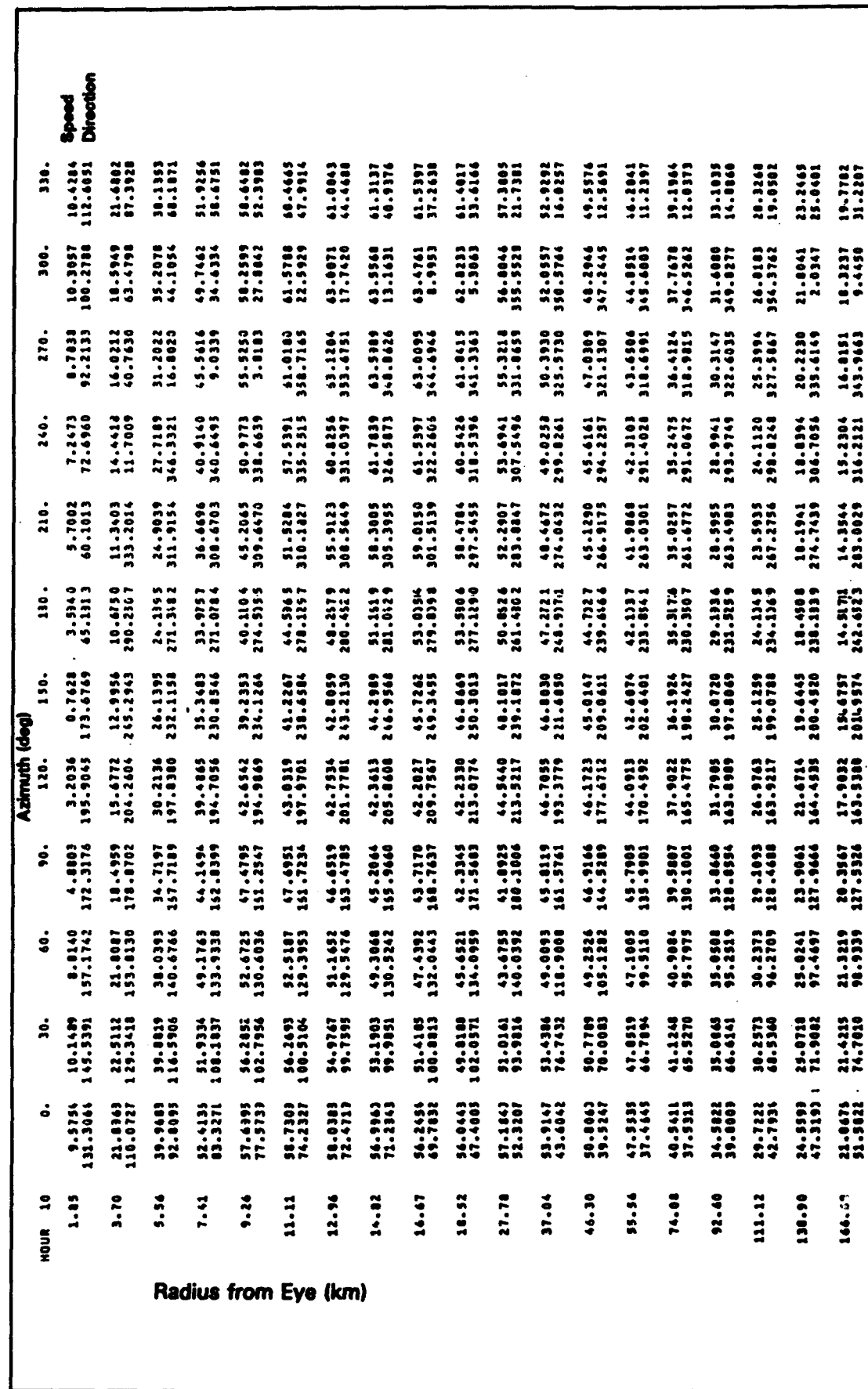


Figure C6. (Concluded)



Radius from Eye (km)

(Continued)

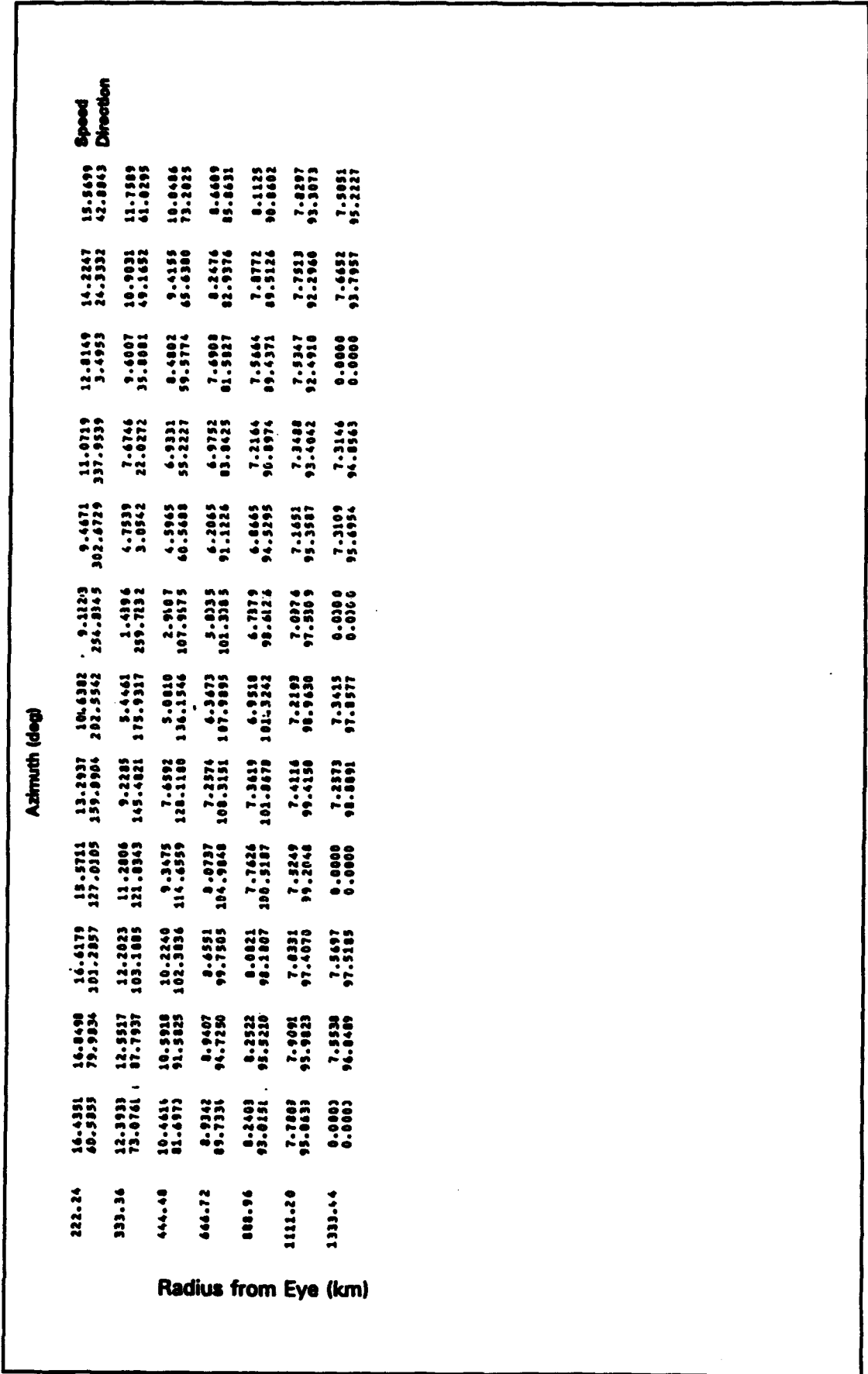


Figure C7. (Concluded)

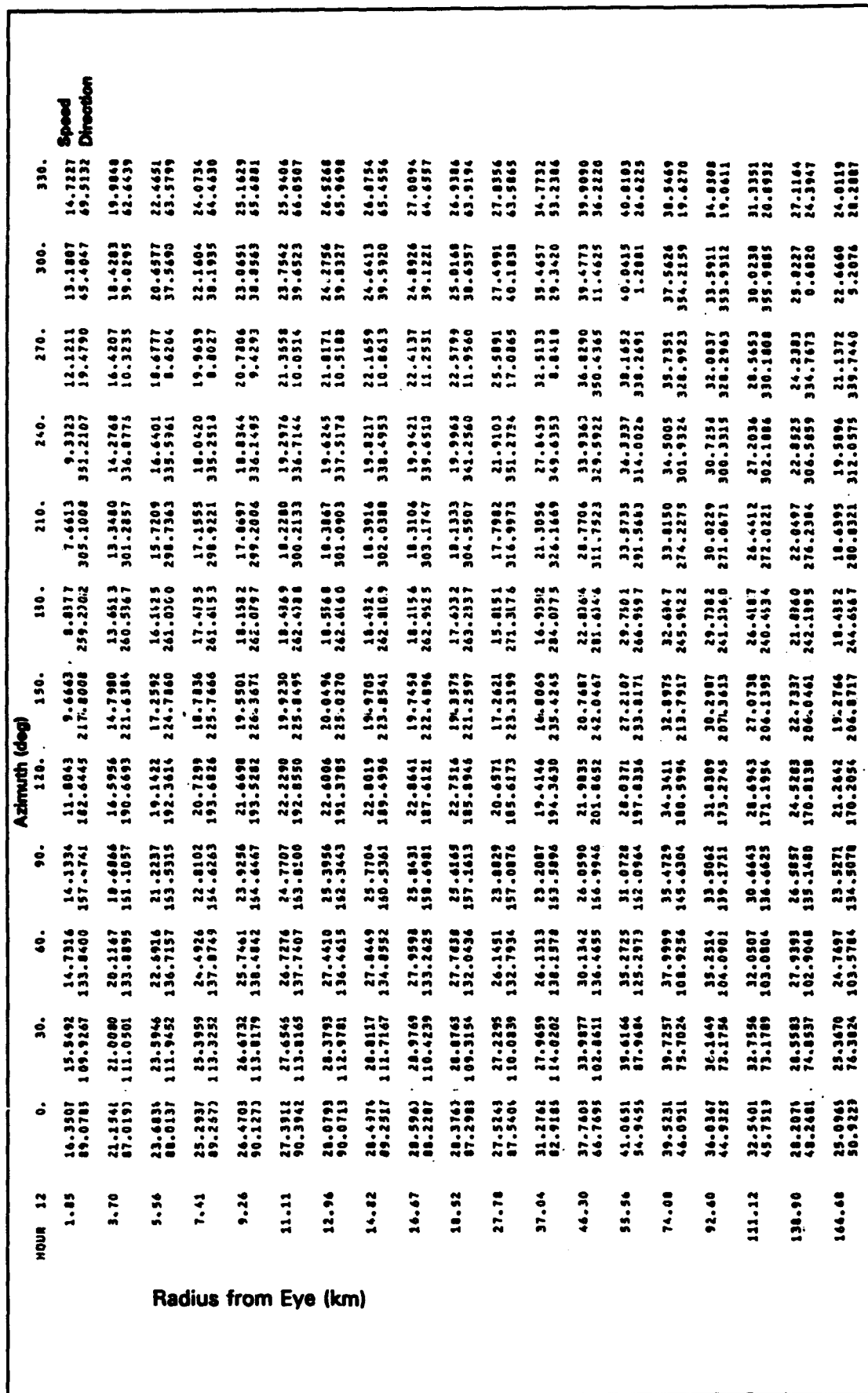


Figure C8. Wind speed and direction fields, Snapshot 7, Hurricane Gilbert (Continued)

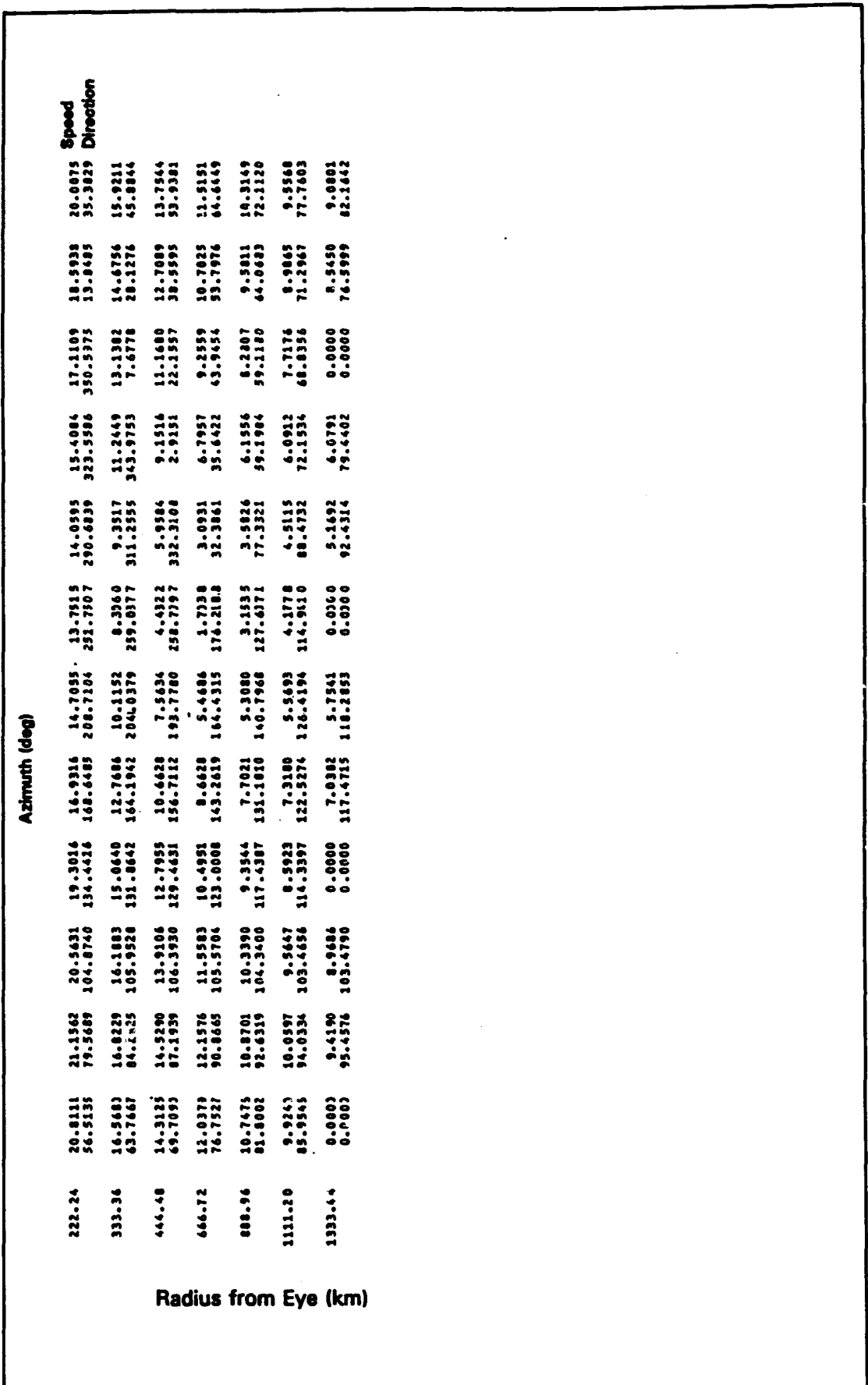


Figure C8. (Concluded)

| HOUR | 14 | Azimuth (deg) | | | | | | | | | | Speed | Direction |
|--------|----------|---------------|----------|----------|----------|----------|----------|----------|----------|----------|----------|----------|-----------|
| | | 0. | 30. | 60. | 90. | 120. | 150. | 180. | 210. | 240. | 270. | | |
| 1.85 | 6.3167 | 6.2123 | 5.7882 | 5.1633 | 4.7461 | 4.7461 | 5.1945 | 5.4502 | 5.9912 | 6.4114 | 6.8043 | 6.7548 | Speed |
| | 113.4983 | 117.9277 | 118.9435 | 115.4730 | 113.5873 | 107.9817 | 101.1154 | 96.6061 | 97.0941 | 101.4559 | 103.3165 | 107.4558 | Direction |
| 3.70 | 9.3112 | 9.0862 | 8.2132 | 6.4910 | 5.1180 | 2.0463 | 2.0463 | 3.6093 | 5.8876 | 7.4573 | 8.6332 | 9.4594 | |
| | 105.5661 | 123.3492 | 135.8164 | 115.0093 | 151.1655 | 143.0505 | 90.4703 | 65.2637 | 64.1703 | 74.3324 | 83.4606 | 96.7249 | |
| 5.56 | 13.2142 | 13.0437 | 12.2754 | 8.4234 | 5.1929 | 3.2935 | 5.1488 | 7.9992 | 10.1942 | 12.7349 | 13.7975 | 12.7349 | |
| | 101.9886 | 125.2039 | 140.1764 | 150.5241 | 105.4784 | 219.9188 | 285.0376 | 349.4021 | 19.9737 | 42.8766 | 63.3147 | 82.7475 | |
| 7.41 | 16.8883 | 17.0289 | 16.2297 | 14.5931 | 12.3905 | 10.0180 | 8.8706 | 9.2825 | 11.5762 | 13.3150 | 15.0022 | 16.1679 | |
| | 97.9123 | 118.8363 | 141.6720 | 165.5396 | 193.5907 | 230.2839 | 277.5774 | 322.8787 | 337.6623 | 26.3930 | 31.7343 | 75.3055 | |
| 9.26 | 20.2743 | 20.4665 | 19.9056 | 18.0361 | 15.9228 | 13.4850 | 12.4596 | 13.1633 | 14.5065 | 16.1560 | 17.9445 | 19.2404 | |
| | 96.4741 | 119.6323 | 142.4737 | 157.1964 | 196.3895 | 231.8090 | 273.3212 | 313.5428 | 348.1594 | 18.3159 | 46.3590 | 72.1667 | |
| 11.11 | 23.1022 | 23.7701 | 23.0663 | 21.1463 | 18.5180 | 16.0879 | 14.9322 | 15.4324 | 16.6294 | 18.3807 | 20.1093 | 21.8452 | |
| | 95.9632 | 119.3792 | 142.4355 | 167.3588 | 194.2962 | 230.9065 | 270.5374 | 307.0006 | 339.8620 | 15.2455 | 44.1015 | 70.3994 | |
| 12.96 | 25.6683 | 26.3959 | 25.6746 | 23.6869 | 20.7933 | 18.0016 | 16.7268 | 17.047 | 18.0205 | 20.1455 | 22.0099 | 24.0113 | |
| | 95.1533 | 118.9341 | 141.2413 | 166.2325 | 194.0393 | 229.2747 | 268.4595 | 306.9566 | 322.0164 | 13.6336 | 43.0226 | 70.1846 | |
| 14.82 | 27.6933 | 27.4618 | 27.6445 | 25.5862 | 22.4223 | 19.3911 | 17.8150 | 18.0439 | 19.4860 | 21.5614 | 23.6559 | 25.7190 | |
| | 93.9031 | 116.5405 | 139.2284 | 164.2486 | 192.3340 | 227.2160 | 267.0525 | 304.0743 | 331.5164 | 13.0553 | 42.1994 | 69.1750 | |
| 16.67 | 29.1255 | 29.9084 | 28.9386 | 26.7639 | 23.5632 | 20.0442 | 18.3133 | 18.7669 | 20.3842 | 22.7364 | 25.0775 | 27.1694 | |
| | 92.1422 | 114.3554 | 136.9860 | 151.9113 | 190.2466 | 225.0539 | 266.0706 | 306.0851 | 341.9314 | 13.0819 | 41.4002 | 67.8509 | |
| 18.52 | 29.4692 | 30.7179 | 29.5451 | 27.2449 | 24.1347 | 20.3251 | 18.397 | 19.0814 | 21.0763 | 23.7232 | 26.1338 | 28.1101 | |
| | 90.2622 | 112.2167 | 136.6950 | 159.7269 | 188.0776 | 223.4422 | 265.3289 | 308.8276 | 343.5373 | 13.6250 | 40.4221 | 66.4047 | |
| 27.78 | 30.7132 | 30.1161 | 28.8644 | 26.4438 | 22.9905 | 19.2543 | 17.7383 | 20.4126 | 25.5789 | 30.1293 | 32.2792 | 31.9115 | |
| | 87.0723 | 109.7474 | 131.7295 | 157.6473 | 186.7729 | 224.4622 | 273.0611 | 310.7719 | 352.2397 | 16.5688 | 39.3419 | 62.5939 | |
| 31.94 | 35.9041 | 30.4543 | 28.3870 | 25.1491 | 21.2310 | 16.0711 | 15.7367 | 16.3924 | 17.8092 | 19.1071 | 22.2181 | 41.1226 | |
| | 86.2313 | 113.9165 | 136.9709 | 154.9368 | 196.1668 | 238.3922 | 286.5193 | 322.8619 | 347.6337 | 5.1933 | 24.0314 | 49.1850 | |
| 44.30 | 43.7292 | 38.1410 | 32.5712 | 27.3968 | 23.1957 | 23.1957 | 27.2599 | 34.3286 | 40.5223 | 43.2903 | 45.9331 | 44.1238 | |
| | 43.3261 | 102.3553 | 137.5450 | 171.5198 | 208.1391 | 248.9361 | 284.3951 | 310.4670 | 326.7548 | 347.1288 | 37.8804 | 52.1669 | |
| 55.94 | 47.7531 | 45.9381 | 39.9193 | 34.2487 | 30.9906 | 31.0531 | 35.6531 | 48.2867 | 43.0494 | 44.7797 | 46.7223 | 47.1961 | |
| | 51.4451 | 85.3982 | 122.0643 | 166.3225 | 204.1390 | 238.4617 | 267.7323 | 289.2571 | 310.8600 | 334.9314 | 357.9331 | 395.9387 | |
| 74.08 | 47.2631 | 47.7271 | 46.1813 | 42.5727 | 43.9469 | 41.1600 | 40.7971 | 42.3924 | 42.4332 | 43.8169 | 45.3205 | 44.3935 | |
| | 41.3381 | 70.0167 | 104.1661 | 161.5234 | 176.6868 | 205.0109 | 240.3930 | 267.7920 | 295.4655 | 322.5900 | 348.3860 | 34.1311 | |
| 92.40 | 44.2671 | 64.4299 | 64.1783 | 62.7220 | 41.4710 | 39.4451 | 38.9101 | 39.0944 | 39.4565 | 40.7029 | 41.7655 | 43.1862 | |
| | 38.2463 | 67.0357 | 91.6673 | 132.5369 | 166.5817 | 199.5909 | 232.5516 | 262.0262 | 290.9577 | 319.0399 | 345.9387 | 31.4524 | |
| 111.12 | 46.4933 | 46.7662 | 46.5590 | 39.3421 | 37.6938 | 36.1250 | 35.0934 | 35.4555 | 36.7140 | 37.8852 | 39.2700 | | |
| | 38.9715 | 64.2596 | 91.0790 | 129.1239 | 143.5459 | 194.9359 | 229.9558 | 261.0335 | 290.8429 | 319.0163 | 344.4371 | 32.3193 | |
| 138.90 | 34.7275 | 35.1190 | 34.9954 | 33.9626 | 32.1515 | 30.4496 | 29.3938 | 29.2223 | 29.5757 | 30.7724 | 32.1345 | 33.4266 | |
| | 40.5929 | 67.0323 | 95.5495 | 127.0322 | 142.9711 | 196.3827 | 230.3771 | 263.6073 | 322.2280 | 350.0075 | 351.1750 | 15.1750 | |
| 144.68 | 30.1893 | 38.4352 | 38.3078 | 29.4091 | 27.3710 | 23.5357 | 24.0243 | 24.2397 | 24.7240 | 26.0802 | 27.4366 | 28.7774 | |
| | 43.9341 | 69.5160 | 97.0643 | 127.8675 | 142.9317 | 197.5369 | 232.4844 | 267.1037 | 298.4638 | 326.8257 | 354.3222 | 19.1913 | |

Figure C9. Wind speed and direction fields, Snapshot 8, Hurricane Gilbert (Continued)

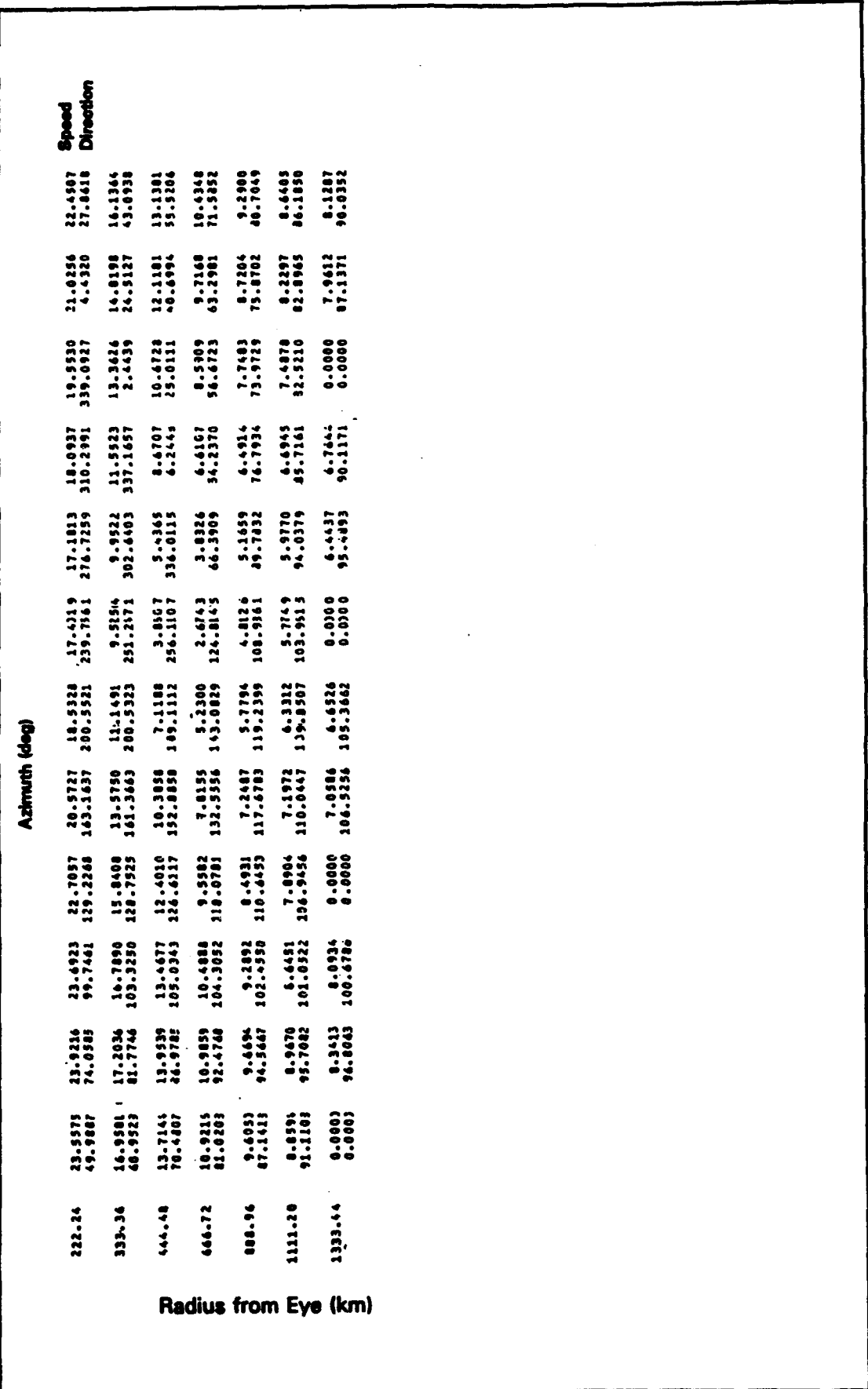


Figure C9. (Concluded)

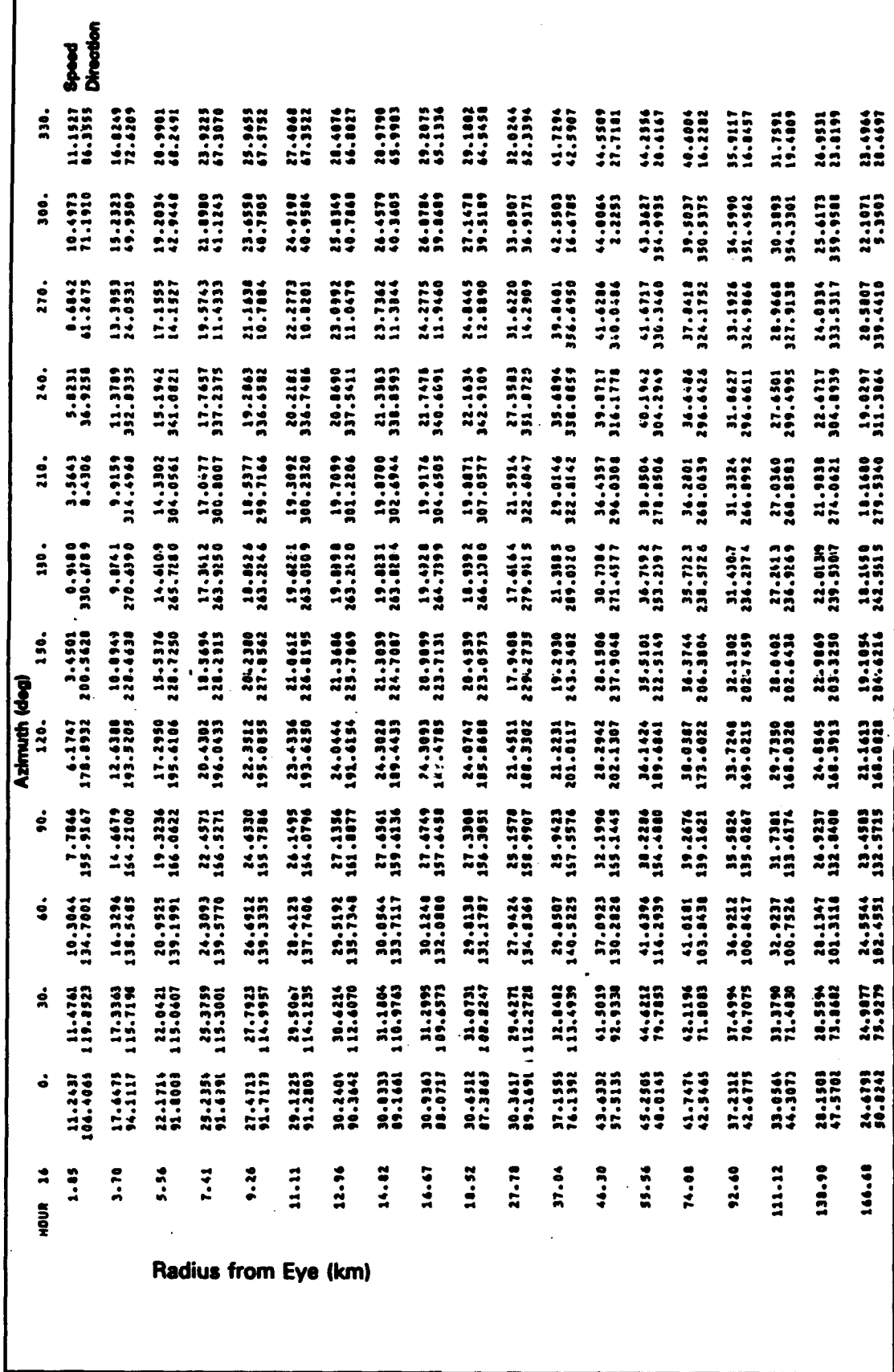


Figure C10. Wind speed and direction fields, Snapshot 9, Hurricane Gilbert (Continued)

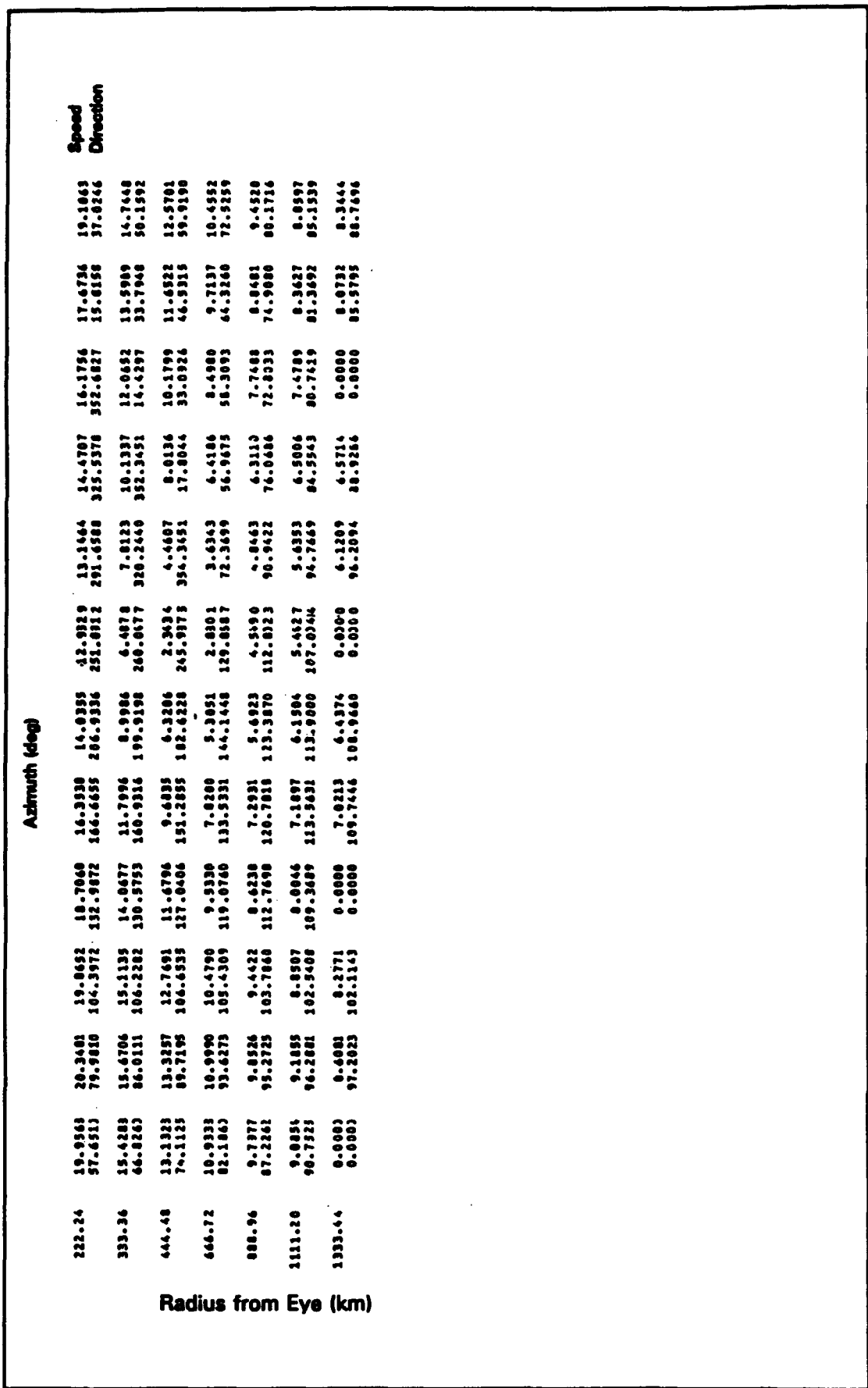


Figure C10. (Concluded)

| Hour | Radius from Eye (km) | Azimuth (deg) | | | | | | | | | | Speed | Direction |
|----------|----------------------|---------------|----------|----------|----------|----------|----------|----------|----------|----------|----------|----------|-----------|
| | | 0. | 30. | 60. | 90. | 120. | 150. | 180. | 210. | 240. | 270. | | |
| 1.05 | 5.8791 | 5.8192 | 5.7591 | 5.724 | 5.7350 | 5.7720 | 5.8250 | 5.8780 | 5.9223 | 5.9668 | 5.9664 | 5.9486 | 5.9486 |
| 104.9437 | 105.1000 | 104.6491 | 103.6973 | 102.8880 | 102.0790 | 101.6304 | 101.4966 | 101.1503 | 102.8366 | 103.1457 | 103.5127 | 103.5127 | 103.5127 |
| 3.70 | 4.0381 | 5.8556 | 5.4873 | 5.4953 | 5.6093 | 5.6977 | 5.8229 | 5.9268 | 6.0137 | 6.0952 | 6.1977 | 6.1777 | 6.1777 |
| 5.56 | 4.4052 | 6.2755 | 5.8663 | 5.4957 | 5.2914 | 5.2809 | 5.5704 | 5.6918 | 5.9702 | 6.2115 | 6.4694 | 6.8159 | 6.8159 |
| 109.5462 | 112.4160 | 113.8568 | 111.2192 | 108.4607 | 104.0910 | 100.2931 | 98.5566 | 97.4455 | 96.6729 | 101.3262 | 101.3813 | 101.3813 | 101.3813 |
| 7.41 | 8.1022 | 7.5052 | 6.7850 | 5.8232 | 4.8059 | 4.0650 | 3.9226 | 4.4891 | 5.6382 | 6.9329 | 7.9069 | 8.1191 | 8.1191 |
| 108.7143 | 117.0380 | 124.8824 | 128.4530 | 125.8730 | 116.1497 | 102.1179 | 91.8890 | 84.4838 | 87.8724 | 93.9237 | 100.7391 | 100.7391 | 100.7391 |
| 9.24 | 10.3157 | 9.8020 | 9.0202 | 7.4588 | 5.1709 | 2.8452 | 0.9344 | 3.0884 | 5.5816 | 7.6019 | 9.2662 | 10.1286 | 10.1286 |
| 105.0439 | 111.8488 | 134.0343 | 148.4417 | 160.4423 | 166.1832 | 168.8815 | 166.7296 | 168.3810 | 167.3143 | 179.2884 | 191.5931 | 191.5931 | 191.5931 |
| 11.11 | 12.8761 | 12.5965 | 11.6469 | 10.1689 | 7.8619 | 5.9521 | 2.3129 | 4.1879 | 7.2315 | 9.7013 | 11.2386 | 12.6221 | 12.6221 |
| 101.4369 | 120.6983 | 139.7655 | 150.4014 | 164.9447 | 217.7013 | 277.3317 | 393.4661 | 267.4537 | 47.4178 | 65.4497 | 83.5906 | 83.5906 | 83.5906 |
| 12.96 | 15.6671 | 15.4980 | 14.5311 | 13.9063 | 11.1054 | 8.8946 | 6.9754 | 7.6100 | 9.9767 | 12.2262 | 14.1036 | 15.2993 | 15.2993 |
| 98.6277 | 111.9411 | 122.3634 | 136.3339 | 133.9177 | 229.0041 | 216.8531 | 326.7876 | 7.5710 | 34.4339 | 56.4631 | 77.8766 | 77.8766 | 77.8766 |
| 14.82 | 18.6273 | 18.5335 | 17.4777 | 16.1361 | 14.1814 | 11.9945 | 10.4265 | 10.7774 | 12.5268 | 14.1664 | 16.8134 | 18.1419 | 18.1419 |
| 96.4916 | 117.8137 | 143.2739 | 166.4552 | 197.9950 | 230.9480 | 273.6273 | 319.2888 | 397.2303 | 267.5179 | 51.5986 | 74.1468 | 74.1468 | 74.1468 |
| 16.47 | 21.4323 | 21.7028 | 20.8665 | 19.2667 | 17.1703 | 14.6755 | 13.3136 | 13.2873 | 14.9666 | 17.2690 | 19.5127 | 21.0934 | 21.0934 |
| 95.2263 | 110.9406 | 143.3261 | 159.1313 | 197.4498 | 230.5236 | 273.3225 | 314.0730 | 391.4125 | 21.4671 | 47.7105 | 71.7387 | 71.7387 | 71.7387 |
| 18.52 | 24.6191 | 24.8264 | 23.9266 | 22.1337 | 19.8816 | 17.0102 | 15.2121 | 15.4523 | 16.1371 | 19.7091 | 22.1439 | 23.8269 | 23.8269 |
| 94.2877 | 110.9921 | 142.2577 | 160.3927 | 196.9398 | 229.3966 | 269.6417 | 310.9637 | 369.0617 | 10.6115 | 45.5471 | 69.9393 | 69.9393 | 69.9393 |
| 27.18 | 35.5222 | 36.8410 | 32.9125 | 30.1679 | 26.4152 | 23.1143 | 21.4590 | 23.1348 | 24.4759 | 30.7759 | 37.1786 | 44.9019 | 44.9019 |
| 85.5997 | 109.4270 | 135.0929 | 162.9338 | 192.0734 | 228.9039 | 270.0502 | 310.9603 | 344.5595 | 12.5334 | 37.2657 | 61.2746 | 61.2746 | 61.2746 |
| 37.04 | 39.3999 | 37.7291 | 34.9976 | 31.6346 | 28.3959 | 25.4676 | 23.7713 | 29.4866 | 38.5245 | 38.4115 | 40.9763 | 46.4726 | 46.4726 |
| 77.1921 | 103.4319 | 110.2506 | 150.2511 | 193.7711 | 232.4534 | 274.7313 | 311.4034 | 338.9324 | 2.5746 | 25.9047 | 50.4494 | 50.4494 | 50.4494 |
| 46.30 | 49.3423 | 39.2836 | 34.9345 | 31.4693 | 28.3984 | 27.0173 | 23.2109 | 33.1790 | 37.8322 | 40.4875 | 42.1611 | 46.4448 | 46.4448 |
| 70.6902 | 99.7431 | 120.8866 | 160.7063 | 194.4644 | 236.4919 | 273.4991 | 305.8359 | 329.1547 | 352.0350 | 15.2129 | 41.1493 | 41.1493 | 41.1493 |
| 55.96 | 41.7935 | 39.9269 | 35.9931 | 31.3238 | 28.7288 | 26.4614 | 21.8145 | 35.4987 | 38.5344 | 40.6359 | 42.3464 | 43.8039 | 43.8039 |
| 64.7161 | 66.4463 | 120.4886 | 162.2574 | 195.1939 | 230.4906 | 273.2194 | 299.1604 | 322.4314 | 36.9380 | 87.1331 | 36.8233 | 36.8233 | 36.8233 |
| -0.04 | 51.0643 | 50.1187 | 46.2899 | 32.2104 | 20.3981 | 16.9071 | 12.9192 | 25.1227 | 36.8094 | 39.3970 | 40.2994 | 40.9471 | 40.9471 |
| 55.5161 | 57.4422 | 122.7976 | 160.1244 | 198.9955 | 233.5294 | 263.1859 | 286.8892 | 313.5711 | 338.4441 | 2.2226 | 27.4732 | 27.4732 | 27.4732 |
| 92.49 | 39.5187 | 39.9413 | 36.7864 | 33.3399 | 31.4998 | 31.2726 | 31.9172 | 33.3039 | 34.6699 | 36.2574 | 37.7727 | 38.7346 | 38.7346 |
| 138.90 | 34.7661 | 34.9126 | 34.9269 | 32.4345 | 30.5914 | 28.9449 | 26.3984 | 29.9449 | 29.7139 | 30.9772 | 32.4236 | 33.6645 | 33.6645 |
| 50.1269 | 60.3433 | 114.2604 | 151.9442 | 188.1002 | 222.8533 | 254.2592 | 281.4391 | 308.6914 | 334.2113 | 358.4581 | 358.4581 | 358.4581 | 358.4581 |
| 121.12 | 37.7722 | 37.4336 | 36.1561 | 32.9693 | 32.0884 | 30.8971 | 28.9148 | 31.7090 | 32.7493 | 34.2408 | 35.7021 | 36.7002 | 36.7002 |
| 47.3269 | 70.4333 | 106.5802 | 144.7343 | 186.1336 | 215.6644 | 247.7752 | 274.7655 | 304.6753 | 331.4695 | 356.4646 | 356.4646 | 356.4646 | 356.4646 |
| 138.90 | 34.7661 | 34.9126 | 34.9269 | 32.4345 | 30.5914 | 28.9449 | 26.3984 | 29.9449 | 29.7139 | 30.9772 | 32.4236 | 33.6645 | 33.6645 |
| 146.68 | 31.8693 | 32.9561 | 31.3974 | 30.6672 | 28.2689 | 26.3565 | 25.5569 | 26.6123 | 26.8729 | 27.976 | 29.5903 | 30.7119 | 30.7119 |
| 44.3329 | 71.3764 | 102.1377 | 134.6385 | 169.2289 | 205.6914 | 246.4537 | 272.9894 | 303.6312 | 331.7113 | 357.6790 | 357.6790 | 357.6790 | 357.6790 |

Radius from Eye (km)

Figure C11. Wind speed and direction fields, Snapshot 10, Hurricane Gilbert (Continued)

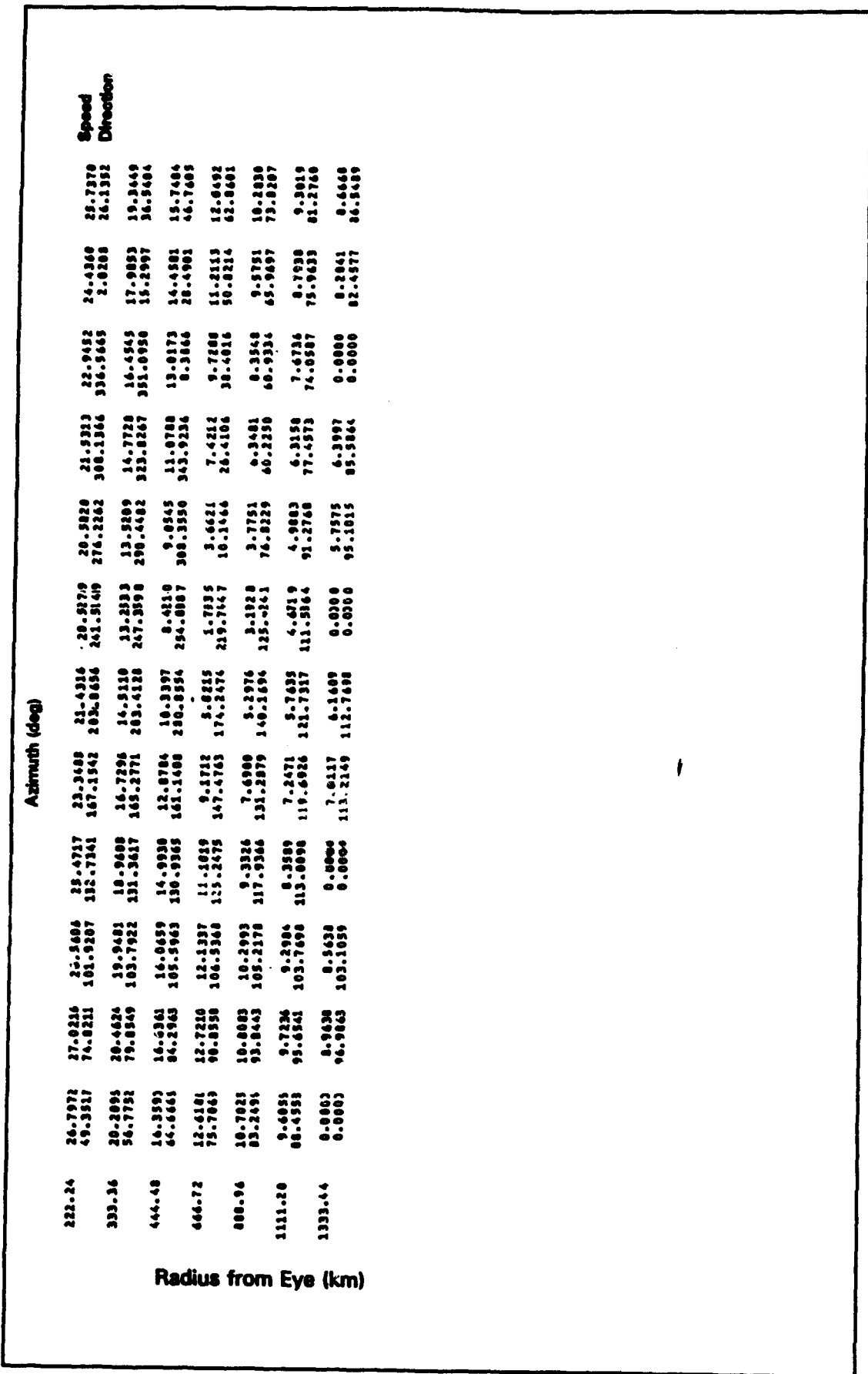
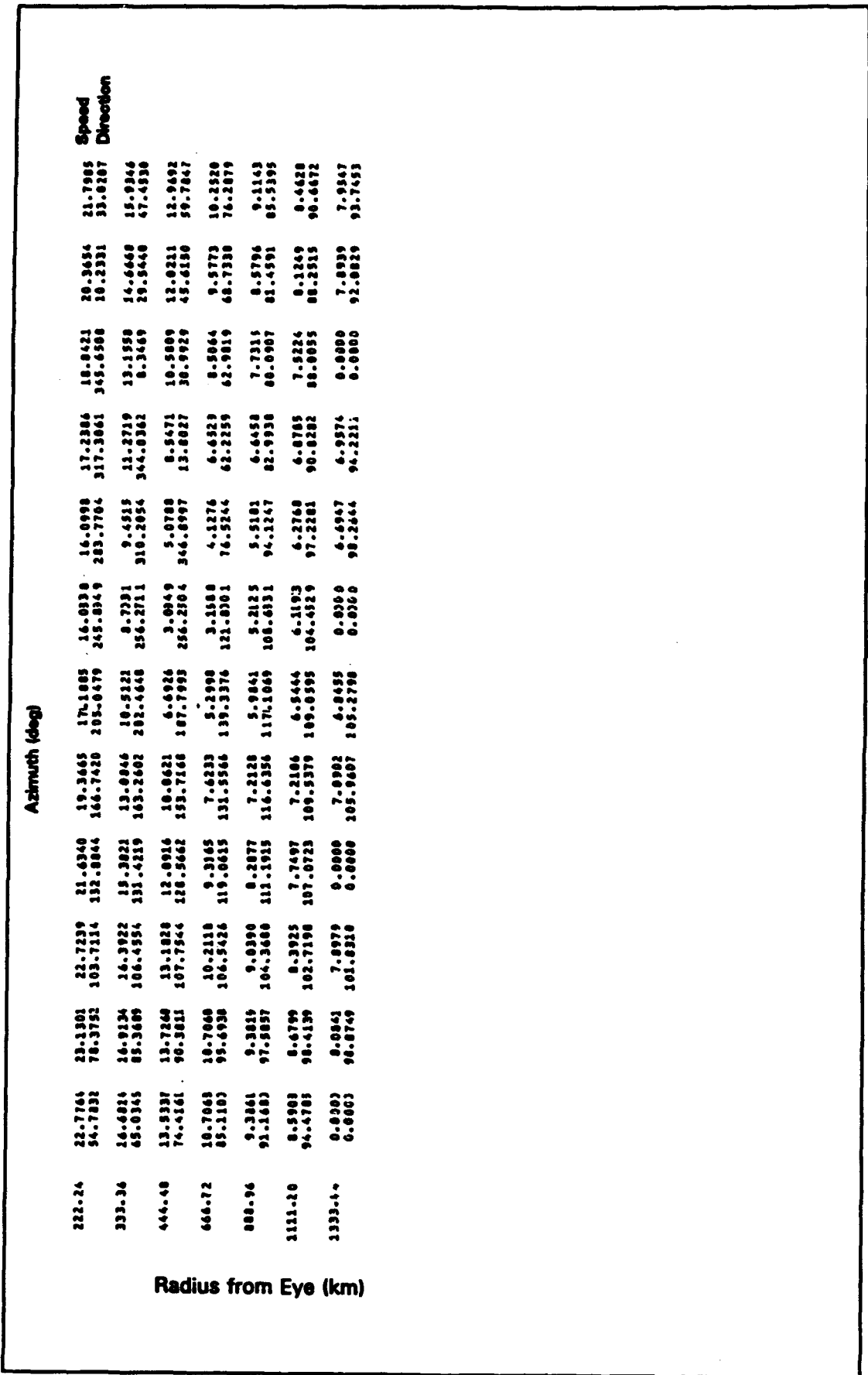


Figure C11. (Concluded)

| Hour | Radius from Eye (km) | Azimuth (deg) | | | | | | | | | | Speed |
|-------|----------------------|---------------|----------|----------|----------|----------|-----------|-----------|-----------|-----------|-----------|-----------|
| | | 0. | 10. | 20. | 30. | 40. | 50. | 60. | 70. | 80. | 90. | |
| 1.45 | 5.9395 | 5.8823 | 5.8475 | 5.8352 | 5.8931 | 5.8916 | 5.9174 | 5.9167 | 6.0003 | 6.0003 | 6.0003 | 5.9767 |
| 3.70 | 3.9811 | 5.8669 | 5.7664 | 5.7365 | 5.7774 | 5.8698 | 5.9524 | 5.9304 | 6.0798 | 6.1027 | 6.1330 | 6.0221 |
| 5.56 | 6.1933 | 5.9303 | 5.7101 | 5.4101 | 5.4446 | 5.7917 | 5.9105 | 6.0720 | 6.1500 | 6.2274 | 6.3004 | 6.3446 |
| 7.41 | 6.7665 | 6.2669 | 5.7929 | 5.781 | 5.3467 | 5.4262 | 5.7160 | 5.9119 | 6.1369 | 6.4120 | 6.7201 | 6.9235 |
| 9.26 | 8.2391 | 7.4281 | 6.4723 | 5.7277 | 4.6736 | 4.1552 | 4.9163 | 5.2863 | 5.7371 | 6.7553 | 7.4339 | 8.1043 |
| 11.11 | 10.9037 | 11.7212 | 12.47192 | 12.6361 | 12.8139 | 11.47497 | 10.0397 | 92.5068 | 87.6621 | 87.5068 | 94.8223 | 101.8703 |
| 12.94 | 12.9992 | 12.5985 | 11.4842 | 10.3957 | 8.2692 | 5.3897 | 2.9532 | 4.1778 | 7.4666 | 10.8225 | 11.7933 | 12.9932 |
| 14.82 | 15.9861 | 15.6482 | 14.9280 | 13.4136 | 11.7990 | 9.3899 | 7.9165 | 7.5269 | 10.2768 | 12.4714 | 14.4066 | 16.2130 |
| 16.67 | 19.2391 | 19.2051 | 18.5467 | 17.1986 | 15.1895 | 12.4795 | 10.5149 | 10.4905 | 12.0813 | 15.6470 | 17.7775 | 19.9106 |
| 18.52 | 22.7201 | 22.8847 | 22.2024 | 20.6210 | 18.3616 | 15.9631 | 12.9013 | 13.3014 | 15.9718 | 18.9824 | 21.0770 | 22.3292 |
| 20.39 | 34.5608 | 32.6769 | 29.9005 | 26.1567 | 22.3295 | 21.4734 | 25.3618 | 31.3325 | 36.2174 | 38.5119 | 37.2980 | 39.1997 |
| 22.25 | 42.5229 | 35.5777 | 32.1298 | 28.8985 | 27.0031 | 29.3277 | 36.4634 | 41.1668 | 44.4955 | 46.7209 | 48.0016 | 50.7563 |
| 24.11 | 42.4135 | 38.2159 | 44.6894 | 48.4440 | 49.4510 | 25.9250 | 27.3.2320 | 31.9.0206 | 35.6.4006 | 39.3.8006 | 41.1.7006 | 43.4.0006 |
| 27.78 | 42.1673 | 37.9512 | 33.7562 | 31.3806 | 31.7468 | 35.1369 | 39.3362 | 42.5312 | 44.4370 | 46.0355 | 48.1.9006 | 50.7.5006 |
| 30.54 | 46.0261 | 46.3777 | 39.7195 | 35.9760 | 34.2357 | 34.9786 | 37.6124 | 39.7897 | 41.5712 | 43.2217 | 44.9356 | 49.6401 |
| 32.40 | 48.3545 | 48.4922 | 39.4321 | 37.5463 | 35.8956 | 34.4616 | 33.9822 | 34.4173 | 35.1465 | 36.4302 | 37.9004 | 39.1431 |
| 34.26 | 49.4595 | 74.6640 | 105.1505 | 10.8722 | 175.2363 | 189.1969 | 242.3194 | 271.4305 | 306.3736 | 328.1291 | 354.0091 | 39.3106 |
| 36.12 | 37.0892 | 37.2925 | 36.4285 | 35.3346 | 33.3221 | 31.6798 | 31.0519 | 31.3381 | 31.7849 | 32.1381 | 34.2634 | 38.0079 |
| 38.08 | 48.8663 | 77.986 | 112.6982 | 116.3196 | 115.6896 | 210.4469 | 249.3781 | 276.9476 | 304.2015 | 330.7660 | 354.2827 | 39.5995 |
| 39.94 | 32.3885 | 32.1023 | 32.2468 | 31.9266 | 29.9466 | 27.2892 | 26.3192 | 26.4103 | 27.9126 | 28.3159 | 29.0994 | 31.1446 |
| 41.80 | 28.5681 | 28.6026 | 28.4113 | 27.3220 | 25.1770 | 25.1219 | 22.3196 | 22.3491 | 22.9469 | 24.4161 | 25.9338 | 27.2816 |
| 43.66 | 48.6255 | 74.5154 | 101.9119 | 125.4059 | 127.8595 | 203.5327 | 239.7195 | 274.7785 | 301.9169 | 330.3402 | 357.2231 | 31.7717 |

Figure C12. Wind speed and direction fields, Snapshot 11, Hurricane Gilbert (Continued)

Figure C12. (Concluded)



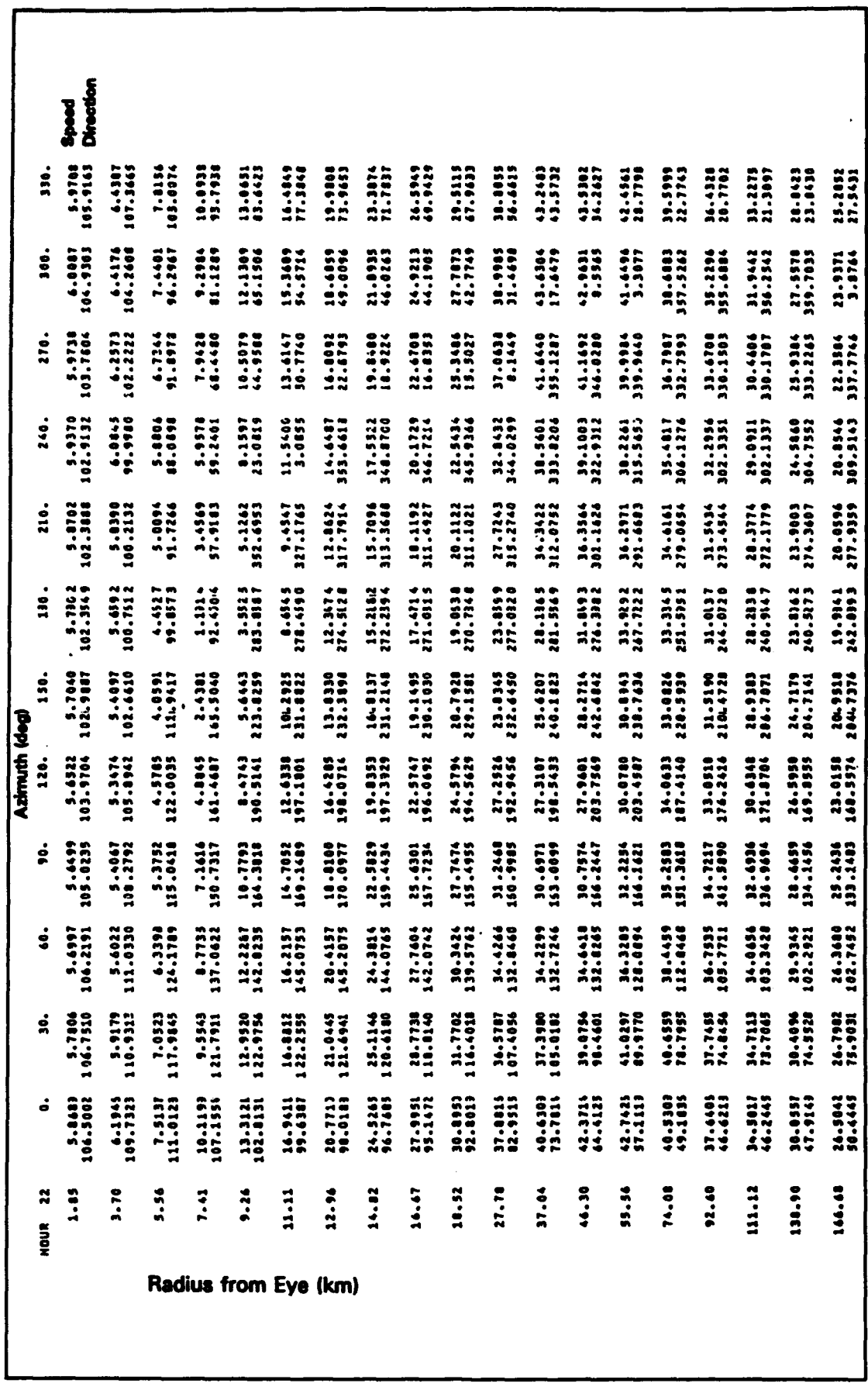


Figure C13. Wind speed and direction fields, Snapshot 12, Hurricane Gilbert (Continued)

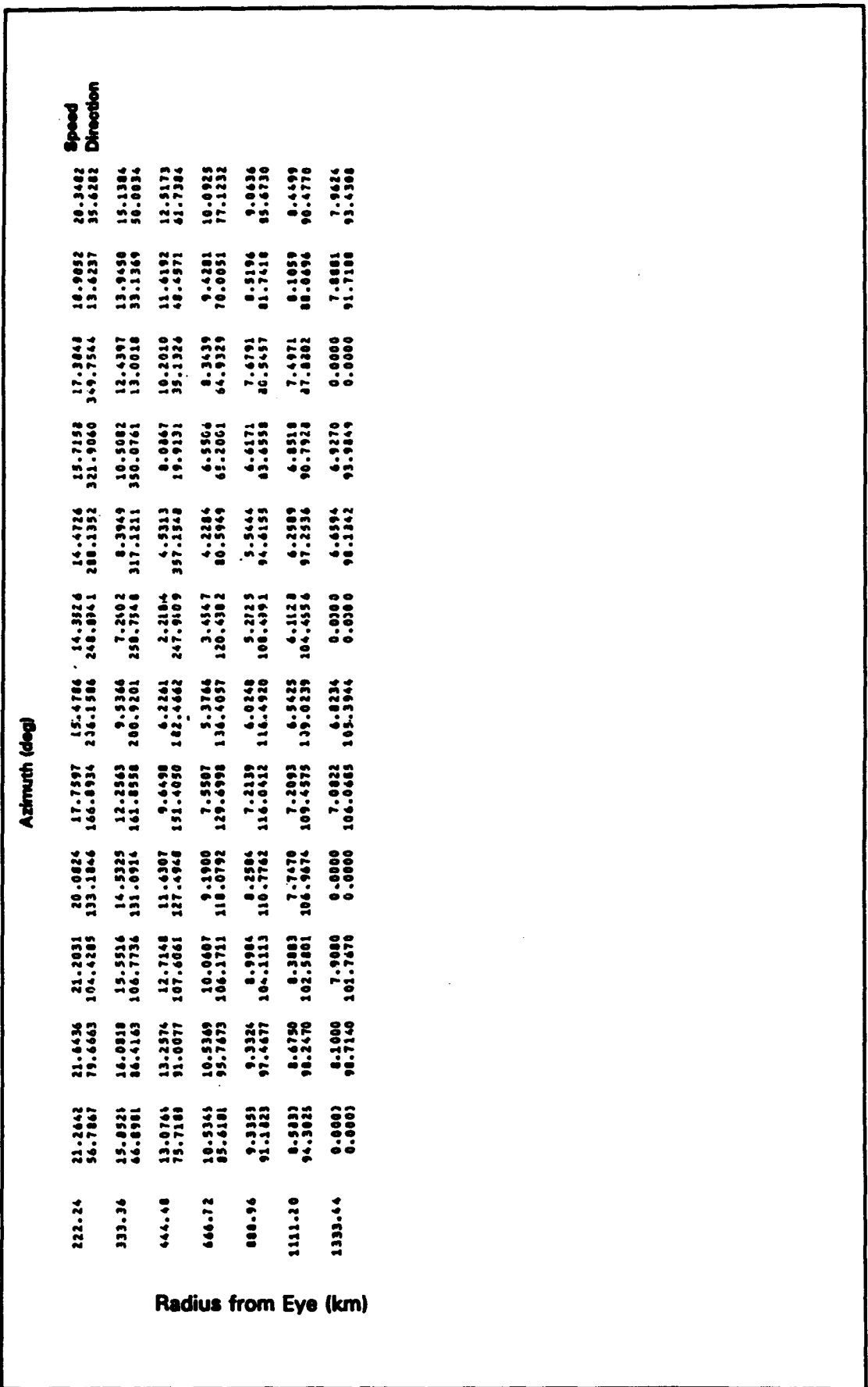


Figure C13. (Concluded)

\$ ASSIGN GILB.WIND21 FOR020
 \$ ASSIGN GILB.WIND18 FOR018
 \$ RUN AZIM_AVER

| Radius (n.m.) | Radius (km) | --- Wind Speed --- | | Inflow Angle, |
|------------------|----------------|------------------------|------------------------|----------------------------|
| | | Scalar Avg. (m/sec) | Vector Avg. (m/sec) | (+ = in, - = out) (deg) |

| | | | | |
|-----------|----------|---------|---------|----------|
| WIND,HOUR | | 20 | 0 | |
| 1. | 1.852 | 5.9405 | 0.0583 | 242.9772 |
| 2. | 3.704 | 5.9437 | 0.1176 | 243.5015 |
| 3. | 5.556 | 5.9498 | 0.1792 | 244.4864 |
| 4. | 7.408 | 5.9595 | 0.2443 | 245.8895 |
| 5. | 9.260 | 5.9755 | 0.3159 | 248.0143 |
| 6. | 11.112 | 5.0049 | 0.4017 | 251.6257 |
| 7. | 12.964 | 5.0747 | 0.5263 | 259.0292 |
| 8. | 14.816 | 5.2682 | 0.7831 | -85.1015 |
| 9. | 16.668 | 5.7908 | 1.4971 | -61.3046 |
| 10. | 18.520 | 7.8736 | 3.2177 | -39.8814 |
| 15. | 27.780 | 25.7127 | 25.8542 | 0.0638 |
| 20. | 37.040 | 39.1360 | 37.0043 | 14.4071 |
| 25. | 46.300 | 39.8450 | 38.6980 | 21.4880 |
| 30. | 55.560 | 39.2075 | 38.2327 | 26.3533 |
| 40. | 74.080 | 35.9664 | 36.4542 | 35.2711 |
| 50. | 92.600 | 36.7457 | 34.4134 | 40.8962 |
| 60. | 111.120 | 32.1222 | 31.8455 | 43.3617 |
| 75. | 138.900 | 27.6395 | 27.3607 | 43.5430 |
| 90. | 166.680 | 23.5362 | 23.2120 | 41.9669 |
| 120. | 222.240 | 17.3512 | 16.8293 | 36.0960 |
| 180. | 333.360 | 13.8521 | 9.6021 | 23.6111 |
| 240. | 444.480 | 7.9560 | 5.4558 | 15.0186 |
| 360. | 666.720 | 7.4514 | 1.7981 | 10.4387 |
| 480. | 888.960 | 7.4233 | 0.6930 | 11.4414 |
| 600. | 1111.200 | 7.4100 | 0.3141 | 6.7318 |
| 720. | 1333.440 | 6.9126 | 0.1089 | -12.1050 |

| | | | | |
|-----------|----------|---------|---------|----------|
| WIND,HOUR | | 20 | 1 | |
| 1. | 1.852 | 5.9644 | 0.0565 | 240.5800 |
| 2. | 3.704 | 5.9677 | 0.1138 | 241.0424 |
| 3. | 5.556 | 5.9738 | 0.1730 | 241.9138 |
| 4. | 7.408 | 5.9834 | 0.2350 | 243.1496 |
| 5. | 9.260 | 5.9985 | 0.3022 | 245.0328 |
| 6. | 11.112 | 5.0250 | 0.3803 | 248.1936 |
| 7. | 12.964 | 5.0830 | 0.4864 | 254.5270 |
| 8. | 14.816 | 5.2368 | 0.6847 | 268.6367 |
| 9. | 16.668 | 5.6499 | 1.2092 | -68.0856 |
| 10. | 18.520 | 7.5427 | 2.5093 | -45.4020 |
| 15. | 27.780 | 23.5379 | 22.5697 | -2.4338 |
| 20. | 37.040 | 33.3208 | 37.1779 | 14.3794 |
| 25. | 46.300 | 42.0500 | 41.0345 | 23.7352 |
| 30. | 55.560 | 41.5028 | 40.6994 | 29.0430 |
| 40. | 74.080 | 37.9929 | 37.5078 | 35.4472 |
| 50. | 92.600 | 36.9229 | 34.5727 | 39.4681 |
| 60. | 111.120 | 32.1931 | 31.8974 | 41.7004 |
| 75. | 138.900 | 23.1118 | 27.8268 | 42.5412 |
| 90. | 166.680 | 24.3038 | 23.9868 | 41.6276 |
| 120. | 222.240 | 13.2532 | 17.7728 | 36.8113 |
| 180. | 333.360 | 11.5444 | 10.4276 | 25.1562 |
| 240. | 444.480 | 3.2821 | 6.0906 | 15.3304 |
| 360. | 666.720 | 7.4668 | 2.0921 | 10.6132 |
| 480. | 888.960 | 7.4237 | 0.8189 | 11.3564 |
| 600. | 1111.200 | 7.4093 | 0.3746 | 7.6189 |
| 720. | 1333.440 | 6.9128 | 0.1289 | -8.0063 |

Snapshot 1

Interpolation between
Snapshots 1 & 2

Figure C14. Azimuthally averaged speed and inflow angle, Hurricane Gilbert (Sheet 1 of 12)

| Radius (n.m.) | Radius (km) | Scalar Avg. (m/sec) | Vector Avg. (m/sec) | Inflow Angle, (+ = in, - = out) (deg) |
|----------------------|----------------|------------------------|------------------------|---|
| ---- Wind Speed ---- | | | | |
| WIND,HOUR | | 20 | 2 | |
| 1. | 1.852 | 5.9885 | 0.0548 | 238.0248 |
| 2. | 3.704 | 5.9919 | 0.1102 | 238.4156 |
| 3. | 5.556 | 5.9982 | 0.1672 | 239.1560 |
| 4. | 7.408 | 5.0076 | 0.2264 | 240.1999 |
| 5. | 9.260 | 5.0220 | 0.2895 | 241.7754 |
| 6. | 11.112 | 5.0457 | 0.3604 | 244.3654 |
| 7. | 12.964 | 5.0921 | 0.4500 | 249.2603 |
| 8. | 14.816 | 5.2074 | 0.5968 | 260.4110 |
| 9. | 16.668 | 5.5173 | 0.9457 | -78.7729 |
| 10. | 18.520 | 7.2460 | 1.8151 | -55.4724 |
| 15. | 27.780 | 20.4553 | 19.1466 | -5.2852 |
| 20. | 37.040 | 33.5064 | 37.3467 | 14.3384 |
| 25. | 46.300 | 46.2971 | 43.3895 | 25.7404 |
| 30. | 55.560 | 43.8676 | 43.1995 | 31.4260 |
| 40. | 74.080 | 39.0180 | 38.5573 | 35.6167 |
| 50. | 92.600 | 35.1224 | 34.7513 | 38.0579 |
| 60. | 111.120 | 32.2916 | 31.9735 | 40.0499 |
| 75. | 138.900 | 23.5935 | 28.3006 | 41.5780 |
| 90. | 166.680 | 25.0731 | 24.7614 | 41.3158 |
| 120. | 222.240 | 19.1630 | 18.7172 | 37.4373 |
| 180. | 333.360 | 12.2446 | 11.2392 | 26.5320 |
| 240. | 444.480 | 3.6870 | 6.7227 | 17.4240 |
| 360. | 666.720 | 7.4862 | 2.3823 | 10.7159 |
| 480. | 888.960 | 7.4253 | 0.9447 | 11.2861 |
| 600. | 1111.200 | 7.4090 | 0.4350 | 8.2587 |
| 720. | 1333.440 | 4.9130 | 0.1493 | -5.0173 |
| WIND,HOUR | | 20 | 3 | |
| 1. | 1.852 | 5.8402 | 0.7731 | -75.1767 |
| 2. | 3.704 | 5.4599 | 3.0543 | -50.1969 |
| 3. | 5.556 | 5.9973 | 8.7711 | -22.2437 |
| 4. | 7.408 | 17.1276 | 16.4325 | -8.7850 |
| 5. | 9.260 | 23.7617 | 23.2580 | -1.7680 |
| 6. | 11.112 | 27.9470 | 27.5536 | 2.6972 |
| 7. | 12.964 | 29.9794 | 29.6319 | 6.0785 |
| 8. | 14.816 | 30.5931 | 30.2645 | 8.6527 |
| 9. | 16.668 | 30.4137 | 30.1121 | 10.4360 |
| 10. | 18.520 | 29.9044 | 29.6449 | 11.3989 |
| 15. | 27.780 | 33.3389 | 32.9973 | 10.4108 |
| 20. | 37.040 | 33.8700 | 38.9509 | 15.7391 |
| 25. | 46.300 | 43.8779 | 39.9576 | 22.2504 |
| 30. | 55.560 | 39.5400 | 36.7501 | 26.6865 |
| 40. | 74.080 | 35.3129 | 35.8119 | 33.3749 |
| 50. | 92.600 | 33.4908 | 33.1396 | 37.8682 |
| 60. | 111.120 | 33.9005 | 30.6016 | 40.2691 |
| 75. | 138.900 | 27.0636 | 26.7709 | 41.2536 |
| 90. | 166.680 | 23.5050 | 23.1748 | 40.4313 |
| 120. | 222.240 | 17.8497 | 17.3439 | 35.7290 |
| 180. | 333.360 | 11.4874 | 10.3226 | 24.5473 |
| 240. | 444.480 | 3.3587 | 6.1182 | 16.4950 |
| 360. | 666.720 | 7.5436 | 2.1977 | 11.5892 |
| 480. | 888.960 | 7.4797 | 0.9074 | 12.1303 |
| 600. | 1111.200 | 7.4515 | 0.4313 | 9.1300 |
| 720. | 1333.440 | 4.9283 | 0.1473 | -3.2681 |

Figure C14. (Sheet 2 of 12)

| Radius (n.m.) | Radius (km) | --- | Wind Speed | --- | Inflow Angle, (+ = in, - = out) |
|------------------|----------------|-------------|-------------|----------|------------------------------------|
| | | Scalar Avg. | Vector Avg. | (m/sec) | (deg) |
| WIND,HOUR | | 20 | | 4 | |
| 1. | 1.852 | 5.8323 | 1.5088 | -73.7257 | |
| 2. | 3.704 | 7.6811 | 5.8655 | -48.3018 | Snapshot 3 |
| 3. | 5.556 | 17.0601 | 16.3827 | -18.8441 | |
| 4. | 7.408 | 31.1340 | 30.6660 | -5.6326 | |
| 5. | 9.260 | 44.1059 | 43.7016 | 1.0484 | |
| 6. | 11.112 | 52.0694 | 51.6435 | 5.5470 | |
| 7. | 12.964 | 55.7219 | 55.1891 | 8.9149 | |
| 8. | 14.816 | 55.9171 | 56.2661 | 11.6026 | |
| 9. | 16.668 | 55.6530 | 55.9352 | 13.6930 | |
| 10. | 18.520 | 55.4595 | 54.7346 | 15.2657 | |
| 15. | 27.780 | 47.2739 | 46.6246 | 17.3370 | |
| 20. | 37.040 | 41.2928 | 40.5148 | 17.0706 | |
| 25. | 46.300 | 37.5578 | 36.6132 | 18.1098 | |
| 30. | 55.560 | 35.4703 | 34.4779 | 20.7272 | |
| 40. | 74.080 | 33.6395 | 33.0831 | 30.7598 | |
| 50. | 92.600 | 31.8519 | 31.5189 | 37.6681 | |
| 60. | 111.120 | 29.5078 | 29.2248 | 40.5194 | |
| 75. | 138.900 | 25.5316 | 25.2342 | 40.8956 | |
| 90. | 166.680 | 21.9416 | 21.5849 | 39.4102 | |
| 120. | 222.240 | 15.5657 | 15.9818 | 33.7018 | |
| 180. | 333.360 | 10.7602 | 9.3951 | 22.2754 | |
| 240. | 444.480 | 3.1825 | 5.5112 | 15.3905 | |
| 360. | 666.720 | 7.6131 | 2.0124 | 12.5970 | |
| 480. | 888.960 | 7.5401 | 0.8702 | 13.0439 | |
| 600. | 1111.200 | 7.4989 | 0.4276 | 10.0139 | |
| 720. | 1333.440 | 6.9463 | 0.1454 | -1.4962 | |
| WIND,HOUR | | 20 | | 5 | |
| 1. | 1.852 | 5.2252 | 2.7628 | -65.8165 | Interpolation between |
| 2. | 3.704 | 10.8849 | 9.7729 | -34.6276 | Snapshots 3 & 4 |
| 3. | 5.556 | 23.9177 | 23.3696 | -10.5852 | |
| 4. | 7.408 | 38.7603 | 38.3208 | -0.9444 | |
| 5. | 9.260 | 43.6471 | 49.2128 | 4.1015 | |
| 6. | 11.112 | 55.1260 | 54.6246 | 7.4212 | |
| 7. | 12.964 | 57.2447 | 56.6338 | 9.9296 | |
| 8. | 14.816 | 57.5303 | 56.8154 | 11.9629 | |
| 9. | 16.668 | 55.7618 | 55.9895 | 13.5702 | |
| 10. | 18.520 | 55.3013 | 54.5162 | 14.8087 | |
| 15. | 27.780 | 47.1459 | 46.3588 | 16.6690 | |
| 20. | 37.040 | 41.7828 | 40.8349 | 17.7450 | |
| 25. | 46.300 | 38.5645 | 37.6181 | 21.1510 | |
| 30. | 55.560 | 35.6946 | 35.9205 | 25.7857 | |
| 40. | 74.080 | 34.4778 | 34.0738 | 35.2891 | |
| 50. | 92.600 | 31.8423 | 31.5568 | 40.0867 | |
| 60. | 111.120 | 28.8347 | 28.5661 | 41.5009 | |
| 75. | 138.900 | 24.3943 | 24.0850 | 40.6594 | |
| 90. | 166.680 | 23.6857 | 20.2947 | 38.4191 | |
| 120. | 222.240 | 15.4411 | 14.7694 | 31.7297 | |
| 180. | 333.360 | 10.0126 | 8.4136 | 20.0608 | |
| 240. | 444.480 | 3.0213 | 4.8038 | 13.9795 | |
| 360. | 666.720 | 7.6176 | 1.7291 | 12.1352 | |
| 480. | 888.960 | 7.5582 | 0.7501 | 12.4990 | |
| 600. | 1111.200 | 7.5163 | 0.3689 | 9.0158 | |
| 720. | 1333.440 | 6.9548 | 0.1238 | -3.6095 | |

Figure C14. (Sheet 3 of 12)

| Radius (n.m.) | Radius (km) | --- Wind Speed --- | | Inflow Angle, (+ = in, - = out) |
|-------------------|----------------|------------------------|------------------------|------------------------------------|
| | | Scalar Avg. (m/sec) | Vector Avg. (m/sec) | |
| WIND, HOUR | | | | |
| 1. | 1.852 | 5.7256 | 3.9907 | -62.4913 |
| 2. | 3.704 | 14.5032 | 13.6544 | -28.3991 |
| 3. | 5.556 | 30.8972 | 30.3899 | -6.2408 |
| 4. | 7.408 | 45.3251 | 45.8593 | 2.2482 |
| 5. | 9.260 | 54.9773 | 54.4563 | 6.4809 |
| 6. | 11.112 | 58.0636 | 57.4492 | 9.0340 |
| 7. | 12.964 | 53.7361 | 58.0230 | 10.8773 |
| 8. | 14.816 | 53.1499 | 57.3589 | 12.3154 |
| 9. | 16.668 | 55.8714 | 56.0365 | 13.4475 |
| 10. | 18.520 | 55.1522 | 54.2988 | 14.3488 |
| 15. | 27.780 | 47.0437 | 46.0940 | 15.9946 |
| 20. | 37.040 | 42.3020 | 41.1548 | 16.4114 |
| 25. | 46.300 | 39.6646 | 38.7001 | 24.0330 |
| 30. | 55.560 | 33.1960 | 37.5633 | 30.4291 |
| 40. | 74.080 | 35.5348 | 35.2260 | 39.5457 |
| 50. | 92.600 | 31.8955 | 31.6439 | 42.5023 |
| 60. | 111.120 | 28.1750 | 27.9150 | 42.5365 |
| 75. | 138.900 | 23.2591 | 22.9323 | 40.3630 |
| 90. | 166.680 | 19.4405 | 19.0049 | 37.2775 |
| 120. | 222.240 | 14.3366 | 13.5521 | 29.3917 |
| 180. | 333.360 | 9.3352 | 7.4333 | 17.3851 |
| 240. | 444.480 | 7.9289 | 4.0952 | 12.1178 |
| 360. | 666.720 | 7.6295 | 1.4431 | 11.4411 |
| 480. | 888.960 | 7.5739 | 0.6301 | 11.7333 |
| 600. | 1111.200 | 7.5351 | 0.3103 | 7.6245 |
| 720. | 1333.440 | 6.9639 | 0.1025 | -6.6188 |
| WIND, HOUR | | | | |
| | | 20 | 7 | |
| 1. | 1.852 | 5.8491 | 4.5236 | -58.1521 |
| 2. | 3.704 | 15.3031 | 15.0616 | -22.8319 |
| 3. | 5.556 | 31.6745 | 31.1321 | -4.0379 |
| 4. | 7.408 | 45.2941 | 44.7367 | 3.0175 |
| 5. | 9.260 | 52.8056 | 52.1772 | 6.3979 |
| 6. | 11.112 | 55.6764 | 54.9776 | 8.3532 |
| 7. | 12.964 | 55.5360 | 55.7612 | 9.8517 |
| 8. | 14.816 | 55.2909 | 55.4289 | 11.1628 |
| 9. | 16.668 | 55.4900 | 54.5386 | 12.3841 |
| 10. | 18.520 | 54.2968 | 53.2621 | 13.5252 |
| 15. | 27.780 | 48.6838 | 47.4276 | 18.2287 |
| 20. | 37.040 | 45.1281 | 44.1740 | 25.3132 |
| 25. | 46.300 | 42.5121 | 41.9100 | 32.3032 |
| 30. | 55.560 | 40.5284 | 40.1261 | 37.4110 |
| 40. | 74.080 | 35.1586 | 35.9069 | 42.6494 |
| 50. | 92.600 | 31.4613 | 31.2270 | 43.5405 |
| 60. | 111.120 | 27.2626 | 27.0013 | 42.3935 |
| 75. | 138.900 | 22.2634 | 21.9178 | 39.4404 |
| 90. | 166.680 | 13.5853 | 18.1153 | 35.9769 |
| 120. | 222.240 | 13.8112 | 12.9681 | 27.9855 |
| 180. | 333.360 | 9.1801 | 7.2034 | 16.8972 |
| 240. | 444.480 | 7.9265 | 4.0666 | 12.5087 |
| 360. | 666.720 | 7.6258 | 1.5307 | 12.1834 |
| 480. | 888.960 | 7.5713 | 0.7078 | 12.4845 |
| 600. | 1111.200 | 7.5257 | 0.3684 | 8.9790 |
| 720. | 1333.440 | 6.9587 | 0.1301 | -2.1435 |

Figure C14. (Sheet 4 of 12)

| Radius (n.m.) | Radius (km) | --- Wind Speed --- | | Inflow Angle, (+ = in, - = out) (deg) |
|-------------------|----------------|------------------------|------------------------|---|
| | | Scalar Avg. (m/sec) | Vector Avg. (m/sec) | |
| WIND, HOUR | | | | |
| 1. | 1.852 | 7.0426 | 5.0716 | -54.7408 |
| 2. | 3.704 | 17.1757 | 16.5115 | -18.2037 |
| 3. | 5.556 | 32.4857 | 31.9070 | -1.9445 |
| 4. | 7.408 | 44.2867 | 43.6128 | 3.8353 |
| 5. | 9.260 | 53.5559 | 49.7581 | 6.2712 |
| 6. | 11.112 | 53.2640 | 52.4012 | 7.5746 |
| 7. | 12.964 | 54.2964 | 53.3844 | 8.7047 |
| 8. | 14.816 | 54.4636 | 53.4694 | 9.9306 |
| 9. | 16.668 | 54.1409 | 53.0254 | 11.2704 |
| 10. | 18.520 | 53.4684 | 52.2117 | 12.6752 |
| 15. | 27.780 | 51.3944 | 48.7947 | 20.3304 |
| 20. | 37.040 | 43.4448 | 47.5966 | 31.2649 |
| 25. | 46.300 | 45.0761 | 45.6723 | 39.2970 |
| 30. | 55.560 | 43.3528 | 43.0839 | 43.4863 |
| 40. | 74.080 | 35.8795 | 36.6723 | 45.6317 |
| 50. | 92.600 | 31.0389 | 30.8200 | 44.6116 |
| 60. | 111.120 | 25.3489 | 26.0853 | 42.2429 |
| 75. | 138.900 | 21.2724 | 20.9049 | 38.3987 |
| 90. | 166.680 | 17.7416 | 17.2313 | 34.5203 |
| 120. | 222.240 | 13.2931 | 12.3823 | 26.4577 |
| 180. | 333.360 | 9.0301 | 6.9736 | 16.3809 |
| 240. | 444.480 | 7.9248 | 4.0382 | 12.9052 |
| 360. | 666.720 | 7.6209 | 1.6167 | 12.8425 |
| 480. | 888.960 | 7.5641 | 0.7856 | 13.0809 |
| 600. | 1111.200 | 7.5185 | 0.4267 | 9.9572 |
| 720. | 1333.440 | 6.9536 | 0.1582 | 0.7499 |
| WIND, HOUR | | | | |
| 1. | 1.852 | 5.9981 | 5.0795 | -54.8159 |
| 2. | 3.704 | 17.1768 | 16.5351 | -18.2056 |
| 3. | 5.556 | 32.5058 | 31.9429 | -1.9150 |
| 4. | 7.408 | 44.2801 | 43.6174 | 3.8725 |
| 5. | 9.260 | 53.4746 | 49.6803 | 6.2548 |
| 6. | 11.112 | 53.1378 | 52.2742 | 7.4287 |
| 7. | 12.964 | 54.1663 | 53.2625 | 8.4029 |
| 8. | 14.816 | 54.3547 | 53.3862 | 9.4955 |
| 9. | 16.668 | 56.0787 | 53.0050 | 10.7557 |
| 10. | 18.520 | 53.4631 | 52.2558 | 12.1347 |
| 15. | 27.780 | 53.7277 | 49.1375 | 19.9558 |
| 20. | 37.040 | 49.0489 | 46.2190 | 31.2943 |
| 25. | 46.300 | 45.7582 | 46.3703 | 39.4880 |
| 30. | 55.560 | 44.0145 | 43.7565 | 43.6872 |
| 40. | 74.080 | 37.4074 | 37.2072 | 45.7600 |
| 50. | 92.600 | 31.4470 | 31.2338 | 44.6753 |
| 60. | 111.120 | 25.6654 | 26.4072 | 42.2520 |
| 75. | 138.900 | 21.4959 | 21.1338 | 38.3407 |
| 90. | 166.680 | 17.9024 | 17.3978 | 34.4100 |
| 120. | 222.240 | 13.3829 | 12.4762 | 26.2241 |
| 180. | 333.360 | 9.0683 | 7.0029 | 15.9467 |
| 240. | 444.480 | 7.9528 | 4.0419 | 12.4316 |
| 360. | 666.720 | 7.6355 | 1.6109 | 12.3296 |
| 480. | 888.960 | 7.5744 | 0.7805 | 12.4548 |
| 600. | 1111.200 | 7.5258 | 0.4218 | 9.4619 |
| 720. | 1333.440 | 6.9565 | 0.1548 | 0.8799 |

Snapshot 5

Interpolation between
Snapshots 5 & 6

Figure C14. (Sheet 5 of 12)

| Radius (n.m.) | Radius (km) | --- Wind Speed --- | Inflow Angle, (+ = in, - = out) |
|------------------|----------------|------------------------|------------------------------------|
| | | Scalar Avg. (m/sec) | Vector Avg. (m/sec) |
| WIND, HOUR | | 20 | 10 |
| 1. | 1.852 | 5.9537 | 5.0869 |
| 2. | 3.704 | 17.1782 | 16.5585 |
| 3. | 5.556 | 32.5267 | 31.9786 |
| 4. | 7.408 | 44.2750 | 43.6215 |
| 5. | 9.260 | 53.3961 | 49.6013 |
| 6. | 11.112 | 53.0167 | 52.1647 |
| 7. | 12.964 | 54.0441 | 53.1380 |
| 8. | 14.816 | 54.2563 | 53.3016 |
| 9. | 16.668 | 54.0279 | 52.9847 |
| 10. | 18.520 | 53.4681 | 52.3011 |
| 15. | 27.780 | 51.0640 | 49.4815 |
| 20. | 37.040 | 49.6522 | 48.8398 |
| 25. | 46.300 | 47.4393 | 47.0666 |
| 30. | 55.560 | 44.6752 | 44.4276 |
| 40. | 74.080 | 37.9347 | 37.7411 |
| 50. | 92.600 | 31.8548 | 31.6470 |
| 60. | 111.120 | 25.9819 | 26.7288 |
| 75. | 138.900 | 21.7196 | 21.3627 |
| 90. | 166.680 | 13.0638 | 17.5646 |
| 120. | 222.240 | 13.4730 | 12.5704 |
| 180. | 333.360 | 9.1069 | 7.0325 |
| 240. | 444.480 | 7.9816 | 4.0458 |
| 360. | 666.720 | 7.6511 | 1.6052 |
| 480. | 888.960 | 7.3856 | 0.7755 |
| 600. | 1111.200 | 7.5338 | 0.4170 |
| 720. | 1333.440 | 4.9598 | 0.1515 |
| WIND, HOUR | | 20 | 11 |
| 1. | 1.852 | 3.7297 | 7.8357 |
| 2. | 3.704 | 15.9519 | 16.5147 |
| 3. | 5.556 | 25.1567 | 25.7571 |
| 4. | 7.408 | 32.9936 | 32.5674 |
| 5. | 9.260 | 35.6307 | 36.1683 |
| 6. | 11.112 | 33.3153 | 37.6633 |
| 7. | 12.964 | 39.0787 | 38.6623 |
| 8. | 14.816 | 39.2626 | 38.8826 |
| 9. | 16.668 | 39.0661 | 38.7132 |
| 10. | 18.520 | 33.3591 | 38.2241 |
| 15. | 27.780 | 35.5052 | 36.1724 |
| 20. | 37.040 | 35.8351 | 36.5306 |
| 25. | 46.300 | 38.2610 | 37.9182 |
| 30. | 55.560 | 39.2255 | 38.8999 |
| 40. | 74.080 | 35.8223 | 36.6041 |
| 50. | 92.600 | 32.2816 | 32.0769 |
| 60. | 111.120 | 29.2033 | 27.9708 |
| 75. | 138.900 | 23.4524 | 23.1454 |
| 90. | 166.680 | 23.0079 | 19.6021 |
| 120. | 222.240 | 15.5677 | 14.8986 |
| 180. | 333.360 | 11.1093 | 9.7741 |
| 240. | 444.480 | 8.9368 | 6.8459 |
| 360. | 666.720 | 7.8636 | 3.9343 |
| 480. | 888.960 | 7.6628 | 2.5745 |
| 600. | 1111.200 | 7.5550 | 1.8281 |
| 720. | 1333.440 | 4.9576 | 0.9003 |

Snapshot 6

Interpolation between
Snapshots 6 & 7

Figure C14. (Sheet 6 of 12)

| Radius (n.m.) | Radius (km) | --- Wind Speed --- | Inflow Angle, | |
|------------------|----------------|------------------------|------------------------|----------------------------|
| | | Scalar Avg. (m/sec) | Vector Avg. (m/sec) | (+ = in, - = out) (deg) |
| WIND,HOUR | | 20 | 12 | |
| 1. | 1.852 | 12.3410 | 11.8551 | 3.7051 |
| 2. | 3.704 | 17.3732 | 17.0704 | 5.5010 |
| 3. | 5.556 | 19.8249 | 19.5672 | 4.8894 |
| 4. | 7.408 | 21.3645 | 21.1058 | 4.0851 |
| 5. | 9.260 | 22.3264 | 22.0409 | 3.5390 |
| 6. | 11.112 | 22.9808 | 22.6516 | 3.4733 |
| 7. | 12.964 | 23.4277 | 23.0439 | 3.8438 |
| 8. | 14.816 | 23.6688 | 23.2223 | 4.4859 |
| 9. | 16.668 | 23.7225 | 23.2100 | 5.1796 |
| 10. | 18.520 | 23.5859 | 23.0055 | 5.6476 |
| 15. | 27.780 | 23.2624 | 22.4453 | 1.8611 |
| 20. | 37.040 | 25.1342 | 25.5009 | 0.3552 |
| 25. | 46.300 | 31.0352 | 30.4071 | 10.2215 |
| 30. | 55.560 | 35.0799 | 34.4948 | 21.2548 |
| 40. | 74.080 | 35.0679 | 35.7961 | 34.1508 |
| 50. | 92.600 | 32.8376 | 32.6266 | 37.4436 |
| 60. | 111.120 | 29.4805 | 29.2604 | 37.3449 |
| 75. | 138.900 | 25.2107 | 24.9394 | 35.4033 |
| 90. | 166.680 | 21.9817 | 21.6405 | 33.0628 |
| 120. | 222.240 | 17.7000 | 17.1812 | 28.0628 |
| 180. | 333.360 | 13.3470 | 12.4114 | 21.4082 |
| 240. | 444.480 | 10.9123 | 9.5324 | 17.4889 |
| 360. | 666.720 | 8.6205 | 6.1845 | 15.2893 |
| 480. | 888.960 | 7.9491 | 4.2965 | 15.4385 |
| 600. | 1111.200 | 7.6724 | 3.1780 | 14.7235 |
| 720. | 1333.440 | 5.0044 | 1.6352 | 13.5201 |
| WIND,HOUR | | 20 | 13 | |
| 1. | 1.852 | 7.7009 | 6.5613 | -2.0170 |
| 2. | 3.704 | 11.4624 | 10.8461 | -1.3424 |
| 3. | 5.556 | 14.6585 | 14.2437 | -0.4667 |
| 4. | 7.408 | 17.3708 | 17.0409 | 0.1374 |
| 5. | 9.260 | 19.5312 | 19.2268 | 0.5209 |
| 6. | 11.112 | 21.1956 | 20.8754 | 0.9853 |
| 7. | 12.964 | 22.4706 | 22.1060 | 1.7251 |
| 8. | 14.816 | 23.3862 | 22.9570 | 2.6858 |
| 9. | 16.668 | 23.9666 | 23.4606 | 3.6873 |
| 10. | 18.520 | 24.2226 | 23.6335 | 4.4648 |
| 15. | 27.780 | 24.8182 | 23.9490 | 1.5678 |
| 20. | 37.040 | 23.1526 | 27.4695 | 0.8347 |
| 25. | 46.300 | 33.2867 | 32.4993 | 10.3299 |
| 30. | 55.560 | 37.8870 | 37.1112 | 21.6899 |
| 40. | 74.080 | 40.1685 | 39.6787 | 37.0295 |
| 50. | 92.600 | 37.2299 | 37.0326 | 41.6416 |
| 60. | 111.120 | 33.6495 | 33.4597 | 42.3094 |
| 75. | 138.900 | 23.6322 | 28.4091 | 40.7412 |
| 90. | 166.680 | 24.6445 | 24.3656 | 38.3392 |
| 120. | 222.240 | 19.1697 | 18.7279 | 32.5782 |
| 180. | 333.360 | 13.6240 | 12.7291 | 23.5062 |
| 240. | 444.480 | 10.6611 | 9.2116 | 17.6683 |
| 360. | 666.720 | 8.2944 | 5.3560 | 14.5539 |
| 480. | 888.960 | 7.7899 | 3.4564 | 14.7954 |
| 600. | 1111.200 | 7.5948 | 2.4277 | 14.0900 |
| 720. | 1333.440 | 6.9736 | 1.1949 | 12.8509 |

Snapshot 7

Interpolation between
Snapshots 7 & 8

Figure C14. (Sheet 7 of 12)

| Radius (n.m.) | Radius (km) | --- Wind Speed --- | Scalar Avg. (m/sec) | Vector Avg. (m/sec) | Inflow Angle, (deg) |
|-------------------|----------------|--------------------|------------------------|------------------------|------------------------|
| WIND, HOUR | | | | | |
| 1. | 1.852 | 20 | 5.7881 | 1.0245 | -54.9114 |
| 2. | 3.704 | | 5.4541 | 3.9720 | -24.5178 |
| 3. | 5.556 | | 9.4686 | 8.6090 | -11.9362 |
| 4. | 7.408 | | 13.4829 | 13.0106 | -6.3961 |
| 5. | 9.260 | | 15.7968 | 16.4585 | -3.6516 |
| 6. | 11.112 | | 19.4415 | 19.1273 | -2.0103 |
| 7. | 12.964 | | 21.5386 | 21.1914 | -0.5934 |
| 8. | 14.816 | | 23.1255 | 22.7110 | 0.8438 |
| 9. | 16.668 | | 24.2274 | 23.7256 | 2.2362 |
| 10. | 18.520 | | 24.8698 | 24.2708 | 3.3539 |
| 15. | 27.780 | | 25.3710 | 25.4490 | 1.3220 |
| 20. | 37.040 | | 30.1687 | 29.4218 | 1.2605 |
| 25. | 46.300 | | 35.5447 | 34.5681 | 10.4418 |
| 30. | 55.560 | | 40.6915 | 39.6964 | 22.0873 |
| 40. | 74.080 | | 44.2657 | 43.9524 | 39.3821 |
| 50. | 92.600 | | 41.6690 | 41.4767 | 44.9398 |
| 60. | 111.120 | | 37.9086 | 37.7362 | 46.1393 |
| 75. | 138.900 | | 32.1717 | 31.9795 | 44.8648 |
| 90. | 166.680 | | 27.4255 | 27.1891 | 42.4840 |
| 120. | 222.240 | | 23.7241 | 20.3404 | 35.3204 |
| 180. | 333.360 | | 13.3054 | 13.0482 | 25.5059 |
| 240. | 444.480 | | 10.4115 | 8.8880 | 17.8943 |
| 360. | 666.720 | | 3.0717 | 4.5179 | 13.6535 |
| 480. | 888.960 | | 7.6928 | 2.6034 | 13.7065 |
| 600. | 1111.200 | | 7.5579 | 1.6662 | 12.8807 |
| 720. | 1333.440 | | 4.9537 | 0.7413 | 11.2863 |
| WIND, HOUR | | | | | |
| | | 20 | | 15 | |
| 1. | 1.852 | | 5.2786 | 3.6952 | -21.4673 |
| 2. | 3.704 | | 9.6598 | 8.8585 | -8.8558 |
| 3. | 5.556 | | 13.9015 | 13.4537 | -3.6465 |
| 4. | 7.408 | | 17.2845 | 16.9501 | -1.3335 |
| 5. | 9.260 | | 19.9031 | 19.5926 | -0.1562 |
| 6. | 11.112 | | 21.8548 | 21.5198 | 0.7374 |
| 7. | 12.964 | | 23.2916 | 22.9027 | 1.7017 |
| 8. | 14.816 | | 24.2837 | 23.8207 | 2.7128 |
| 9. | 16.668 | | 24.8923 | 24.3430 | 3.6006 |
| 10. | 18.520 | | 25.1624 | 24.5209 | 4.1324 |
| 15. | 27.780 | | 25.3268 | 25.4590 | 0.4130 |
| 20. | 37.040 | | 30.7382 | 30.0349 | 2.6953 |
| 25. | 46.300 | | 35.3498 | 35.5371 | 14.4592 |
| 30. | 55.560 | | 40.5023 | 39.6200 | 25.8454 |
| 40. | 74.080 | | 41.5230 | 41.2674 | 39.3602 |
| 50. | 92.600 | | 37.9830 | 37.7975 | 43.0899 |
| 60. | 111.120 | | 34.0207 | 33.8370 | 43.3371 |
| 75. | 138.900 | | 23.6710 | 26.4499 | 41.4519 |
| 90. | 166.680 | | 24.4793 | 24.1978 | 39.8258 |
| 120. | 222.240 | | 13.7628 | 18.3017 | 32.6069 |
| 180. | 333.360 | | 13.0273 | 12.0419 | 22.6556 |
| 240. | 444.480 | | 10.0310 | 8.3815 | 16.5407 |
| 360. | 666.720 | | 9.0627 | 4.5075 | 13.6395 |
| 480. | 888.960 | | 7.6978 | 2.7350 | 13.7344 |
| 600. | 1111.200 | | 7.5589 | 1.8231 | 12.9673 |
| 720. | 1333.440 | | 4.9534 | 0.8437 | 11.6417 |

Figure C14. (Sheet 8 of 12)

| Radius (n.m.) | Radius (km) | --- Wind Speed --- | | Inflow Angle, (+ = in, - = out) |
|-------------------|----------------|------------------------|------------------------|------------------------------------|
| | | Scalar Avg. (m/sec) | Vector Avg. (m/sec) | |
| WIND, HOUR | | | | |
| | | 20 | 16 | |
| 1. | 1.852 | 7.5921 | 6.3574 | -15.8577 |
| 2. | 3.704 | 13.8447 | 13.4131 | -2.9746 |
| 3. | 5.556 | 13.2339 | 17.9469 | 0.7354 |
| 4. | 7.408 | 21.1606 | 20.8925 | 1.7934 |
| 5. | 9.260 | 23.0540 | 22.7538 | 2.2868 |
| 6. | 11.112 | 24.2866 | 23.9272 | 2.8904 |
| 7. | 12.964 | 25.0617 | 24.6285 | 3.6555 |
| 8. | 14.816 | 25.4596 | 24.9436 | 4.4044 |
| 9. | 16.668 | 25.5713 | 24.9689 | 4.8958 |
| 10. | 18.520 | 25.4633 | 24.7739 | 4.8956 |
| 15. | 27.780 | 25.2953 | 25.4727 | -0.4949 |
| 20. | 37.040 | 31.3771 | 30.6556 | 4.0804 |
| 25. | 46.300 | 37.3395 | 36.6335 | 18.2633 |
| 30. | 55.560 | 41.5397 | 40.0771 | 29.5947 |
| 40. | 74.080 | 33.7619 | 38.5545 | 39.3625 |
| 50. | 92.600 | 34.2823 | 34.0974 | 40.8550 |
| 60. | 111.120 | 33.1596 | 29.9541 | 39.8027 |
| 75. | 138.900 | 25.2403 | 24.9730 | 37.0471 |
| 90. | 166.680 | 21.6228 | 21.2727 | 34.0914 |
| 120. | 222.240 | 15.8975 | 16.3266 | 27.8725 |
| 180. | 333.360 | 12.1601 | 11.0181 | 19.3734 |
| 240. | 444.480 | 9.6775 | 7.8774 | 15.0447 |
| 360. | 666.720 | 3.0558 | 4.4971 | 13.6266 |
| 480. | 888.960 | 7.7047 | 2.8664 | 13.7609 |
| 600. | 1111.200 | 7.5622 | 1.9796 | 13.0339 |
| 720. | 1333.440 | 4.9545 | 0.9461 | 11.9152 |
| WIND, HOUR | | | | |
| | | 20 | 17 | |
| 1. | 1.852 | 5.1944 | 3.3138 | -17.8760 |
| 2. | 3.704 | 3.2681 | 7.2138 | -6.8815 |
| 3. | 5.556 | 13.7056 | 10.0051 | -6.1496 |
| 4. | 7.408 | 12.7647 | 12.1956 | -3.0712 |
| 5. | 9.260 | 14.7353 | 14.2314 | -2.2659 |
| 6. | 11.112 | 15.6943 | 16.2217 | -1.2967 |
| 7. | 12.964 | 13.5415 | 18.0779 | -0.2965 |
| 8. | 14.816 | 23.2149 | 19.7445 | 0.5915 |
| 9. | 16.668 | 21.6830 | 21.1906 | 1.2304 |
| 10. | 18.520 | 22.9397 | 22.4105 | 1.6022 |
| 15. | 27.780 | 27.8821 | 27.2105 | 1.1748 |
| 20. | 37.040 | 32.6080 | 32.0467 | 5.5850 |
| 25. | 46.300 | 35.3954 | 35.8652 | 14.8451 |
| 30. | 55.560 | 38.1757 | 37.7211 | 22.5590 |
| 40. | 74.080 | 37.0872 | 36.7704 | 30.7857 |
| 50. | 92.600 | 34.6084 | 34.3532 | 34.4098 |
| 60. | 111.120 | 32.1141 | 31.8807 | 36.0672 |
| 75. | 138.900 | 28.4567 | 28.2119 | 36.6382 |
| 90. | 166.680 | 25.2441 | 24.9620 | 35.9514 |
| 120. | 222.240 | 23.3278 | 19.9233 | 32.5304 |
| 180. | 333.360 | 16.6386 | 13.8605 | 25.1756 |
| 240. | 444.480 | 11.3865 | 10.1154 | 19.1383 |
| 360. | 666.720 | 8.4428 | 5.7836 | 14.1522 |
| 480. | 888.960 | 7.8172 | 3.5385 | 13.6463 |
| 600. | 1111.200 | 7.5980 | 2.3437 | 12.9271 |
| 720. | 1333.440 | 4.9691 | 1.0852 | 11.8318 |

Interpolation between
Snapshots 9 & 10

Figure C14. (Sheet 9 of 12)

| Radius (n.m.) | Radius (km) | --- Wind Speed --- | | Inflow Angle, |
|-------------------|----------------|------------------------|------------------------|----------------------------|
| | | Scalar Avg. (m/sec) | Vector Avg. (m/sec) | (+ = in, - = out) (deg) |
| WIND, HOUR | | | | |
| | | 20 | 18 | |
| 1. | 1.852 | 5.8467 | 0.1474 | -88.3850 |
| 2. | 3.704 | 5.8913 | 0.3323 | -80.3511 |
| 3. | 5.556 | 5.9854 | 0.7624 | -51.3616 |
| 4. | 7.408 | 5.1382 | 2.1004 | -27.6604 |
| 5. | 9.260 | 5.7706 | 4.7446 | -17.3690 |
| 6. | 11.112 | 9.0271 | 8.0799 | -12.3260 |
| 7. | 12.964 | 12.0708 | 11.4742 | -8.8906 |
| 8. | 14.816 | 15.0533 | 14.6107 | -6.1866 |
| 9. | 16.668 | 17.8664 | 17.4786 | -4.1897 |
| 10. | 18.520 | 23.4882 | 20.1007 | -2.5294 |
| 15. | 27.780 | 29.5051 | 28.9509 | 2.6555 |
| 20. | 37.040 | 33.9718 | 33.4147 | 6.9510 |
| 25. | 46.300 | 35.6832 | 35.1937 | 11.2949 |
| 30. | 55.560 | 35.3991 | 35.8866 | 14.7093 |
| 40. | 74.080 | 35.2753 | 35.7456 | 21.5719 |
| 50. | 92.600 | 35.3740 | 34.9881 | 28.1950 |
| 60. | 111.120 | 34.2038 | 33.9125 | 32.8383 |
| 75. | 138.900 | 31.6678 | 31.4230 | 36.3589 |
| 90. | 166.680 | 28.8703 | 28.6221 | 37.3360 |
| 120. | 222.240 | 23.8659 | 23.5513 | 35.6325 |
| 180. | 333.360 | 17.1794 | 16.6087 | 29.1446 |
| 240. | 444.480 | 13.2542 | 12.2959 | 22.2227 |
| 360. | 666.720 | 9.1195 | 7.0444 | 14.5881 |
| 480. | 888.960 | 7.9716 | 4.2027 | 13.5547 |
| 600. | 1111.200 | 7.6452 | 2.7066 | 12.8437 |
| 720. | 1333.440 | 4.9840 | 1.2224 | 11.7472 |
| WIND, HOUR | | | | |
| | | 20 | 19 | |
| 1. | 1.852 | 5.8873 | 0.1315 | 267.8173 |
| 2. | 3.704 | 5.9185 | 0.2864 | -85.9611 |
| 3. | 5.556 | 5.9876 | 0.5704 | -62.3600 |
| 4. | 7.408 | 5.0828 | 1.4068 | -35.5898 |
| 5. | 9.260 | 5.4022 | 3.4218 | -21.5389 |
| 6. | 11.112 | 7.7488 | 6.4805 | -15.1524 |
| 7. | 12.964 | 10.6217 | 9.8852 | -11.4492 |
| 8. | 14.816 | 13.7639 | 13.2437 | -8.3193 |
| 9. | 16.668 | 15.7812 | 16.3407 | -5.9519 |
| 10. | 18.520 | 13.6647 | 19.2310 | -4.1128 |
| 15. | 27.780 | 30.2064 | 29.6647 | 1.3036 |
| 20. | 37.040 | 35.6643 | 35.1813 | 7.1232 |
| 25. | 46.300 | 37.6751 | 37.1826 | 12.9720 |
| 30. | 55.560 | 33.4773 | 37.9349 | 17.8365 |
| 40. | 74.080 | 37.8872 | 37.4660 | 26.6277 |
| 50. | 92.600 | 35.1374 | 35.8437 | 32.4841 |
| 60. | 111.120 | 34.0912 | 33.8478 | 35.6165 |
| 75. | 138.900 | 33.5693 | 30.3335 | 37.1984 |
| 90. | 166.680 | 27.2103 | 26.9485 | 36.9100 |
| 120. | 222.240 | 21.8017 | 21.4339 | 33.6695 |
| 180. | 333.360 | 15.3121 | 14.5863 | 25.7770 |
| 240. | 444.480 | 11.6306 | 10.3863 | 18.7814 |
| 360. | 666.720 | 3.3756 | 5.5758 | 13.0014 |
| 480. | 888.960 | 7.7792 | 3.2149 | 12.4173 |
| 600. | 1111.200 | 7.5839 | 2.0212 | 11.7434 |
| 720. | 1333.440 | 4.9611 | 0.8834 | 10.6389 |

Snapshot 10

Interpolation between
Snapshots 10 & 11

Figure C14. (Sheet 10 of 12)

| Radius (n.m.) | Radius (km) | --- Wind Speed --- | | Inflow Angle, (+ = in, - = out) (deg) |
|-------------------|----------------|------------------------|------------------------|---|
| | | Scalar Avg. (m/sec) | Vector Avg. (m/sec) | |
| WIND, HOUR | | 20 | 20 | |
| 1. | 1.852 | 5.9287 | 0.1162 | 262.9969 |
| 2. | 3.704 | 5.9470 | 0.2442 | 266.3879 |
| 3. | 5.556 | 5.9963 | 0.4185 | -82.6926 |
| 4. | 7.408 | 5.0763 | 0.7876 | -57.0778 |
| 5. | 9.260 | 5.1921 | 2.0833 | -30.7253 |
| 6. | 11.112 | 5.8094 | 4.8376 | -19.6630 |
| 7. | 12.964 | 3.1999 | 8.2625 | -14.5830 |
| 8. | 14.816 | 12.4422 | 11.8214 | -10.8999 |
| 9. | 16.668 | 15.7084 | 15.2023 | -7.9758 |
| 10. | 18.520 | 18.8605 | 18.3726 | -5.8433 |
| 15. | 27.780 | 33.9314 | 30.3868 | 0.0276 |
| 20. | 37.040 | 37.4365 | 36.9167 | 7.2898 |
| 25. | 46.300 | 39.7792 | 39.1634 | 14.4881 |
| 30. | 55.560 | 40.6823 | 40.0401 | 20.6426 |
| 40. | 74.080 | 33.7404 | 39.3892 | 31.2106 |
| 50. | 92.600 | 37.0910 | 36.8561 | 36.5571 |
| 60. | 111.120 | 34.0673 | 33.8533 | 38.4093 |
| 75. | 138.900 | 23.4841 | 29.2478 | 38.1131 |
| 90. | 166.680 | 25.5521 | 25.2662 | 36.4341 |
| 120. | 222.240 | 13.7706 | 19.3250 | 31.2195 |
| 180. | 333.360 | 13.5125 | 12.5523 | 21.3094 |
| 240. | 444.480 | 13.1318 | 8.4430 | 14.2101 |
| 360. | 666.720 | 3.0124 | 4.0795 | 10.4747 |
| 480. | 888.960 | 7.6745 | 2.2099 | 10.1812 |
| 600. | 1111.200 | 7.5460 | 1.3164 | 9.3948 |
| 720. | 1333.440 | 6.9515 | 0.5429 | 8.0716 |
| WIND, HOUR | | 20 | 21 | |
| 1. | 1.852 | 5.8757 | 0.1576 | 268.9495 |
| 2. | 3.704 | 5.9111 | 0.3922 | -77.2274 |
| 3. | 5.556 | 5.9792 | 1.0670 | -45.1869 |
| 4. | 7.408 | 5.2267 | 2.7191 | -27.0611 |
| 5. | 9.260 | 7.1538 | 5.5461 | -17.8151 |
| 6. | 11.112 | 9.9381 | 9.1108 | -12.9344 |
| 7. | 12.964 | 13.2739 | 12.7167 | -9.3226 |
| 8. | 14.816 | 15.5174 | 16.0578 | -5.5766 |
| 9. | 16.668 | 13.5786 | 19.1314 | -4.5214 |
| 10. | 18.520 | 22.3568 | 21.8765 | -2.8559 |
| 15. | 27.780 | 31.7253 | 31.1325 | 1.6857 |
| 20. | 37.040 | 35.4453 | 35.8979 | 7.4276 |
| 25. | 46.300 | 33.1408 | 37.5264 | 13.7821 |
| 30. | 55.560 | 33.9178 | 38.2712 | 19.6641 |
| 40. | 74.080 | 33.2284 | 37.8720 | 30.4967 |
| 50. | 92.600 | 35.6980 | 35.4598 | 35.9404 |
| 60. | 111.120 | 32.7401 | 32.5198 | 37.7223 |
| 75. | 138.900 | 23.2836 | 28.0357 | 37.3035 |
| 90. | 166.680 | 24.4976 | 24.1939 | 35.5394 |
| 120. | 222.240 | 13.9903 | 18.5127 | 30.2212 |
| 180. | 333.360 | 13.0686 | 12.0446 | 20.4458 |
| 240. | 444.480 | 9.6837 | 8.1095 | 13.8851 |
| 360. | 666.720 | 7.9783 | 3.9614 | 10.7447 |
| 480. | 888.960 | 7.5647 | 2.1807 | 10.4799 |
| 600. | 1111.200 | 7.5406 | 1.3178 | 9.6954 |
| 720. | 1333.440 | 6.9487 | 0.5516 | 8.3981 |

Snapshot 11

Interpolation between
Snapshots 11 & 12

Figure C14. (Sheet 11 of 12)

| Radius (n.m.) | Radius (km) | --- Wind Speed --- | | Inflow Angle, (+ = in, - = out) |
|------------------|----------------|------------------------|------------------------|------------------------------------|
| | | Scalar Avg. (m/sec) | Vector Avg. (m/sec) | (deg) |
| | | 20 | 22 | |
| 1. | 1.852 | 5.8255 | 0.2000 | -87.6107 |
| 2. | 3.704 | 5.8812 | 0.5546 | -70.1721 |
| 3. | 5.556 | 5.0218 | 1.8204 | -37.1198 |
| 4. | 7.408 | 5.7394 | 4.6981 | -21.8820 |
| 5. | 9.260 | 9.6611 | 8.8197 | -14.1624 |
| 6. | 11.112 | 13.5649 | 13.0636 | -9.2704 |
| 7. | 12.964 | 17.2198 | 16.8280 | -6.1336 |
| 8. | 14.816 | 20.5720 | 20.1906 | -3.9692 |
| 9. | 16.668 | 23.4862 | 23.0649 | -2.2587 |
| 10. | 18.520 | 25.8745 | 25.3865 | -0.7408 |
| 15. | 27.780 | 32.5430 | 31.8957 | 3.2647 |
| 20. | 37.040 | 35.4582 | 34.8746 | 7.5786 |
| 25. | 46.300 | 35.5038 | 35.8823 | 13.0151 |
| 30. | 55.560 | 37.1546 | 36.4978 | 18.5939 |
| 40. | 74.080 | 35.7130 | 36.3500 | 29.7262 |
| 50. | 92.600 | 38.3014 | 34.0590 | 35.2759 |
| 60. | 111.120 | 31.4108 | 31.1831 | 36.9782 |
| 75. | 138.900 | 27.0841 | 26.8226 | 36.4202 |
| 90. | 166.680 | 23.4467 | 23.1226 | 34.5579 |
| 120. | 222.240 | 13.2176 | 17.7032 | 29.1176 |
| 180. | 333.360 | 12.6231 | 11.5294 | 19.5335 |
| 240. | 444.480 | 9.6441 | 7.7750 | 13.5450 |
| 360. | 666.720 | 7.9456 | 3.8433 | 11.0326 |
| 480. | 888.960 | 7.6550 | 2.1516 | 10.7810 |
| 600. | 1111.200 | 7.5351 | 1.3193 | 9.9973 |
| 720. | 1333.440 | 6.9459 | 0.5603 | 8.7143 |
| FORTRAN STOP | | | | |

Snapshot 12

Figure C14. (Sheet 12 of 12)

Appendix D

Sample Application of Upgraded CE Model to Simulation of 36-Hr Period of Hurricane Gilbert in the Gulf of Mexico

This appendix provides information related to a 36-hr simulation of Hurricane Gilbert in the Gulf of Mexico. The simulation was performed by OWI as an additional test with the upgraded CE model. The simulation time period begins 1200 UTC (Universal Time Coordinate, formerly known as Greenwich Mean Time) 15 September 1988. The four snapshots used in the simulation all took advantage of the double exponential form for pressure profile specification. Input file information on the snapshots and storm track specification is provided in this appendix.

The appendix also includes plots of Hurricane Gilbert wind fields. Model wind fields at 19-m elevation are given at 6-hr intervals throughout the simulation period. Wind speed and direction is represented with the conventional weather map "wind barb" notation. The shaft of each wind arrow indicates the direction and the barbs or "feathers" indicate wind speed. A half-barb denotes 5 knots, full barb denotes 10 knots, and solid flag denotes 50 knots.

```

$ type 05gilbert88.dat
$name1 Kzm = 8809, Kdh = 151100, Kmin = 60, inside=1,
    nstres=17227, Kstres = 0, kwind = 19, nwind = 4661, hh=500. $end
    lns2 eyelat=22, eypres=951, pfar=1012, radius=11.88,46.85, holl=.56,2.52,
    dpi=45.07, direc=290, speed=11, sqw=7, oni=120 $end
$name2 eyelat=23, eypres=949, pfar=1010, radius=11.88,43.53, holl=.75,2.52,
    dpi=40.67, sqw=8 $end
$name2 eyelat=24, eypres=953, pfar=1010, radius=27,64.21, holl=1.33,2.52,
    dpi=46.62, sqw=9 $end
$name2 eyelat=24, eypres=954, pfar=1009, radius=21.6,60.61, holl=1.19,2.52,
    dpi=44.98 $end
$name2 eyelat = 999 $end
    0 21 54 -91 42 1
    1 21 54 -91 42 1
    7 22 5 -92 48
    13 22 30 -93 48 2
    19 22 54 -94 48
    25 23 42 -95 54
    31 23 54 -97 0 3
    37 24 24 -98 12 4
999
$what Kstep2 = 37 $enc

```

Figure D1. Snapshot and storm track specification, Hurricane Gilbert

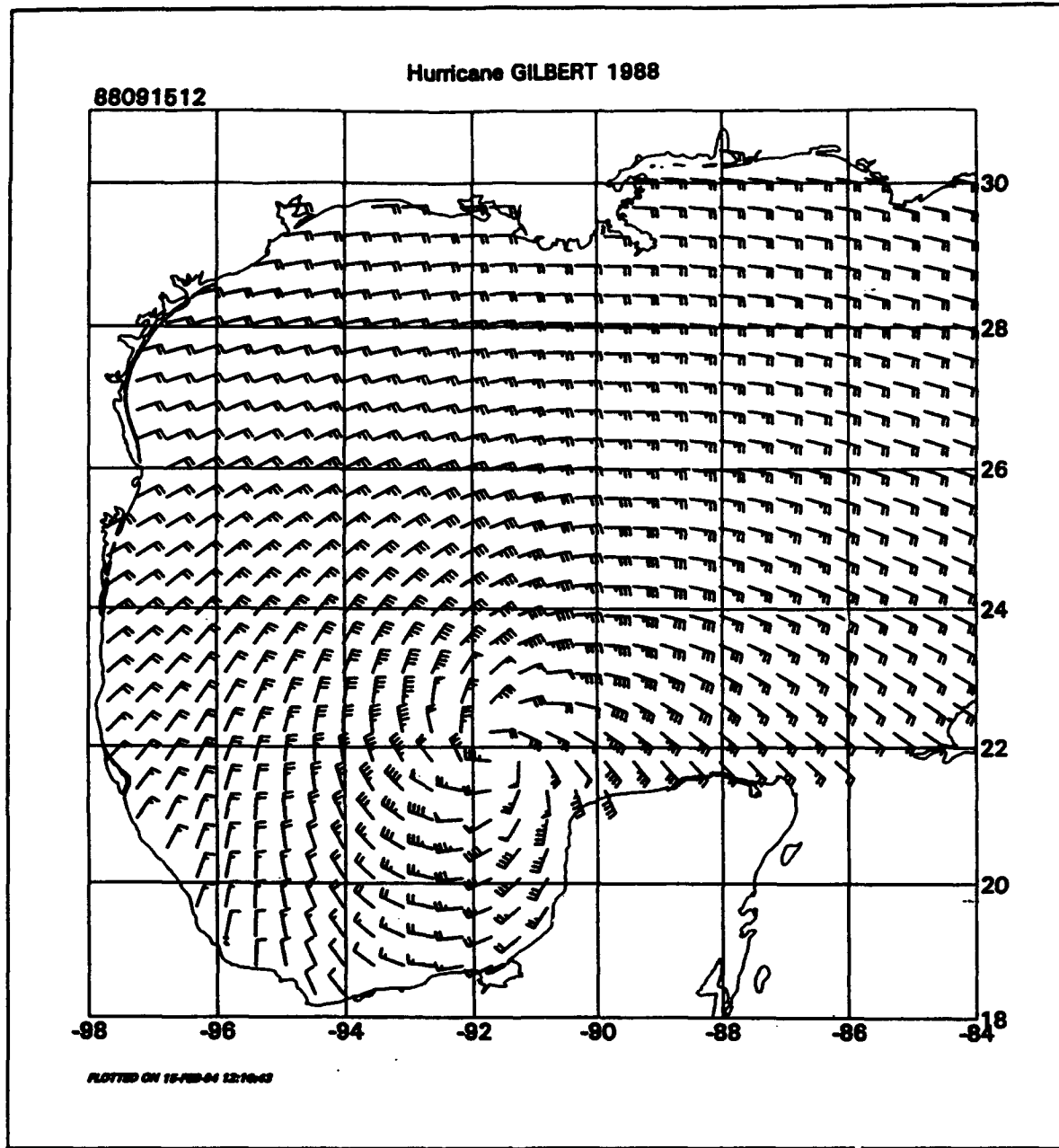


Figure D2. Modelled surface wind field in Hurricane Gilbert (Sheet 1 of 7)

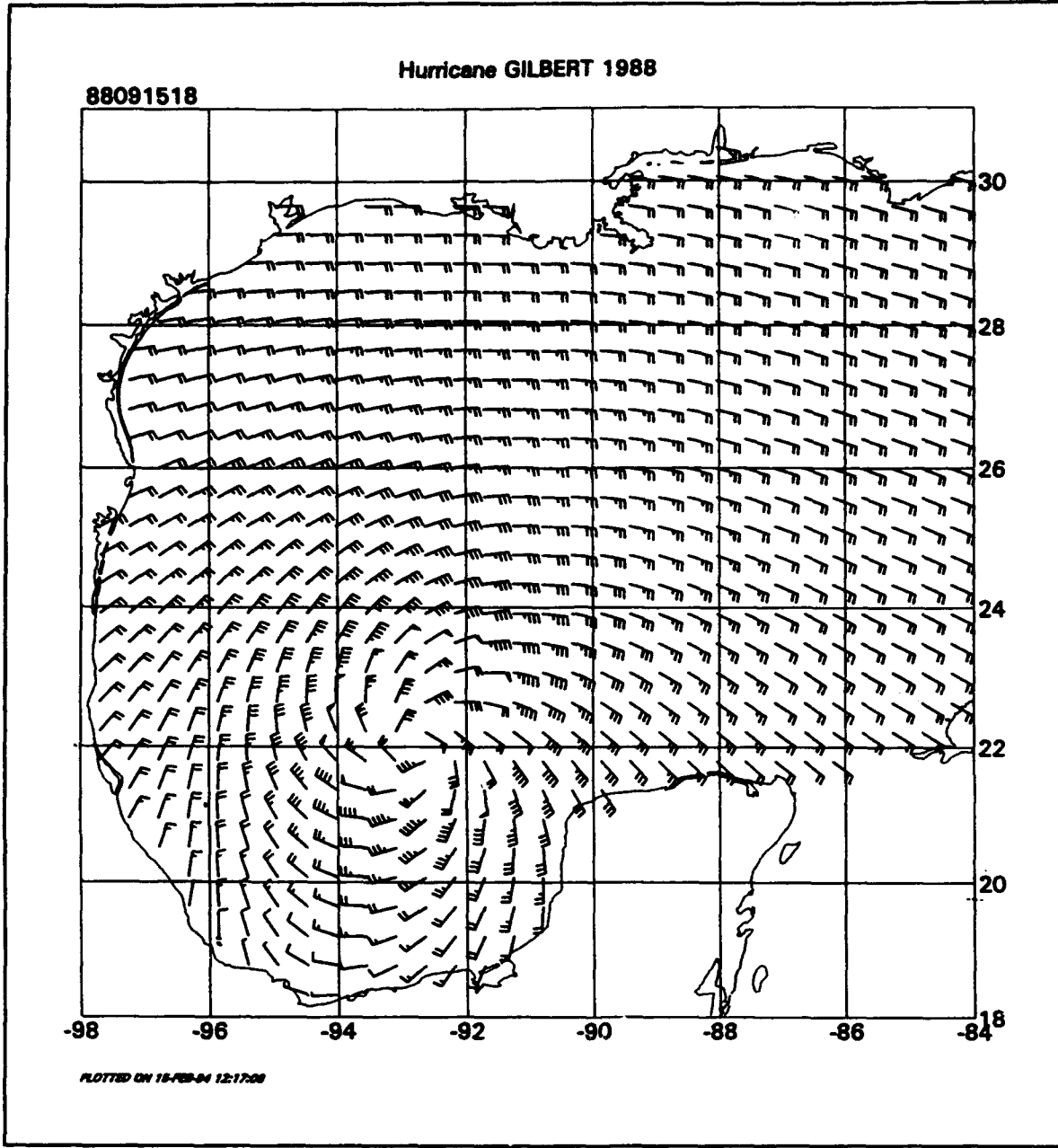


Figure D2. (Sheet 2 of 7)

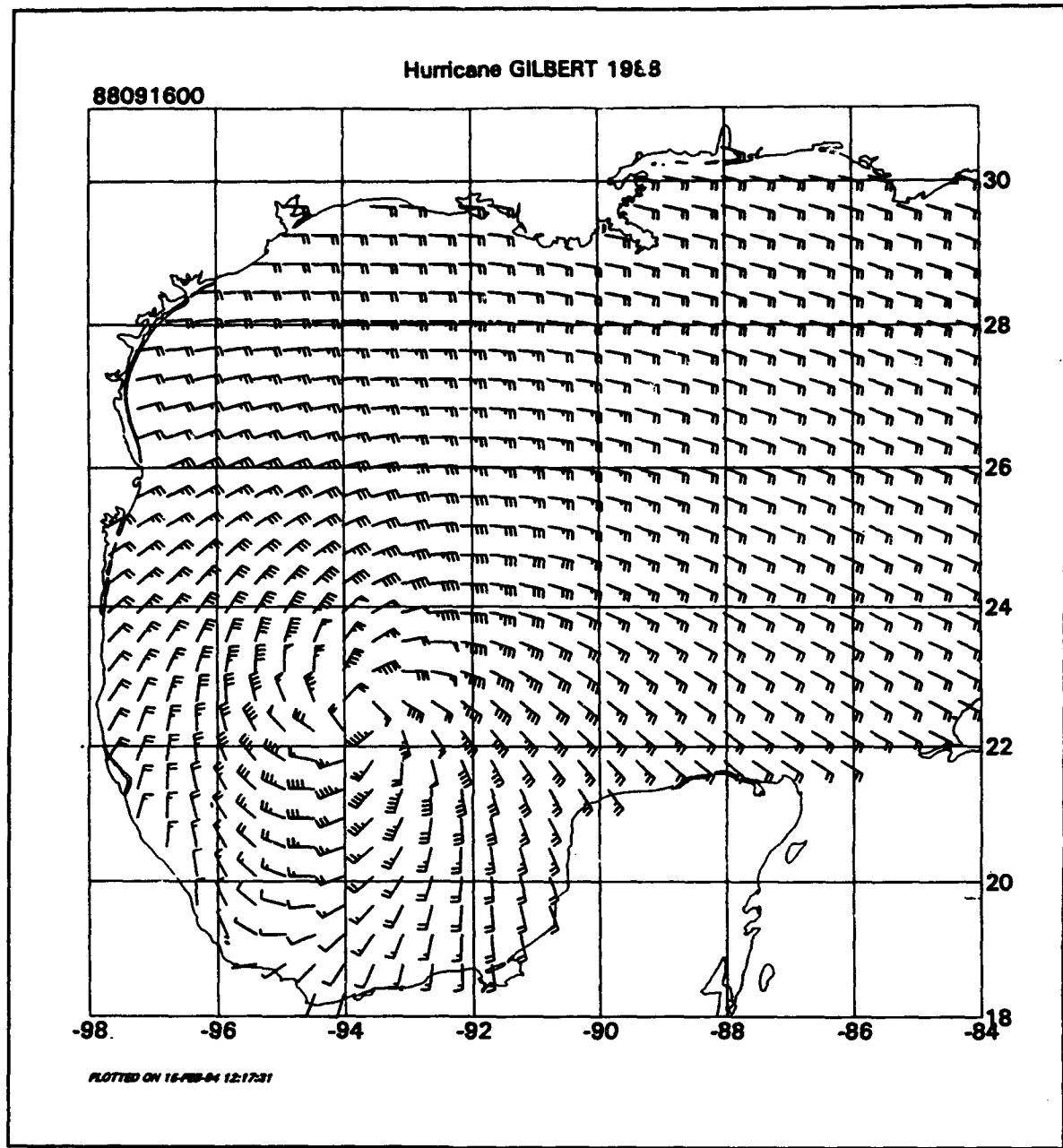


Figure D2. (Sheet 3 of 7)

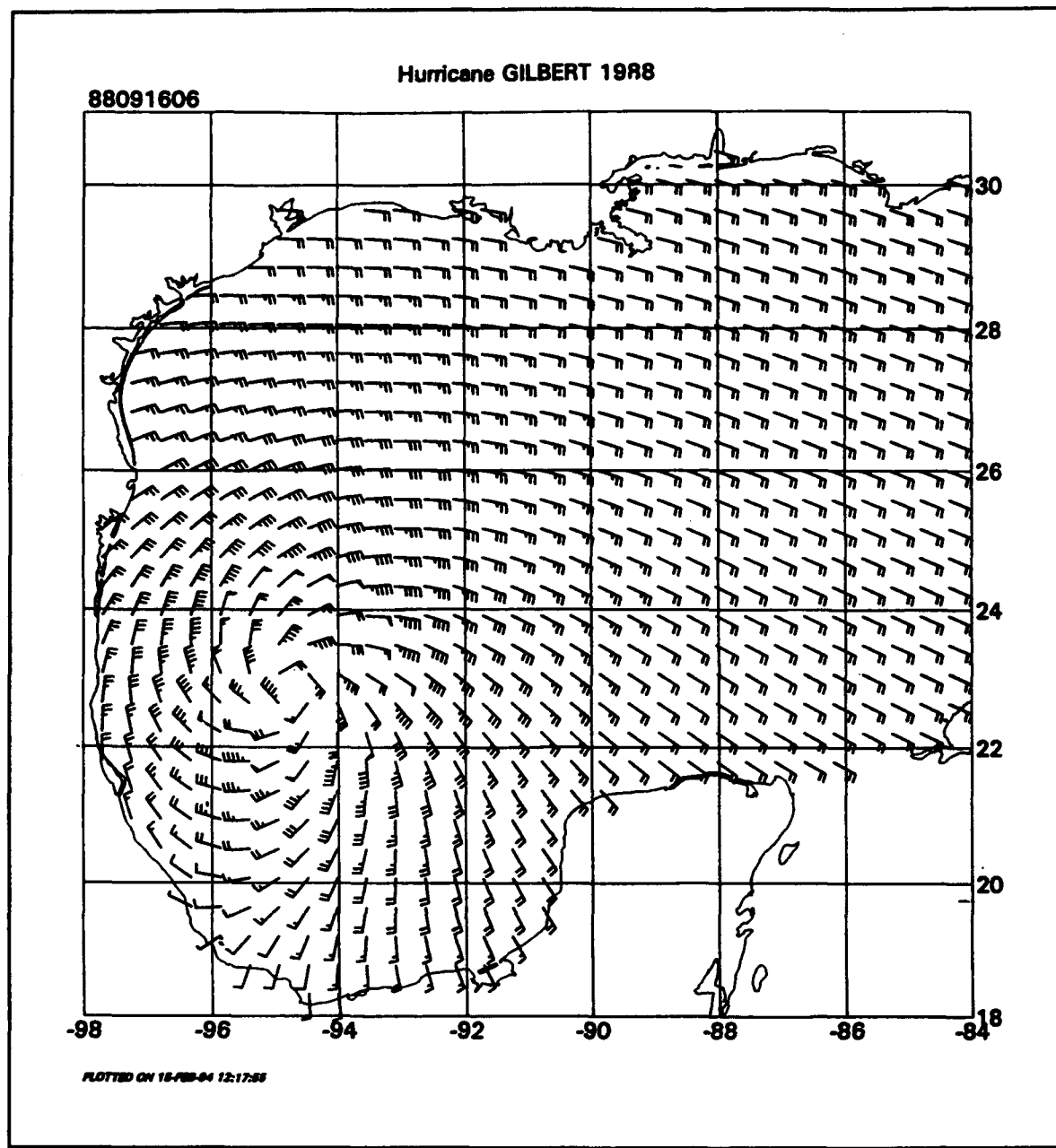


Figure D2. (Sheet 4 of 7)

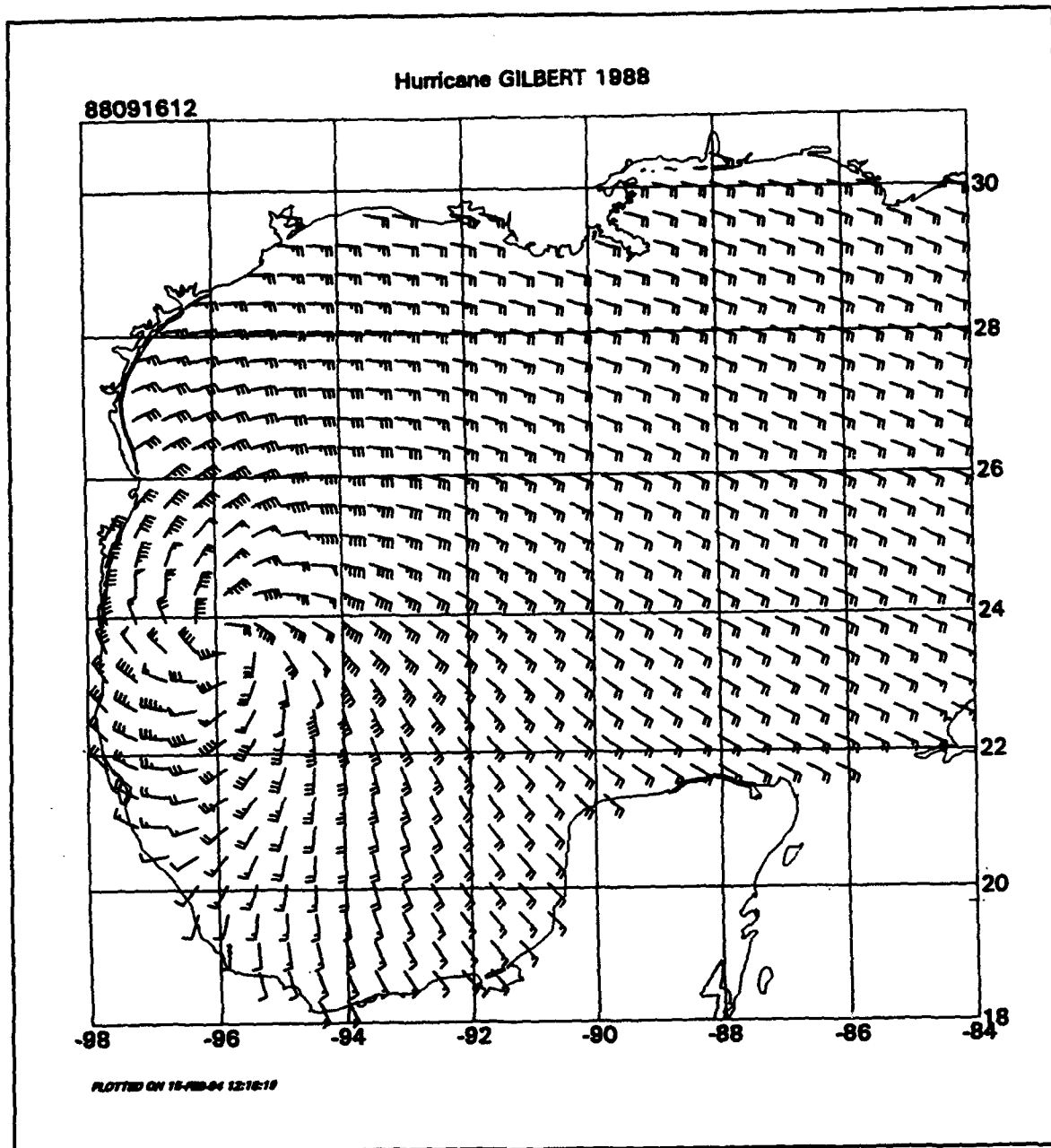


Figure D2. (Sheet 5 of 7)

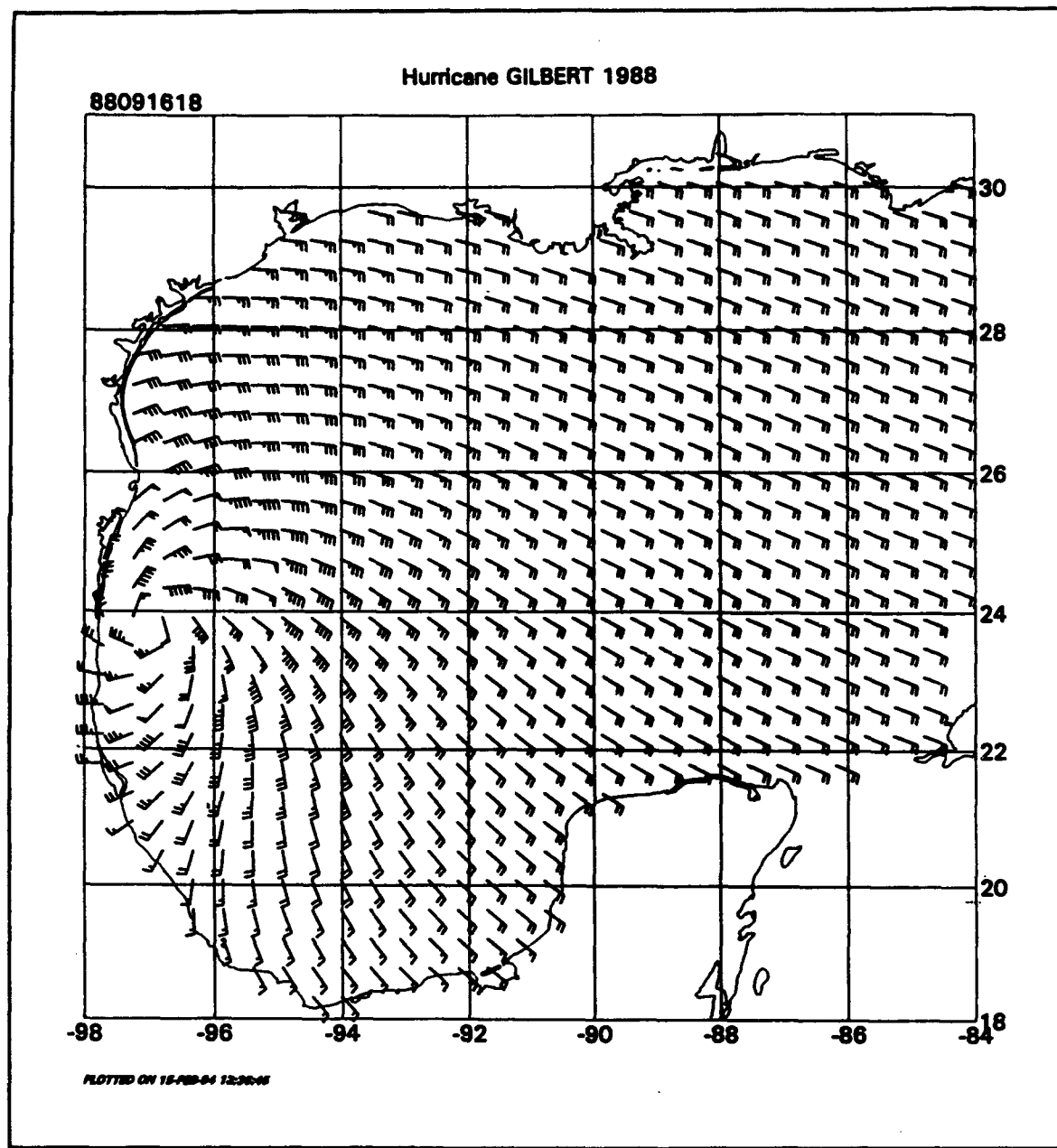


Figure D2. (Sheet 6 of 7)

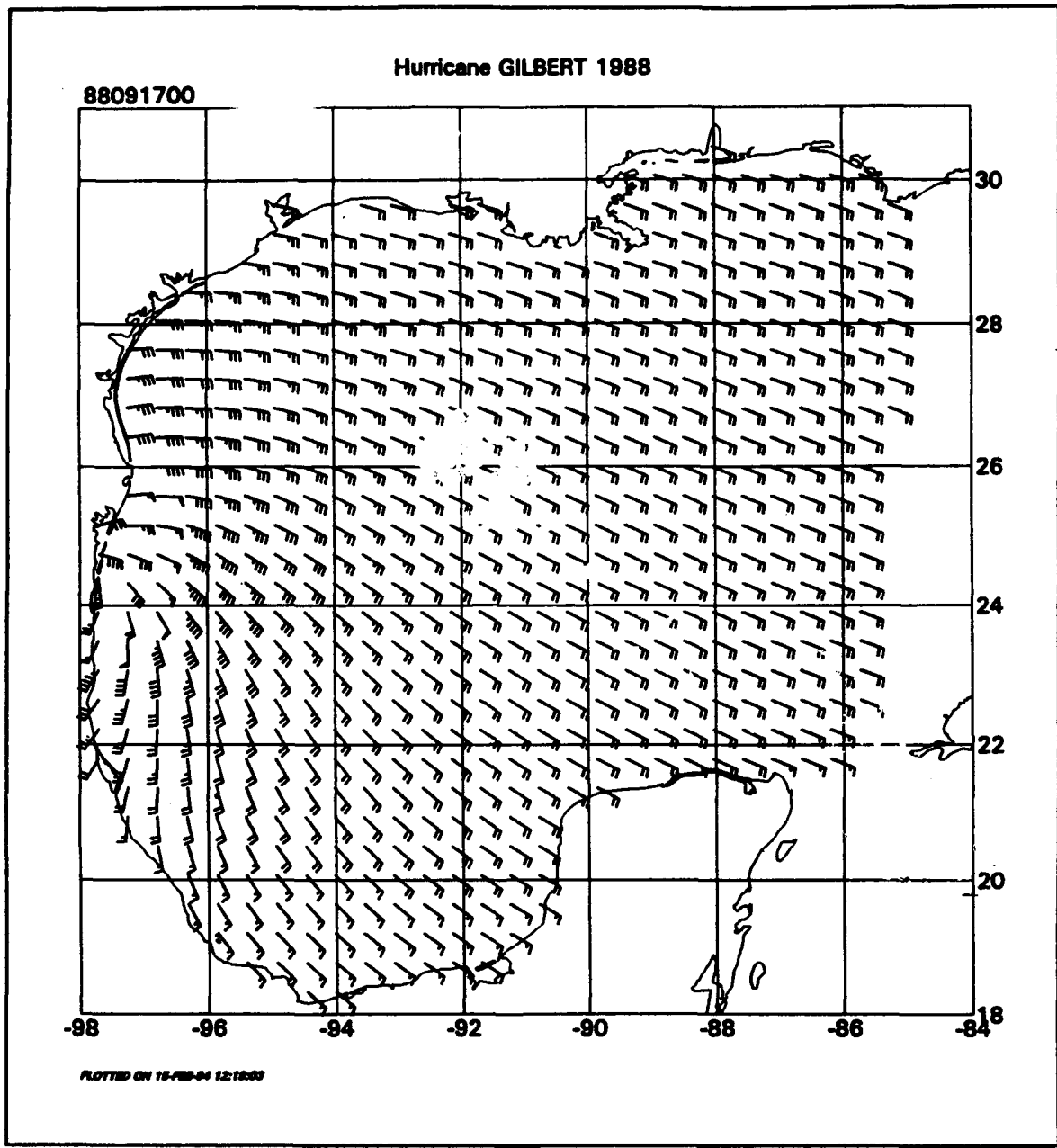


Figure D2. (Sheet 7 of 7)

REPORT DOCUMENTATION PAGE

Form Approved
OMB No. 0704-0188

Public reporting burden for this collection of information is estimated to average 1 hour per response, including the time for reviewing instructions, searching existing data sources, gathering and maintaining the data needed, and completing and reviewing the collection of information. Send comments regarding this burden estimate or any other aspect of this collection of information, including suggestions for reducing this burden, to Washington Headquarters Services, Directorate for Information Operations and Reports, 1215 Jefferson Davis Highway, Suite 1204, Arlington, VA 22202-4302, and to the Office of Management and Budget, Paperwork Reduction Project (0704-0188), Washington, DC 20503.

| | | |
|--|----------------|---|
| 1. AGENCY USE ONLY (Leave blank) | 2. REPORT DATE | 3. REPORT TYPE AND DATES COVERED |
| | July 1994 | Final report |
| 4. TITLE AND SUBTITLE Upgrade of Tropical Cyclone Surface Wind Field Model | | 5. FUNDING NUMBERS WU 32683 |
| 6. AUTHOR(S) Vincent J. Cardone, Andrew T. Cox, J. Arthur Greenwood, Edward F. Thompson | | 8. PERFORMING ORGANIZATION REPORT NUMBER Miscellaneous Paper CERC-94-14 |
| 7. PERFORMING ORGANIZATION NAME(S) AND ADDRESS(ES) Oceanweather, Inc., 5 River Road, Suite 1, Cos Cob, CT 06807 U.S. Army Engineer Waterways Experiment Station 3909 Halls Ferry Road, Vicksburg, MS 39180-6199 | | |
| 9. SPONSORING/MONITORING AGENCY NAME(S) AND ADDRESS(ES) U.S. Army Corps of Engineers Washington, DC 20314-1000 | | 10. SPONSORING/MONITORING AGENCY REPORT NUMBER |
| 11. SUPPLEMENTARY NOTES Available from National Technical Information Service, 5285 Port Royal Road, Springfield, VA 22161. | | |
| 12a. DISTRIBUTION/AVAILABILITY STATEMENT Approved for public release; distribution is unlimited. | | 12b. DISTRIBUTION CODE |

13. ABSTRACT (Maximum 200 words)

The U.S. Army Corps of Engineers (CE) tropical cyclone surface wind field model has been a very useful tool in ocean response modeling for more than a decade. Recently, its limitations were assessed in light of present knowledge and technology. Model limitations were identified and evaluated in terms of their perceived importance to ocean response modeling and the level of effort required to develop improved solutions. The limitations are summarized in this report.

Two aspects of the CE model were targeted for improvement. This report describes the improvements developed for the upgraded model. First, the model was upgraded to include more computationally intensive options which give improved resolution and areal coverage. Up to seven nested grids are now available, compared to only five nests in the standard model. In a typical application, this upgrade can be used to achieve 2-km resolution around the eye (as compared to 5-km resolution often used in the standard model) and an expanded total coverage area.

The second upgrade allows a more general specification of the axisymmetric pressure profile. This upgrade can be used to create wind fields with maxima at two different radii or with a broad maximum extending over a range of radii. It also provides more flexibility in fitting the shape of single peaked wind profiles.

(Continued)

| | | | |
|--|---|--|----------------------------|
| 14. SUBJECT TERMS Hurricanes Numerical modeling Tropical storms | | 15. NUMBER OF PAGES 101 | |
| | | 16. PRICE CODE | |
| 17. SECURITY CLASSIFICATION OF REPORT UNCLASSIFIED | 18. SECURITY CLASSIFICATION OF THIS PAGE UNCLASSIFIED | 19. SECURITY CLASSIFICATION OF ABSTRACT | 20. LIMITATION OF ABSTRACT |

13. (Concluded).

The upgraded model is demonstrated with historical hurricanes. The five-nest and seven-nest models are applied to Hurricane Camille. The fully upgraded model, with seven nests and general pressure specification, is applied to Hurricane Gilbert. This hurricane was chosen because it is well-documented by Black and Willoughby (1992) and it evolved into some nontraditional storm structures. The upgraded model was more effective than the standard CE model in simulating the storm.